# Roles of Msb2p and other putative sensors in environmental responses of *Candida albicans*

Inaugural - Dissertation

Presented by

**Fabien COTTIER**
From Lyon, France

Submitted to attain the doctoral degree of the
Mathematisch-Naturwissenschaftlichen Fakultät
der Heinrich-Heine-Universität Düsseldorf

DÜSSELDORF
December 2007

Referee: Prof. Dr. J.F. Ernst

Co-referee: Prof. Dr. K. Jäger

müdlichen Prüfung: 18.01.2008

# 1. Introduction

## 1.1 *Candida albicans*: friend and foe

Christine Berkhout described the genus *Candida* as follows: “Few hyphae, prostrate, breaking up into shorter or longer pieces. Conidia, arising by budding from the hyphae or on top of each other, are small and hyaline“(Berkhout CM., 1923). Since this first description, *Candida* species became well known in microbiology and medicine, particularly due to the fact that candidiasis is a major health concern. Indeed with 9 % of nosocomial bloodstream infections (BSIs), *Candida* species are the fourth most common cause of nosocomial BSIs in the United States (Wisplinghoff *et al*., 2004), at the same time for any *Candida* species the overall mortality rate was 44 % within 30 days of the first positive blood culture in 2005 (Klepser *et al.*, 2006). The main agent of these diseases is commensal yeast, which acts as an opportunistic pathogen: *Candida albicans* (Soll *et al.*, 2002). This yeast lives in the human gastrointestinal tract without harmful effects but can become virulent particularly in immunocompromised persons (AIDS, cancer chemotherapy, organ transplantation). This pathogen presents different forms from oral and vaginal infection to systemic infections, which can be lethal.

*C. albicans* is a yeast-type fungus belonging to the phylum ascomycota of fungi, like baker ´s yeast *Saccharomyces cerevisiae*. *C. albicans* is a diploid and asexual fungus, since no complete sexual cycle had been identified until now. Its genome is constituted of 8 pairs of chromosomes, and the haploid genome has a size of approximately 16 Mbp containing more than 6000 predicted genes. This genome has been sequenced and annotated (www.candidagenome.org; Costanzo *et al.*, 2006). Even if *S. cerevisiae* and *C. albicans* contain a high number of homologous genes with similar biological functions, *C. albicans* has the particularity to be diploid and to have a particular genetic code, since the CUG codon does not encode leucine, like in others organism, but serine (Santos *et al.*, 1995). This finding requires the development of specific genetic tools for *C. albicans* (Berman *et al.*, 2002)

*C. albicans* exists in at least 4 different morphologies: yeast (single round cells proliferating by budding), true hyphae (apically growing, tubular filamentous cells), pseudohyphae (elongated budding cells that remain attached, constrictions at the cell-cell junctions) and chlamydospores (Fig. 1). This last form, specific to *C. albicans* and *C. dubliniensis*, corresponds to large spherical cells with a thick cell wall, which are obtained in microaerobic conditions at 28 °C, on nutrient-poor medium. Their functions are not understood, although they were identified during infections of AIDS patients (Chabasse *et al.*, 1988). Another morphological specificity of *C. albicans* is the occurence of so-called *white* (spherical) and *opaque* (rod-like) yeast cells. Strains homozygous at the mating type locus MTL (a/α) are able to switch frequently between these two forms. *White* cells are the common form for growth and *opaque* cells are necessary for mating of an *MTLa* cell and an *MTLα* cell. After nuclear fusion, cells will revert to normal diploidy by loss of chromosomes, constituting the parasexual cycle of *C. albicans* (Soll *et al.*, 2003). Nevertheless, dimorphism of *C. albicans*, which allows its growth in either yeast or hyphal form, is the prominent characteristic responsible for the high virulence

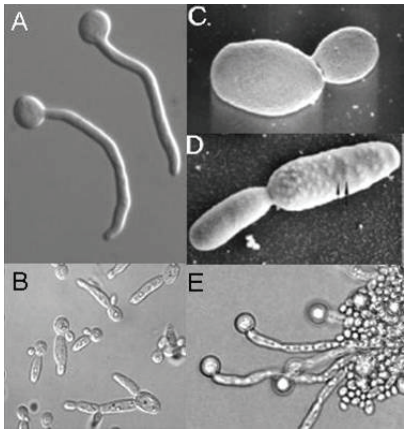


Fig. 1: Morphologies of *C. albican*s. Microscopic appearance of hyphae (A), pseudohyphae (B), *white* (C) and *opaque* yeast cells (D) and chlamydospores (round cells at the tips of filaments (E).

of *C. albicans*. Yeast allows rapid propagation of *C. albicans*, while the hyphae are important for adherence and invasion. Once yeasts have attached to a surface (tissue, plastic), cells can differentiate into hyphae to colonize the surface or invade tissues. Yeasts can then develop into a biofilm consisting of a mixture of yeast and hyphal cells, embedded in an extracellular matrix. These biofilms can grow on different plastic surfaces used during chirurgical operations (catheter, heart valves) and can be the origin of a systemic infection. Moreover, cells present in biofilms are more resistant to drugs than single cells and this makes treatment of candidiasis more difficult (d´Enfert *et al.*, 2006). Hyphae are also the growth form that allows *C. albicans* to escape from phagocytes. Indeed, once *C. albicans* yeast is inside an immune cell, hyphal growth can occur, penetrating the plasma membrane of the phagocytes and releasing *C. albicans* into the environment and at the same time killing the immune cell. *C. albicans* is able to grow in different environments (including skin, gastrointestinal track, plastic, organs), presenting each their own specific features (including different temperatures, pH, $O_2$ and $CO_2$ concentrations). *C. albicans* has the exceptional ability to adapt itself to its environment, which is a crucial reason of its high virulence.

Dimorphism and the ability to grow in different environments require a lot of environmental information to be integrated by cells. All these external cues are received by proteins on the cell surface, called sensors. Many sensors are localised at the cell surface to sense the environment and to activate signalling pathway to respond to the different conditions.

## 1.2 Dimorphism: from yeast to hyphae.

Two main activation pathways for dimorphism have been identified in *C. albicans*: the Cph1p-mediated mitogen-activated protein kinase (MAPK) pathway and the Efg1p-mediated cAMP pathway. These pathways permit the transfer of information from the environment to the nucleus, where genes will be activated by specific transcription factors to establish the program in response to the environment. Different stimuli can induce the switch from yeast to hypha including high temperature (37 °C), serum, N-acetylglucosamine (GlcNAc), starvation, $CO_2$, adherence or neutral pH. All proteins, activators or repressors implicated in yeast to hypha transition, form a complex regulatory network (Biswas *et al.*, 2007).

### 1.2.1 MAPK cascade pathways

MAPK pathways were particularly well described in *S. cerevisiae* and some homologous proteins implicated in similar phosphorylation cascades can be found in *C. albicans*. In yeast five MAPKs were identified (Martin *et al.*, 2005). Fus3p and Kss1p are implicated in response to pheromones and cell wall damage (Wang *et al.*, 2004). Kss1p is also acting in pseudohyphal differentiation of diploid cells and in invasive growth of haploid cells (Roberts *et al.*, 1994); furthermore, it is required to maintain cell integrity during vegetative growth (Lee et al., 1999). Cell wall integrity is also controlled by the MAPK Slt2p (Garcia-Rodrigez *et al.*, 2005). Hog1p (high osmolarity glycerol) plays a role during the response to high osmolarity (Brewster *et al.*, 1993), heat shock (Winkler *et al.*, 2002), oxidative (Singh, 2000) and citric acid stress (Lawrence *et al.*, 2004). Finally, Smk1p is required for spore cell wall morphogenesis (Huang *et al.*, 2005).

Regarding dimorphism, the *C. albicans* pathway that is homologous to the Kss1p-mediated MAPK pathway in *S. cerevisiae* consists of Cst20p (homologue of Ste20p), Hst7p (homologue of Ste7p) and Cek1p (homologue of Fus3p and Kss1p) (Fig. 2). The transcription factor at the end of the pathway is Cph1p (homologue of Ste12p). All null mutants of this pathway lead to a deficit in hypha formation on solid inducing medium (SLAD) but they are

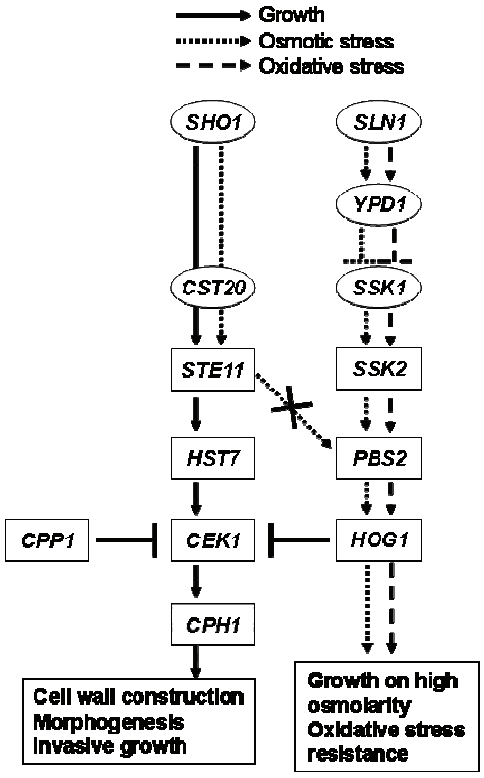


Fig. 2: Interaction of two MAPK pathways in *C. albicans* (according to a model of E. Roman *et al., 2005*). The absence of interaction between Ste11p and Pbs2p is represented by a cross in agreement with the result from Cheetham *et al.*, 2007.

still forming hyhae in response to serum (Csank *et al.*, 1998). Upstream sensors of this pathway are still unknown but it is established that Cdc42p (GTPase), which is required for hypha formation, binds to Ste20p and activates the pathway. A null mutant of *CDC24*, encoding the exchange factor of Cdc42p, is also hypha-deficient (Bassilana, 2003). Activation of the MAPK pathway induces phosphorylation of Cek1p, whose level is controlled by the phosphatase Cpp1p (Csank *et al.*, 1997). A homozygous mutant for this gene is hyper-filamentous, but this phenotype is suppressed in a double mutant *cpp1 cek1* (Csank *et al.*, 1998). A *cek1* mutant presents a deficit in filamentation on inducing solid medium containing mannitol, like Lee- and Spider-medium, but also on low-ammonia-dextrose medium (SLAD). These phenotypes are shared by *cst20*, *hst7* and *cph1* mutants. Downstream of this cascade, the transcription factor Cph1p activates transcription of hypha-specific genes. Indeed a *cph1* mutant strain is defective in hypha differentiation and in hypha-specific gene induction (Liu *et al.*, 1994). Recently, a link between this MAPK pathway and other phosphorylation cascades (Hog1 pathway) was discovered in *C. albicans* (Roman *et al.*, 2005). Cek1p is repressed by the phosphorylated form of Hog1p, which is itself activated by another cascade of kinases (containing Sln1p, Ssk1p, Ssk2p, and Pbs2p) (Fig. 2). Indeed, a *hog1* mutant is hyperfilamentous in serum media (Alonso-Monge *et al.*, 1999)**,** revealing Hog1p-repression on the *CEK1* pathway. Upstream of this pathway, Sho1p, a membrane protein containing 4 transmembrane domains, was identified to activate the Hog-pathway in *C. albicans*. A *sho1* mutant is sensitive to oxidative and osmotic stress, as an *ssk1* mutant. Furthermore, a *sho1 ssk*1 double mutant has the same osmosensitivity as a *hog1* single mutant, placing Ssk1p and Sho1p on 2 different activation pathways for Hog1p. In *C. albicans* Sho1p is partially implicated in the Hog1 pathway but also in the activation of Cek1p (Roman *et al.*, 2005). Fig. 2 shows a model of MAPK pathway regulation with Sho1p on top of the Cek1p MAP kinase cascade. A recent publication (Cheetham *et al.*, 2007) demonstrate that contrary to the precedent model (Fig. 2) only one kinase is responsible for activation of Pbs2p which is Ssk2p. Ste11p was found to have no role in this phenomenon. But these results do not disprove the hypothesis that a protein acting upstream of Ste11p can have a role in Hog1 pathway activation by acting through a compound upstream of Pbs2p.

### 1.2.2 cAMP-PKA pathway

The cAMP-PKA pathway (Fig. 3) was first characterised in *S. cerevisiae* and was shown to lead to pseudohypha formation on solid nitrogen starvation medium (Kronstad *et al.*, 1998). In *C. albicans* a transient increase of the cAMP concentration is related to the yeast-to-hypha transition (Sabie *et al.*, 1992). On top of this cascade, a 6- transmembrane-domain-protein, Gpr1p (G protein-coupled receptor), is associated with a Gα protein, Gpa2p. This interaction was demonstrated by two-hybrid experiments between Gpa2p and the C-terminal

tail of Gpr1p. In *S. cerevisiae* as in *C. albicans*, inactivation of one of these proteins leads to a defect in pseudohypha or, respectively, hypha differentiation, which can be restored by addition of exogenous cAMP. Activators of this pathway are still not completely defined but some experiments show that amino acids and particularly methionine could be possible inducer molecules. Mutants of *CYR1* (adenylate cyclase) and *RAS1* genes also present the same phenotypes as *gpr1* or *gpa2* mutants (defect in hypha formation and lower cAMP levels). Moreover, by a two-hybrid experiment, an interaction was discovered between Ras1p and Cyr1p, supporting their function in the cAMP-PKA pathway (Fang *et al.*, 2006). Ras1p also has a role in MAPK pathway activation due to the fact that the *ras1* hyphal deficit can be complemented by overexpression of components of the MAPK cascade (Leberer *et al.*, 2001). Three other proteins involved in Cyr1p regulation are also present in *C. albicans*: Srv2p (adenylate cyclase-associated protein), Pde1p and Pde2p (low- and high-affinity phosphodiesterases). Like the previous mutants, the *srv2* mutant morphogenesis defect is rescued by addition of cAMP, but the fact that the cAMP concentration is elevated in this mutant suggests a possible negative feedback loop (Bahn *et al.*, 2001). Compared to mutants with lower AMP levels a *pde2* mutant with high cAMP signalling presents different phenotypes: sensitivity to SDS, calcofluor white, amphotericin B, flucytosine, fluconazole (Jung *et al.*, 2005), cadmium ions but also oxidative and osmotic stress (Wilson *et al.*, 2007). An analysis of the cell wall demonstrates a reduction in its thickness and a modification of glucan and ergosterol composition (Jung *et al.*, 2005). *PDE2* inactivation results in a constitutive activation of the PKA pathway, due to an absence of cAMP degradation. But when a *pde2* mutant shows an important decrease of its virulence, strains become avirulent only with inactivation of *PDE1* in the same *pde2* background (Wilson *et al.*, 2007).

The target of cAMP is the protein kinase A (PKA). This conserved class of proteins consists of two catalytic subunits, which are silenced by the association with a homodimer of regulatory subunits (*BCY1*). Increase of internal cAMP levels leads to a binding of cAMP to the regulatory subunits, liberating and activating the catalytic subunit. In *C. albicans* only 2 PKA isoforms were identified as compared to 3 isoforms in *S. cerevisiae*: Tpk1p and Tpk2p. Both act positively on hypha differentiation. A *tpk1* mutant is deficient in hyphae formation on solid media (serum-containing and Spider-medium) but partially affected in liquid media, while for a *tpk2* mutant, the phenotypes are reversed. Exchange of the N-terminal domains between Tpk1p and Tpk2p, in which most differences occur, leads to hybrid Tpk molecules that show phenotypes consistent with the conclusion that the N-terminal domain responsible for agar invasion (Bockmühl *et al.*, 2001). A null *bcy1* mutant is not viable in a wild-type background and analyses of this regulatory subunit of PKA were possible only by analysis of a *bcy1 tpk2* mutant. In this double mutant, PKA activity is constitutive and the strain is delayed during germination on serum- and GlcNAc-containing media. Furthermore, instead of a nuclear localisation, a GFP-Tpk1p fusion is mainly dispersed in the cytoplasm. Therefore, Bcy1p probably has a role in the regulation of PKA enzymatic activity through its ability to differently localise PKA (Cassola *et al.*, 2004).

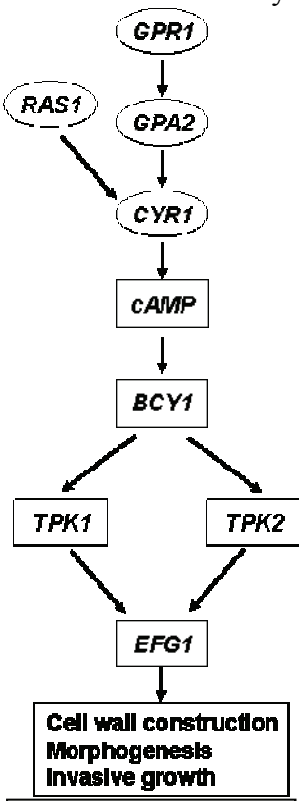


Fig. 3: Model of the cAMP-PKA pathway in *C. albicans* (in normoxic condition).

Downstream of PKA in the cAMP-PKA pathway the transcriptional factor Efg1p is localised. The contribution of Efg1p to this pathway was proven by the fact that an overexpression of *EFG1* can rescue the filamentation defect of a *tpk2* mutant, while the

inverse is not possible (Sonneborn *et al.*, 2000). *EFG1* is required for hypha induction by serum, which requires PKA-activity. An *efg1* mutant has a nearly complete hyphal defect on different induction media. These results indicated that in presence of serum or GlcNAc, Efg1p is a positive factor of hypha formation. However, the same mutant presents an enhanced level of filamentation in hypoxia and in embedded conditions compared to a wild-type strain (Sonneborn *et al.*, 2000 ; Giusani *et al.*, 2002; Setiadi *et al.,* 2006 ), leading to the conclusion that under these conditions Efg1p represses rather than activates hypha differentiation. Efg1p contains a basic helix-loop-helix (bHLH) domain that is highly conserved among members of the APSES family of transcription factors in fungi, which all are involved in fungal morphogenesis (Doedt *et al.*, 2004). As expected for bHLH-type proteins Efg1p was found to bind DNA containing E-boxes (5´-CANNTG-3´) in vitro (Leng *et al.*, 2001), although direct regulation of a gene by Efg1p via an E-box was not yet reported. If the two transcriptional factors of MAPK- and cAMP-PKA- pathways are inactivated (*efg1 cph1* double mutant), the residual hypha formation of an *efg1* mutant is completely abolished (Lo *et al.*, 1997) (although hypoxic hypha formation still does occur). These results demonstrate the importance of these pathways during the yeast-to-hypha transition, particularly during normoxia.

### 1.2.3 Other pathways

A *tec1* mutant is unable to produce hyphae in liquid serum-containing media, while overexpression of this gene can partially complement phenotypes of *cph2* and *efg1* mutants (Schweizer *et al.*, 2000). Tec1p appears to act downstream of these two components.

The pH-response pathway in *C. albicans* is ensured by the transcriptional factor Rim101p, which is activated by proteolysis and regulated by Rim8p and Rim20p. Rim101p is essential for filamentation under alkaline conditions and the expression of alkaline-responsive genes (*PHR1*), while repressing alkaline-repressed genes (e. g. *PHR2*).

*CZF1* encodes a zinc-finger protein known to have a role in hyphal differentiation, when cells are in a surrounding matrix (Brown *et al.*, 1999). Deletion or overexpression of *CZF1* in an *efg1* mutant background does not change the hyperfilamentation of this strain during growth in a matrix. Czf1p is acting upstream of Efg1p and known to inhibit its repressor function, apparently by direct binding to Efg1 (Vinces *et al.*, 2006).

A major transcriptional repressor of the yeast-to-hypha switch identified in *C. albicans* is Tup1p, which is a general repressor affecting numerous genes. In the absence of this protein, pseudohyphae and even true hypha appear on all media tested. A *tup1* deletion also causes a growth-defect at 42 °C and misshapen cell walls. Presence of seven conserved WD40 domains at the C-terminal end of Tup1p suggests that this protein is probably a DNA-binding protein (Braun *et al.*, 1997). It was shown that Tup1p represses several filament-specific genes encoding components that are mostly secreted or cell surface proteins (*HWP1*, *WAP1*, *RBT1*, *RBT5*, *RBT2*, *RBT4* and *RBT7*).

## 1.3 Sensing the environment

Yeasts but also other fungi and bacteria colonise a large range of environments, where conditions are highly variable. Some microorganisms are highly adapted to certain environments, while others like *C. albicans* are able to grow under many variable conditions. This is probably due to a high number of sensors able to transmit information about the environment and activate appropriate response pathways to develop the optimal adaptation to keep cells alive.

### 1.3.1 Pheromones

*S. cerevisiae* produces two pheromones, a-factor by *MATa* cells and α-factor by *MATα* cell. Each cells reacts to the pheromone of the other mating type by remodelling its cytoskeleton to allow cell and nuclear fusion to complete the sexual cycle. Pheromones are sensed by G-protein-coupled receptors (GPCR) in the plasma membrane, Ste2p and Ste3p in *S. cerevisiae* (Versele *et al.*, 2001). Ste2p (receptor of *α* pheromone) is a 431 residue-long protein with 7 transmembrane (TM) domains and a cytoplasmic C-terminal tail of 132 residues Ste3p (receptor of *a* pheromone) contains 470 residues with 7 TM domains and a cytoplasmic C-terminal tail of 182 residues. Once a pheromone binds to the appropriate receptor, it induces a GDP-GTP exchange on the Gα protein Gpa1p. After activation of Gpa1p by GTP, this protein separates from the βγ dimmer consisting of Ste4p and Ste18p. Gpa1p-GTP activates the Ste12p-MAPK pathway and results in cell-cycle arrest and cells fusion. In *C. albicans*, genes involved in both pheromones synthesis were identified: *MFA1* for *a*-factor pheromone (Dignard *et al.*, 2007) and *MFα* for *α*-factor (Bennett *et al.*, 2003). These genes are critical to induce mating if they are express respectively in *MTLa* and *MTLα* cells. It was observed that the homologue of Ste2p in *C. albicans* is required for the morphological response of *a*-cells to *α*-factor (Bennett *et al.*, 2003). Homologues of the two receptors present the same topology than in *S. cerevisiae* but are less characterised in *C. albicans*. Nevertheless, majority of proteins involved in mating in *S. cerevisiae* present ortholog in *C. albicans* like Hst6p, which is essential in both organisms for the export of **a**-pheromone, or protein of the MAPK pathway (Bennett *et al.*, 2005).

### 1.3.2 Glucose

In many environments, the main carbon energy source is glucose and other sugars. All organisms have developed different strategies to incorporate glucose with maximum efficiency. In *S. cerevisiae*, glucose and sucrose are sensed by GPCR of 6 TM domains: Gpr1p, a 961 residue-long protein with a cytoplasmic loop of 345 a.a. This protein can activate the cAMP-PKA pathway through a direct interaction with the Gα protein Gpa2p (Xue *et al.*, 1998). Homologues of these 2 proteins were identified in *C. albicans*. The Gpr1p homologue is a 823 a.a long protein with 7 TM domains and a cytoplasmic loop and C-terminal tails of 151 and 327 a.a., respectively. Surprisingly, it was found that CaGpr1p does not respond to glucose but to methionine (Maidan *et al.*, 2005) and thereby activates the cAMP-PKA pathway to induce the yeast-to-hypha switch.

Another aspect of glucose sensing in *S. cerevisiae* is provided by hexose transporters of the HXT family, consisting of 12 TM domain-proteins: Hxt1-17p, Snf3p and Rgt2p. *HXT*s genes encode different high- or low-affinity hexose transporters. Snf3p and Rgt2p have the same topology as HXT transporters, except that they possess a long cytoplasmic C-terminal tail of 328 a.a and 204 a.a, respectively. These 2 proteins have been named “transceptors”, due to their homology with transporters, as well as receptors (Forsberg *et al.*, 2001). These proteins sense extracellular glucose and regulate *HXT*-expression through Rgt1p regulation. *C. albicans* contains only one homologue for Snf3p and Rgt2p: Hxt4p, a 12 TM domain-protein with a C-terminal cytoplasmic tail of 254 a.a. This protein shares 56 % identity and 73 % similarity with Snf3p and Rgt2p, which is the best match with the 21 hexose transporter orthologs found in the *C. albicans* genome, but the C-terminal tail sequence shows a higher variability. A *hgt4* mutant is less active in filamentation and virulence as compared to the wild-type strain and shows constitutive repression of *HGT7*, *HXT10* and *HGT12*. Contrary to inactivation of glucose transporters, *hgt4* presents a growth deficit on solid media containing fructose or low concentration of mannose or glucose, but also in condition where the

respiratory system is reduced. Furthermore *HGT4* expression is repressed at high concentration of glucose (> 0.1 %). All together these results are in agreement with the hypothesis that Hgt4p is a glucose sensor in *C. albicans* (Brown *et al.*, 2006).

### 1.3.3 N-Acetylglucosamine

Recently, an *N*-acetylglucosamine (GlcNAc) transporter implicated in hypha differentiation has been identified in *C. albicans* (Alvarez *et al.*, 2006). This is Ngt1p, a 509 a.a. protein with 12 TM domains and a cytoplasmic N-terminal tail of 64 a.a. No homologue of this protein has been discovered in *S. cerevisiae*, which is not able to transport and metabolize GlcNAc. A GFP fusion to Ngt1p showed the plasma membrane localisation of this protein in the presence of GlcNAc. Expression of this protein in *S. cerevisiae* allowed GlcNAc uptake. In *C. albicans*, a *ngt1* mutant is defective in hypha formation in standard hypha induction condition (2.5 mM GlcNAc), but mutants can filament in the presence of 100 mM GlcNAc or in the presence of serum. This result suggests that GlcNAc acts as a signalling molecule in the cytoplasm and that Ngt1p acts mainly by allowing entry of the inducer. In this sense, Ngt1p may act mainly as a transporter.

### 1.3.4 Amino acids

Amino acid-sensors were well described in *S. cerevisiae* for the SPS complex consisting of Ssy1p-Ptr3p-Ssy5p. Only Ssy1p (852 a.a.) is a plasma membrane protein with 12 TM domains and a 287 a.a. long cytoplasmic N-terminal tail. Ssy1p is also a transceptor. Ptr3p and Ssy5p are predicted to interact with Ssy1p. If an amino acid binds to Ssy1p, it induces Ssy5p activation, which leads to a proteolytic processing of the two transcription factors Stp1p and Stp2p (Martinez *et al.*, 2005). This allows expression of genes involved in transport and metabolism of amino acids (Andreasson *et al.*, 2006). A homologue of Ssy1p in *C. albicans*, Csy1p, is an 880 a.a. protein predicted to contain 12 TM domains and a 312 a.a. cytoplasmic N-terminal tail. A *csy1* mutant shows a deficit in transcription of amino acid transporters but also an alteration in hyphae formation on solid media (Serum-, Lee-medium), except inducing media that do not contain amino acids, such as Spider- and SLAD-medium). Like in *S. cerevisiae*, Csy1p is linked to gene activation through the proteolytic cleavage of Stp1p and Stp2p. Activated Stp1p migrates to the nucleus and positively regulates expression of genes implicated in the degradation of extracellular proteins (*SAP2*) and uptake of peptides (*OPT1*). Truncated Stp2p induces genes required for amino acid uptake (Martinez *et al.*, 2005).

A second amino acid sensor in *S. cerevisiae* and *C. albicans* is Gap1p (582 a.a.) with 12 TM domains and a N-terminal cytoplasmic tail of 82 a.a. A *gap1* mutant is hypofilamentous in GlcNAc-containing and nitrogen starvation media but not in the presence of serum; consequently, it is avirulent. Interestingly, *GAP1* expression is activated by GlcNAc during the yeast to hypha switch in a Cph1p-dependent manner, but it is not known if this MAPK pathway is used for Gap1p-mediated filamentation (Biswass *et al.*, 2003). Another amino acid sensor responding to methionine is Gpr1p (see above).

### 1.3.5 Ammonium

Mep1p and Mep2p are the two ammonium permeases of *C. albicans* required for growth, when a low concentration of ammonium is the only nitrogen source. Mep2p is a less efficient ammonium transporter compared to Mep1p but it has also a sensor function which is responsible of hypha differentiation under nitrogen starvation conditions (SLAD medium).

Mep2p is another example of a transceptor. Mep2p is a 480 a.a. protein with 11 TM domains and a cytoplasmic C-terminal tail of 74 a.a. Deletion of the C-terminal 57 a.a. of Mep2p do not block ammonium uptake but inhibit filamentation on SLAD medium. A full deletion of the C-terminal tail produces a non-functional protein. This tail is essential for the sensing role of Mep2p but not for the transport function (Biswas *et al.*, 2005). In an *efg1 cph1* double mutant or *ras1* single mutant, a hyperactive form of Mep2p ($Mep2^{\Delta C440}p$) cannot complement the filamentation deficit on SLAD plates of these strains, contrary to what is obtain in an *efg1* or *cph1* single mutant. These results suggest an activation of the MAPK and cAMP-PKA pathways by Mep2p through Ras1p activation.

### 1.3.6 Gases

Fungi like *C. albicans* are able to grow in many environments, including a $CO_2$ concentration of 0.033 % like on a skin surface, to 5-6 % in intestine or blood. $CO_2$ contributes to hyphal differentiation and invasion of the agar. A wild-type strain placed on SD, YPD or serum medium differentiates hypha in the presence of 5 % $CO_2$, while it presents a yeast growth in normoxia. However, while a *ras1* mutant does not show any particular phenotype in comparison to a wild-type strain, a *cyr1* (adenylate cyclase) mutant looses the ability to differentiate hypha and to invade agar in high concentrations of $CO_2$. $CO_2$ induced dimorphism therefore does not appear to be Ras1p- dependant but need the adenylate cyclase and thereby cAMP. It is known in plants and mammalian cells that $CO_2$ can be transported through aquaporin channels. In *C. albicans*, inactivation of the only identified aquaporin Aqy1p does not induce an inability to form hyphae (Klengel *et al.*, 2005). The $CO_2$ effect can be mimicked by bicarbonate, the hydrated form of $CO_2$ which is formed spontaneously in aqueous solutions. But bicarbonate can be formed faster with carbonic anhydrase, which is encoded by *NCE103* in *C. albicans*. Inactivation of this gene results in incapacity of cells to grow in condition where $CO_2$ concentration is lower than 0.5 %. Cyr1p activity increases with the $NaHCO_3$ concentration, suggesting that Cyr1p is a cytoplasmic sensor for $CO_2$.

Low concentrations of $O_2$ can also induce hyphae formation. It is known that microaerophilic conditions are necessary to induce chlamydospore formation (Sonneborn *et al.*, 1999) where Efg1p plays a critical role. This protein is also involved in yeast-to-hyphae regulation in hypoxic conditions (99.9% $N_2$) (Setiadi *et al.*, 2006) and embedded condition (Doedt, 2004). Indeed while a wild-type strain shows moderate hyphae formation in hypoxic conditions, an *efg1* mutant is hyperfilamentous. This suggests that contrary to its positive regulation role in normoxia, in hypoxic condition, Efg1p has a hypha-repressioning function.

### 1.3.7 Thigmotropism and galvanotropism

Thigmotropism is a morphological response to contact or touch stimuli, as in appressorium formation in the rice pathogen *Magnaporthe grisea*, which is induced by contact with the surface of a rice leaf. Galvanotropism is also a change in morphology but due to an electrical field. Recent studies have shown that *C. albicans* answers to these two stimuli (Brand *et al.*, 2007). These responses involve a high-affinity calcium uptake (HACS) system consisting of Mid1p, a 558 a.a. protein with 4 TM domains and Cch1p, a 2254 a.a. protein with 24 TM domains. There is also a low-affinity calcium (LACS) system consisting of Fig1p, a 265 a.a. protein with 4 TM domains. Wild-type cells fixed on a slide and incubated at 37 °C with serum modify their growth axis when they are in contact with a 0.79 μm ridge in 60 % of the cases. Single mutants of the mentioned three genes reorient their growth axis to the ridges less frequently. Regarding galvanotropism, only the *cch1* mutant responds differently than the wild-type to an electrical field. This analysis reveals also that these

phenotypes are $Ca^{2+}$ dependent. The hypothesis is that calcium-transporters are essential to accumulate $Ca^{2+}$ locally and that activation of the calcium pathway at this location induces a growth response.

### 1.3.8 Stress

The above described MAPK pathway (see 1.2.1) is involved in dimorphism but other MAPK pathways are also involved in stress signalling as a response to osmotic and oxidative shock, temperature, UV irradiation and antifungal drugs. In fungi, these stresses are transmitted through the HOG pathway containing the key MAP kinase Hog1p. This pathway was first described in *S. cerevisiae*. It shows that under normal (non-stress) conditions, Sln1p, a sensor histidine kinase, phosphorylates itself leading to constitutive activation but also Ypd1p. This protein transfers its phosphate on Ssk1p. This active form of Ssk1p phosphorylates and thereby inhibits Ssk2p and Ssk22p, which in turn cannot activate Pbs2p and Hog1p. If stress is detected by Sln1p, the phosphorylation cascade does not take place, keeping Ssk2p and Ssk22p active to induce Pbs2p and Hog1p. Phosphorylated Hog1p migrates to the nucleus for activation of transcriptional activators (Hot1p, Msn2p, Msn4p and Skn7p) or a repressor (Sko1p). As described above, Hog1p can be activated not only by Sln1p but also by the Sho1p branch. In *C. albicans*, a third branch involving the plasma membrane protein Msb2p has also been identified for Hog1p activation (see 1.4). Furthermore, in *C. albicans*, Sln1p (1373 a.a with 3 TM domains, a cytoplasmic loop of 134 a.a. and a large extracytoplasmic carboxy terminus), is not the only sensor histidine kinase. Chk1p and Nik1p, two cytoplasmic proteins, are involved in osmosensing, cell-wall biogenesis, morphogenesis, quorum sensing and virulence (Kruppa *et al.*, 2006).

Contrary to what occurs in *Schizosaccharomyces pombe*, where Sty1p, homologue of Hog1p, is the main regulator to different stresses (Chen *et al.*, 2003), in *C. albicans* Hog1p contributes only partially to the regulation of the core transcriptional response to stress (Enjalbert *et al.*, 2006). Core stress was defined in *C. albicans* by genes positively regulated during 3 different stresses: oxidative, osmotic and heavy metal. A list of 24 genes was proposed to constitute this core stress, but this number decreases to 9 in addition of the transcriptional response to heat shock (Enjalbert *et al.*, 2003). Genes constituting the core stress are involved in carbohydrate metabolism, cell wall biogenesis, multidrug resistance, protein folding, redox regulation.

Regulation of stress genes occur also in a *pmt1* mutant as in a wild-type strain in presence of a Pmt inhibitor (Cantero *et al.*, 2007). In parallel, *CEK1* transcription and Cek1p phosphorylation are increased in the same condition while no particular modification was observed for Hog1p. Kss1p, homologue of Cek1p in *C. albicans*, is needed for the *STE* vegetative growth (SVG) pathway when *N*-glycosylation is defective (Lee *et al.*, 1999). And a *cek1* mutant presents a transitory growth deficit in the presence of Pmt inhibitor. This growth deficit is not recovered in a *cna1* mutant (Sanglard *et al.*, 2003), which suggest that calcineurin can rescue cell growth during a protein mannosylation defect.

## 1.4 Msb2p

Msb2p is a 1306 a.a. protein with only 1 TM domain and a large extracytoplasmic N-terminal tail (1184 a.a) and a 97 a.a. long carboxy terminal tails. It was first discovered in 1992 in a search for suppressors of a temperature-sensitive (ts-) *cdc24* mutation in *S. cerevisiae* (Bender *et al.*, 1992). High levels of *MSB2* expression were able to rescue the lethality of a Ts- *cdc24* mutation, which induced alterations in the cytoskeleton. In this study

the *msb2* mutant did not appear to have particular phenotypes: standard growth in all tested temperatures, normal morphology, sporulation and response to pheromone were observed.

The next paper about *MSB2* appeared only 10 years later to show its function in the MAPK pathway (O'Rourke *et al.*, 2002). This time *MSB2* was selected during a screening for new osmosensors. It is known that Hog1p is mainly activated by the Sln1p pathway, but Sho1p of the *KSS1* MAPK pathways is also partially involved in this activation (see 1.2) through Ste11p. In a *hog1* or *pbs2* mutant, it was proven that induction due to high osmolarity (1 M sorbitol) can activate the pheromone pathway, which normally is not activated by this stimulus. Activation of a pathway by a component of another pathway is called cross-talk Sho1p is implicated in this cross-talk, and a defect in Ste11p or Ste50p, which are downstream in the Sho1-pathway, completely blocked any cross-talk in a *hog1* background. The partial cross-talk activity in a *hog1 sho1* mutant suggested the existence of another osmosensor. *FUS1-lacZ* is a reporter construct used to quantify pheromone pathway activation. In a *hog1 sho1* mutant, expression of this fusion is highly deteriorated. Random mutagenesis of this double mutant revealed 2600 strains with a higher reduction of *FUS1-lacZ* expression, but only 56 were still able to mate meaning that mutations in these strains were not localised in the pheromone pathway. From these 56 mutants, only 37 showed an increase of *FUS1-lacZ* activity when Sho1p was reintroduced. Transformation of these mutants with a genomic bank revealed 3 different plasmids that were able to restore *FUS1-lacZ* activity. 2 plasmids contained members of the MAPK pathway: *STE7* and *STE20*, and the last encoded Msb2p. These data show the implication of Msb2p in cross talk.

Inactivation of *MSB2* in a *hog1* background showed almost the same *FUS1-lacZ* activity as a *hog1 sho1* mutant in response to addition of 1 M sorbitol and in a *hog1 sho1 msb2* mutant, *lacZ* activity was highly decreased (O'Rourke *et al.*, 2002). Thus, Sho1p and Msb2p appear to have partially redundant roles in cross-talk in a *hog1* background. Results about cell elongation, which is a response to pheromone, confirmed these results. *hog1 sho1* and *hog1 msb2* double mutants showed a reduction in cell elongation induced by osmotic stress, but strangely the triple mutant did not present any major morphological defects. Then, it was analysed how Msb2p acts in the presence of Hog1p. It was demonstrated that an *ssk1 ste11* mutant is highly osmosensitive (1 M KCl) due to lack of Hog1p activation, while a single mutation does not cause this effect. An *ssk1 msb2* mutant had the same osmosensitivity as an *ssk1* single mutant, whereas an *ssk1 sho1* mutant was clearly more sensitive. An *ssk1 sho1 msb2* triple mutant presented almost the same phenotype as an *ssk1 ste11* strain, suggesting that the contribution of *MSB2* in this phenotype is not predominant. These results were confirmed by a Hog1p phosphorylation study, which showed an absence of phosphorylation of Hog1p in osmotic stress for *ssk1 sho1* and *ssk1 sho1 msb2* mutant but not for *ssk1* and *ssk1 msb2* strains. This led to the conclusion that the signal coming from Msb2p was too weak to have been detected in the Hog1 phosphorylation assay or that Msb2 is acting on osmosensitivity through another mechanism. Thus, Msb2p was proven to be an osmosensor and to act in cross- talk pathway in *S. cerevisiae*.

*MSB2* was discovered a third time during microarray comparisons (Cullen *et al.*, 2004). The authors were interested to find new targets for the MAPK pathway (FG pathway) leading to filamentous growth, which involves Ste11p, Ste20p, Ste7p and Ste12p. For this purpose, they compared two sets of microarrays. The first array experiment was to find targets in a glycosylation mutant (*pmi40-101*), where the FG pathway is activated due to the absence of glycosylation, while mannose suppressed this phenotype. Transcriptomal comparisons were done in the mutant strain with or without mannose in the growth medium. This revealed genes implicated in the FG pathway. The second array experiment was done using the same strain, with or without inactivation of *STE12*. This experiment provided a list of Ste12p-dependent genes. Comparison of these 2 experiments provided a list of *STE12* dependent

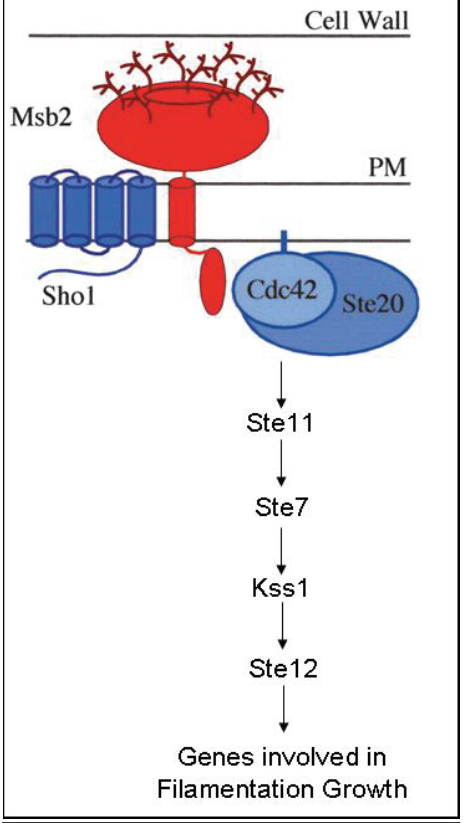


Fig. 4: Model of FG pathway (modified after Cullen *et al.*, 2004) in *S.cerevisiae*. Msb2p and/or Hkr1p (in red) are interacting with Sho1p to transduce the signal to activate the FG pathway. Cross talk with the HOG pathway is not represented.

genes involved in FG pathway. These genes included known components of the FG pathway but 3 new genes were identified including *MSB2*. In parallel, a screen of mutants deficient in agar-invasion revealed that an *msb2* mutant is not able to invade agar. This invasion defect was also observed in a single-cell invasive-growth assay (Cullen *et al.*, 2000) which showed Msb2p importance in unipolar budding and polarized growth. These phenotypes are relevant with mutants implicated in the FG pathway. Expression of *MSB2-lacZ* fusions and biosynthesis of Msb2-HA showed a dependence on Ste12p. Furthermore, two consensus Ste12-binding sites had been identified in the upstream sequence of *MSB2*, suggesting that this gene not only is a target of the FG pathway but that it also implicated in it. The *msb2* phenotype in agar invasion is identical to *sho1* or *ste12* mutants, encoding for proteins of the FG pathway. To definitively prove that Msb2p is involved in the FG pathway, the expression of target genes of this pathway was confirmed in an *msb2* mutant. In conclusion, these data imply Msb2p in the FG pathway of *S. cerevisiae*. A second strong argument was obtained by an experiment regarding the level of phosphorylation of Kss1p in different *msb2* mutants. Indeed an *msb2* mutant showed a defect in Kss1p phosphorylation, while a hyperactive form of Msb2p induced hyperphosphorylation. Kss1p phosphorylation is known to be involved in FG pathway activation. Results are summarized in a model (Fig. 4).

A GFP and HA labelled Msb2p chimera proved the integral-membrane localisation of the protein and its concentration to polarized sites like for Sho1p (Tatebayashi *et al.*, 2007). Protein interactions of Msb2p, probably through their TM domains, were identified with Sho1p by coimmunoprecipitation and with Cdc42p by two-hybrid experiments using only the cytoplasmic tail of Msb2p. Identification of positive and negative regulatory (PRD and NRD) domains in Msb2p revealed that a mucin motif (Ser/Thr/Pro-rich repeat), probably due to its high level of glycosylation (Hollingworth *et al.*, 2004), reduces Msb2p function. A domain between a.a. 100 and a.a. 500 is also involved in regulation of the active form of Msb2p. In mutants lacking these previous regions or mucin domains, expression of FG genes is increased and morphologically strains are hyperfilamentous and bud in a unipolar fashion. These phenotypes are not suppressed by expression of a wild type Msb2p, indicating that these deletions are dominant. In contrast, the region between a.a. 500-1000 is essential for Msb2p function.

A recent publication described new functional domains in Msb2p (Tatebayashi *et al.*, 2007). An Hkr1-Msb2 homology (HMH) domain (a.a. 961-1117) is essential for the cross-talk activity of Msb2p. Without this domain, the Hog pathway can not be activated anymore. An STR (serine threonine rich) domain localised between a.a. 51 and 950 was identified as a repressor of this cross talk. Hkr1p shares 30.3 % of similarity and 18.5 % of identity with Msb2p. It has the same domains and organisation as Msb2p and it is functionally redundant of Msb2p. The fact that hyperactive forms of Hkr1p and Msb2p strongly induced the HOG pathway in a *SHO1*-dependent manner and that hyperactive mutants of Sho1p have the same

phenotype in wild-type as well as in *hkr1* and *msb2* mutant backgrounds prove that Hkr1p and Msb2p are acting upstream of Sho1p. These two proteins could be the actual osmosensors.

In *C. albicans*, research of homologs to ScMsb2p or ScHkr1p by Blast analysis (http://www.candidagenome.org/cgi-bin/nph-blast) gave an identical result. The best match for these 2 proteins is a protein encoded by *orf19.1940* (alias *IPF6003*, *CA1435*) or *CaMSB2*, the second candidate is *orf19.207* predicted to encode Pga55p. *CaMSB2* is a 4230 bp gene predicted to encode a 1410 a.a. protein. The topology of this protein obtain by TMHMM (http://www.cbs.dtu.dk/services/TMHMM/) is a 1 TM protein with a C-terminal cytoplasmic tail of 89 a.a., which is in agreement with ScMsb2p and ScHkr1p topology. CaMsb2p shares 36.1 % of similarity and 21.9 % of identity with ScMsb2p, when these values decrease to 29.5 % and 17.1 % with ScHkr1. CaMsb2p presents a closer homology with ScMsb2p than ScHkr1p. For ScMsb2, ScHkr1p and CaMsb2p their respective STR region contained 49 %, 44% and 43 % of serine or threonine (Fig. 5). Two other motifs were identified between these proteins: an Hkr1-Msb2 Homology (HMH) and the TM domain (Tatebayashi *et al.*, 2007).

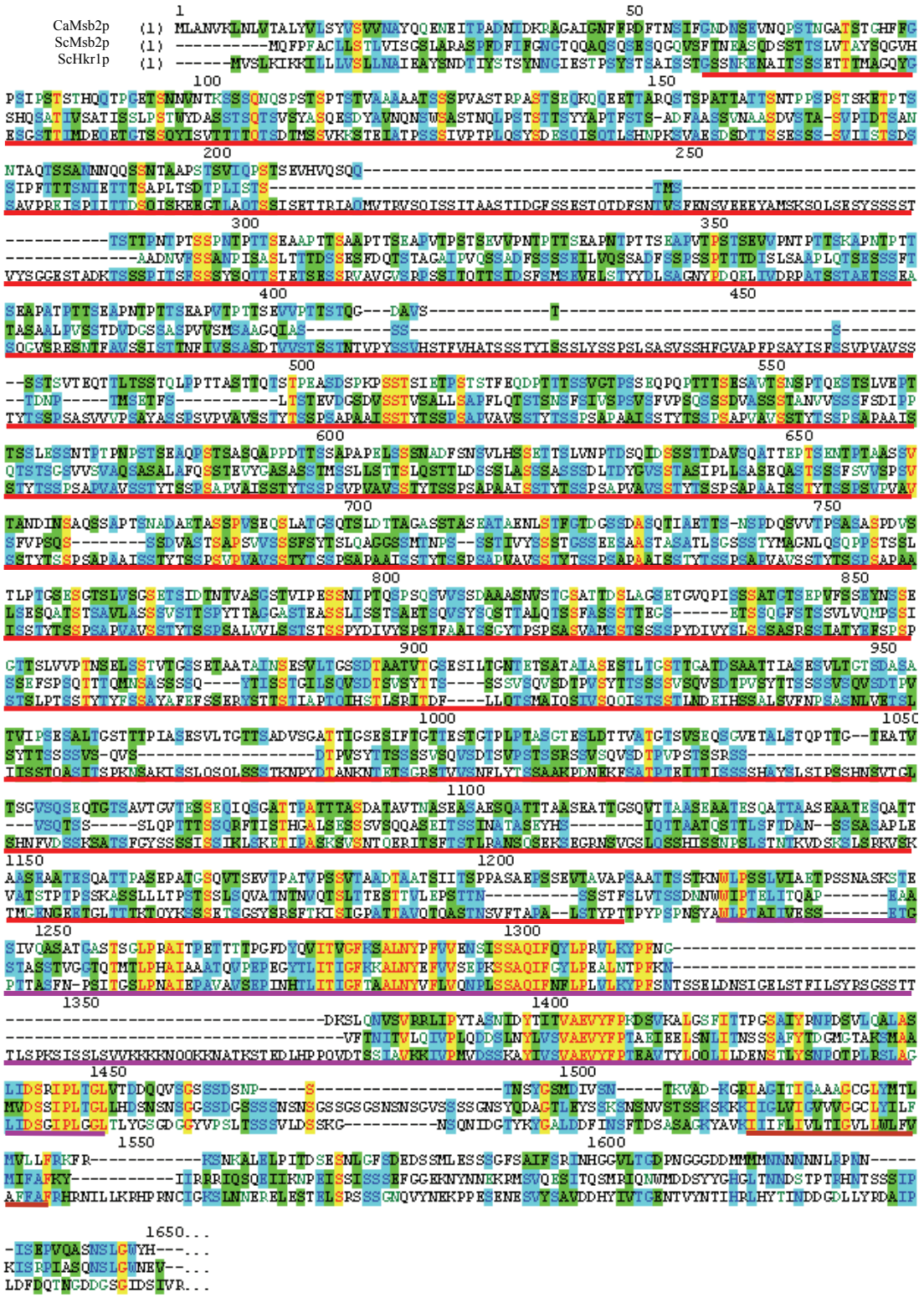


Fig. 5: Alignment of ScMsb2p, ScHkr1p and CaMsb2p protein sequences. Identical a.a. in 3 sequences are written in red with a yellow background, identical a.a. in 2 sequences are written in blue with a cyan background, similar a.a. are written in black with green background. STR, HMH and TM domains are, respectively, deffined by a.a. underline in red, purple and maron.

## 1.5 Aims of this work

This work was mainly focused on the identification and characterisation of a *MSB2* homologue in *C. albicans*. Once this homologue was found, inactivation of both alleles was undertaken in wild-type and other genetic backgrounds. These mutants were tested for any particular morphologies, sensitivities to drugs, chemical compounds or other phenotypes in environmental conditions. The results of all genetic interaction data led to a model of Msb2p function in *C. albicans*.

Research of further, yet unknown sensor proteins in *C. albicans* was started by a bioinformatics approach. Sensors were predicted among membrane proteins of unknown function by using general characteristics of well-known sensors. Thereby, a list of genes predicted to encode putative sensors was produced. After genes were selected and inactivated in a wild-type background, phenotypic analyses of two mutants were performed. Phenotypic characterisations of potential sensor-encoding genes also included previously generated mutant strains deleted for theoretical membrane proteins.

# 2. Material and methods

## 2.1 Chemical products and enzymes

Chemical products and enzymes were obtained from the following companies : Amersham (Braunschweig), B. Braun Biotech International GmbH (Melsungen), Biorad (München), Clontech laboratories (Montain View, Californie), Difco (Michigan), Eurogentech (Seraing, Belgium), Gibco BRL (Eggenstein), ICN Biomedicals INC. (Ohio, USA), IKA® (Staufen, Germany), Kodak (New Haven), Merck AG (Darmstadt), MBI Fermentas (St. Leon Rot), Millipore (Eschborn), New England Biolabs (Schwalbach), Oxoid (Wesel), Pierce (Rockford), Promega (Madison), Qiagen (Hilden), Roche (Mannheim), Roth (Karlsruhe), Sigma (Deisenhofen), Whatman (Maidstone, GB), Zymo research (Orange, Californie)

## 2.2 Strains and media

### 2.2.1 Bacterial strain

Tab. 1: *E. coli* strain used in this work

| Strain | Genotype | Reference |
|---|---|---|
| DH5αF‘ | F‘[Φ80 (Δ*lacZ*) *M15*] Δ(*lacZYA-argF*) *U169 recA1 endA1 hsdR17* $r_k^-$ $m_k^+$ *supE44 thi-1 gyrA relA* | Hanahan, 1983 |

### 2.2.2 Media and growth of *E. coli*

LB: 1 % trypton, 0.5 % yeast extract, 0.5 % NaCl

2 % agar was added to obtain solid medium. Bacterial cells were cultivated at 37 °C. Antibiotic resistance of the plasmid-transformed cells was selected with the following concentrations: ampicillin, 100 µg/ml; kanamycin, 50 µg/ml. *lacZ*-activity was checked by addition of 100 µl IPTG / X-gal to the plates (10 mg X-Gal, 2.4 mg IPTG / ml in DMF).

### 2.2.3 Yeast strains

Tab. 2: *C. albicans* strains used in this work.

| Strain | Genotype | Reference |
|---|---|---|
| SC5314 | prototroph | Fonzi *et al.*, 1993 |
| CAF2-1 | *URA3*/ *ura3*::*imm434* | Fonzi *et al.*, 1993 |
| CAI4 | *ura3*::*imm434*/*ura3*::*imm434* | Fonzi *et al.*, 1993 |
| HLC52 | like CAI4, but *efg1*::*hisG*/*efg1*::*hisG-URA3-hisG* | Lo *et al*., 1997 |
| RM100 | like CAI4, but *his1Δ::hisG/his1Δ::hisG-URA3-his* | Negredo *et al.*, 1997 |
| REP3 | like CAI4, but *his1Δ::hisG/his1Δ::hisG sho1::hisG/sho1::hisG-URA3-hisG* | Roman *et al.*, 2005 |
| REP12 | like CAI4,but *his1Δ::hisG/his1Δ::hisG ssk1::hisG/ssk1::hisG sho1::hisG-URA3-hisG /sho1::hisG* | Roman *et al.*, 2005 |

| | | |
|---|---|---|
| CSSK21 | like CAI4, but *ssk1::hisG/ssk1::hisG-URA3-hisG* | Calera *et al.*, 2000 |
| REP16 | like RM100, but *msb2Δ::FTR/ msb2Δ:: SAT1-FLIP*$^{b}$ | J.Pla |
| REP21 | like REP3, but *msb2Δ::FTR/ msb2Δ::FTR* | J.Pla |
| REP25 | like CSSK21, but *msb2Δ::FTR/ msb2Δ:: SAT1-FLIP*$^{b}$ | J.Pla |
| REP29 | like REP12, but *msb2Δ::FTR/ msb2Δ:: SAT1-FLIP* | J.Pla |
| CK43B-16L | like CAI4, but *cek1*Δ::*his*G/cek1Δ::*His*G | Csank *et al.*, 1998 |
| HLC67 | like CAI4, but *efg1* Δ*::hisG/efg1* Δ*::hisG* | Lo *et al.*, 1997 |
| HLC52 | as CAI4, but *efg1* Δ*::hisG/efg1* Δ*::hisG-URA3-hisG* | Lo *et al.*, 1997 |
| SPCa2 | *pmt1*Δ::*hisG*/*pmt1*Δ::*hisG ura3*Δ::*imm434*/*URA3* | Prill *et al*.,2005 |
| SPCa4 | *pmt2*Δ::*hisG*/*PMT2 ura3*Δ::*imm434/URA3* | Prill *et al*.,2005 |
| SPCa6 | *pmt4*Δ::*hisG*/*pmt4*Δ::*hisG ura3*Δ::*imm434/URA3* | Prill *et al*.,2005 |
| SPCa10 | *pmt5*Δ::*hisG*/*pmt5*Δ::*hisG ura3*Δ::*imm434/URA3* | Prill *et al*.,2005 |
| SPCa8 | *pmt6*Δ::*hisG*/*pmt6*Δ::*hisG ura3*Δ::*imm434/URA3* | Prill *et al*.,2005 |
| NHSF | like CAI4, but *nhs1*Δ::*his*G/*nhs1*Δ::*his*G-*URA3*-h*is*G | Ernst collection n°146 |
| 1HB3G | like CAI4, but *hgt11*Δ::h*is*G/*hgt1*Δ::*his*G-*URA3-his*G | Ernst collection n°185 |
| FCCa1 | like CAI4, but *ipf4949*Δ::*his*G-*URA3-his*G/*IPF4949* | This work |
| FCCa2 | like CAI4, but *ipf4949*Δ::*his*G/*IPF4949* | This work |
| FCCa3 | like CAI4, but *ipf4949*Δ::*his*G/*IPF4949* | This work |
| FCCa4 | like CAI4, but *ipf4949*Δ::*his*G/*ipf4949*Δ::*his*G-*URA3-his*G | This work |
| FCCa5 | like CAI4, but *ipf4949*Δ::*his*G/*ipf4949*Δ::*his*G-*URA3-his*G | This work |
| FCCa6 | like CAI4, but *ipf4949*Δ::*his*G/*ipf4949*Δ::*his*G | This work |
| FCCa7 | like CAI4, but *ipf4949*Δ::*his*G/*ipf4949*Δ::*his*G | This work |
| FCCa8 | like FCCa6, but *ura3*Δ::*λimm434*/*URA3* | This work |
| FCCa9 | like FCCa7, but *ura3*Δ::*λimm434*/*URA3* | This work |
| FCCa10 | like CAI4, but *ipf5005*Δ::*hisG-URA3-hisG*/*IPF5005* | This work |
| FCCa11 | like CAI4, but *ipf5005*Δ::*hisG-URA3-hisG*/*IPF5005* | This work |
| FCCa12 | like CAI4, but *ipf5005*Δ::*hisG*/*IPF5005* | This work |
| FCCa13 | like CAI4, but *ipf5005*Δ::*hisG*/*IPF5005* | This work |
| FCCa14 | like CAI4, but *ipf5005*Δ::*hisG*/ *ipf5005*Δ::*hisG-URA3-hisG* | This work |
| FCCa15 | like CAI4, but *ipf5005*Δ::*hisG*/ *ipf5005*Δ::*hisG-URA3-hisG* | This work |
| FCCa16 | like CAI4, but *ipf5005*Δ::*hisG*/ *ipf5005*Δ::*hisG* | This work |
| FCCa17 | like CAI4, but *ipf5005*Δ::*hisG*/ *ipf5005*Δ::*hisG* | This work |
| FCCa18 | like FCCa16, but *ura3*Δ::*λimm434*/*URA3* | This work |
| FCCa19 | like FCCa17, but *ura3*Δ::*λimm434*/*URA3* | This work |
| FCCa20 | like CAI4, but *ipf5005*Δ::*hisG*/ *ipf5005*Δ::*hisG*-p5005+URA | This work |
| FCCa21 | like FCCa12, but *ura3*Δ::*λimm434*/*URA3* | This work |
| FCCa22 | like CAI4, but *msb2*Δ::*hisG-URA3-hisG*/*MSB2* | This work |
| FCCa23 | like CAI4, but *msb2*Δ::*hisG-URA3-hisG*/*MSB2* | This work |
| FCCa24 | like CAI4, but *msb2*Δ::*hisG*/*MSB2* | This work |
| FCCa25 | like CAI4, but *msb2*Δ::*hisG*/*MSB2* | This work |
| FCCa26 | like CAI4, but *msb2*Δ::*his*G/ *msb2*Δ::*his*G-*URA3-his*G | This work |
| FCCa27 | like CAI4, but *msb2*Δ::*his*G/ *msb2*Δ::*his*G-*URA3-his*G | This work |
| FCCa28 | like CAI4, but *msb2*Δ::*his*G/ *msb2*Δ::*his*G | This work |
| FCCa29 | like CAI4, but *msb2*Δ::*his*G/ *msb2*Δ::*his*G | This work |
| FCCa30 | like FCCa28, but *ura3*Δ::*λimm434*/*URA3* | This work |
| FCCa31 | like FCCa29, but *ura3*Δ::*λimm434*/*URA3* | This work |
| FCCa34 | like CK43B-16L, but *msb2*Δ::*his*G/ *msb2*Δ::*his*G | This work |
| FCCa35 | like FCCa34, but *ura3*Δ::*λimm434*/*URA3* | This work |
| FCCa36 | like FCCa28, but *LEU2*/*LEU2*::p2297UE | This work |
| FCCa37 | like FCCa28, but *LEU2*/*LEU2*::p2297T2 | This work |
| FCCa38 | like FCCa28, but *LEU2*/*LEU2*::p2297T1 | This work |
| FCCa42 | like HLC67, but *msb2*Δ::*his*G/ *msb2*Δ::*his*G | This work |
| FCCa43 | like FCCa43, but *ura3*Δ::*λimm434*/*URA3* | This work |

Tab. 3: *S. cerevisiae* strains used in this work.

| Strain | Genotype | Reference |
|---|---|---|
| PJ69-4A | *MATa trp1-901 leu2-3, 112 ura3-52 his3-200 gal4Δ gal80Δ LYS2::GAL1p-HIS3 GAL2p-ADE met2::GAL7p-lacZ* | James *et al.*, 1996 |
| SY3964 | *MATa leu2-3, 112 ura3-52* | Cullen *et al.*, 2000 |
| SY3969 | *MATa leu2-3, msb2::KanMX6* | Cullen *et al.*, 2004 |
| THY.AP4 | *MAT*a *ura3 leu2 lexA::lacZ::trp1 lexA::HIS3 lexA::ADE2* | Obrdlik *et al.,*2004 |
| THY.AP5 | *MAT*α *URA3 leu2 trp1 his3 loxP::ade2* | Obrdlik *et al.*, 2004 |

### 2.2.4 Media and growth conditions for yeast

YPD : 1 % yeast extract, 2 % pepton, 2 % glucose

SD : 0.67 % YNB (Yeast Nitrogen Base, without amino acid but with ammonium sulfate), 2 % glucose; pH 6.9 adjusted with NaOH.

MM : 0.67 % YNB (Yeast Nitrogen Base, without amino acid but without ammonium sulfate), 2 % glucose; pH 6.9 adjusted with NaOH, amino acid are added 0.48 g/l of arginine, methionine and uracil, 0.72 g/l of tyrosine, lysine, valine and threonine, 1.44 g/l of isoleucine and 1.2 g/l of phenylalanine. Adeine, leucin, tryptophane and histidine can be added with respective concentration of 0.28, 1.44 and 0.48 g/l.

YPM : 1 % yeast extract, 2 % pepton, 2 % mannitol

Lee´s medium : Lee *et al*., 1975

Spider (Liu *et al*., 1994) : 1 % nutrient broth, 1 % mannitol, 0.2 % $K_2HPO_4$

SLADH : Gimeno *et al.*, 1994

F-FOA medium : 0.17 % YNB (Yeast Nitrogen Base, without amino acid but with ammonium sulfate), 0.1 % proline, 2 % glucose, 0.002 % uridin and 0.06 % 5-FOA.

2 % agar was added to these media to obtain solid media. Spider plates contained 1.35 % agar. Yeast cells were cultivated at 30 °C or 37 °C.

### 2.2.5 *C. albicans* hyphal induction in liquid media

Different media were used to induce hyphae formation in *C. albicans*. In all cases the first step was to wash the cells (overnight culture at 30 °C) with water. Induction media were inoculated with a final cells concentration of $OD_{600nm}$= 0.1 or 0.2 and placed at 37 °C. Media used for this purpose were YPD + 10 % or 5 % horse serum, Lee's medium, Spider or YPM. Hyphal differentiation was estimated every 30 min during 2 hours by counting around 200 cells.

### 2.2.6 *C. albicans* hyphal induction on solid media

Hyphae were induced on solid media using the same media as for liquid induction, after addition of agar. Horse serum plates contained water instead of YPD. Hyphal induction was followed at 37 °C during 3 to 7 days.

### 2.2.7 Thigmotropism

From an overnight culture in SD medium at 30 °C, 7.5 µl of this suspension were used to inoculate 10 ml of sterilised water, and then placed on slide containing ridges. Cells had let to adhere during 25 min, before washing carefully the slide. Next, slides were placed in 20 ml of water with 2% glucose and 20% serum. Incubation occurred during 6 h at 37° C. A new washing step of the slide was done before counting. Then, slides were placed in nitric acid 70 % during overnight and washed under a stream of water for 3 h before to be used again.

## 2.3 Plasmids and primers

### 2.3.1 Reference plasmids

Tab. 4: Plasmids used for genetics constructions

| Name | Selection marker/ Replication sequence | Description | Source |
|---|---|---|---|
| pUC18 | $Amp^R$ / no | vector for *E. coli* | Yanisch-Perron *et al*., 1985 |
| pUC19 | $Amp^R$ / no | vector for *E. coli* | Yanisch-Perron *et al*., 1985 |
| pUC21 | $Amp^R$ / no | vector for *E. coli* | Viera und Messing, 1991 |
| pMOS-BLUE | $Amp^R$ / no | vector for *E. coli* | Amersham |
| p5921 | $Amp^R$ / no | vector containing Ura blaster cassette | Ernst collection n° 814 |
| pHB-5 | $Amp^R$ / no | vector for *URA3* complementation | Ernst collection n° 636 |
| pBI-HAHYD | $Amp^R$ CaURA3 CaLEU2/ARS | p*PKC1-EFG1* | Sonneborn *et al.*, 2000 |
| pLJ19 | $Amp^R$ CaURA3/ARS | p*ADH1-CPH1* | Csank *et al.*, 1998 |
| p1367/1 | $Amp^R$ CaURA3 / no | *CaURA3*-Gen in pUC18 | Losberger *et al.*, 1989 |
| pUK21 | $Kan^R$ / no | vector for *E. coli* | Vieira *et al.*, 1991 |
| p2297UE | $Amp^R$ CaLEU2 CaURA3 / no | ACTp + CaEFG1with UTR | Ernst collection n° 2306 |
| p2297T1 | $Amp^R$ CaLEU2 CaURA3 / no | ACTp + CaTPK1 | Ernst collection n° 2311 |
| p2297T2 | $Amp^R$ CaLEU2 CaURA3 / no | ACTp + CaTPK2 | Ernst collection n° 2308 |
| pBM150 | $Amp^R$ *Sc*URA3 / yes | Gal1p promoter for *S.c.* | Phizicky et al., 1986 |
| pGBD-C1 | $Amp^R$ / no | Two-hybrid vector, *TRP1* | James *et al.*, 1996 |
| pGAD-C(x) | $Amp^R$ / no | Two-hybrid vector, *LEU2* | James *et al.*, 1996 |
| pMetYgate | $Amp^R$ / yes | Split ubiquitin vector, *LEU2* | Boles, Centromerplasmid |
| pNXgate | $Amp^R$ / no | Split ubiquitine vector, *TRP1* | Boles, Centromerplasmid |
| pXNgate | $Amp^R$ / no | Split ubiquitine vector, *TRP1* | Boles, Centromerplasmid |

### 2.3.2 Constructed plasmids

Tab. 5: Plasmids contruct in this work

| Name | Selection marker/ Replication sequence | Construction |
|---|---|---|
| pMos-*IPF4949* | $Amp^R$ / no | 2.9 kbp of *IPF4949* integrated in pMOS-BLUE vector |
| p4949.KO.URAb | $Amp^R$ / no | *SnaB*I-*Nsi*I fragment (Ura blaster) of p5921 in pMos-*IPF4949* |
| pMosBlue-5005 | $Amp^R$ / no | 1.7 kbp of *IPF5005* integrated in pMOS-BLUE vector |
| p5005.KO.URAb | $Amp^R$ / no | Ura blaster in pMosBlue-5005 between *Cla*I and *Xmn*I |
| p5005+URA | $Amp^R$ / no | Insertion of *URA3* in pMosBlue-5005 |
| pUK21-6003ns | $Kan^R$ / no | 3.8 kbp of CaMSB2 integrated in pUK21 |
| pUK-6003.Ko.Urab | $Kan^R$ / no | Ura blaster in pMosBlue-5005 between *Kpn*I and *Bam*HI |
| pGBD-6003-C-tail | $Amp^R$ / no | PCR of *MSB2* gene in pGBD-C1, *TRP1* |
| pGAD-CDC42 | $Amp^R$ / no | PCR of *CDC42* gene in pGAD-C1, *LEU2* |
| p2228-MSB2-Cub | $Amp^R$ / yes | PCR of *MSB2* gene in pMetYgate, *LEU2* |
| p2229-SHO1-Nub | $Amp^R$ / no | PCR of *SHO1* gene in pXNgate, *TRP1* |
| p2230-Nub-SHO1 | $Amp^R$ / no | PCR of *SHO1* gene in pNXgate, *TRP1* |
| p2229-MSB2-Nub | $Amp^R$ / no | PCR of *MSB2* gene in pXNgate, *TRP1* |
| p2228-SHO1-Cub | $Amp^R$ / yes | PCR of *SHO1* gene in pMetYgate, *LEU2* |

### 2.3.3 Primers

Tab. 6: Primers used in this work

| Name | Sequence (5’ to 3’) |
|---|---|
| ipf4949-3’p | gcgacattgccgccgacggc |
| ipf4949-5’proche | tgttgcccgacgcctacggc |
| 5005-5´ | ctgaaccattctccagcagc |
| 5005-3´ | aggattcaacagcagtgata |
| IPF6003-NotI | atctagcggccgcgtctattttgatacccacccc |
| IPF6003-SacII | tcagtaccgcggcttgatggctcagctgatgc |
| i-p2-Ura3ver | ttacaatcaaaggtggtcc |
| IPF6003-3verif | ctgctgaaggagcaactgcg |
| HWP1-L1 | tcagcctgatgacaatcctc |
| HWP1-R1 | gtagctggagttgttggcttt |
| IPF16939-L1 | acaacggcaggttctcctat |
| IPF16939-R1 | acatgctaatgatgttgaaccc |
| IPF17558-L1 | aaagcagggtaatgatgcaa |
| IPF17558-R1 | gatgcggtagtaatcacggtt |

| | |
|---|---|
| PRP8-L1 | tatttggccatcacttagcg |
| PRP8-R1 | gcgtcaacgattggatattg |
| ACT1-for RT | caactgggacgatatggaaaaaa |
| ACT1-rev RT | ttcggtcaacaaaactggatgt |
| IPF6003RT-for | agttaccgcagttgctcctt |
| IPF6003RT-ver | ctcgatggtgtctcagcaat |
| 6003-ATG-BglII | cttaagatcttatc*atg*ttggccaacg |
| 6003-Stop-BglII | attagatgtttgaaatggatctaacac |
| 6003-C-term-PstI | ctatactgcagttctctaatgataccaac |
| CDC42-Gal4AD-1 | gagatcgaattccaaactataaaatgtgttg |
| CDC42-Gal4AD-2 | cgaaaaagtgtactattttatagatctatgaat |
| 6003tot-su1 | atggccgctccagcacctgccttggctgctccagccaccaccatgttggccaacgttaaattg |
| 6003tot-su2 | agctgcggttggaacagccaatggggcagctggagcaggatgataccaacccaatgaatt |
| ShoI Cub for | atggccgctccagcacctgccttggctgctccagccaccaccatgggattttcactttca |
| ShoI long Cub rev | agctgcggttggaacagccaatggggcagctggagcaggagtatctaataatttaacata |

### 2.3.4 Plasmid construction

***MSB2***. The first step to inactivate *MSB2* was to create a plasmid containing the URA blaster cassette flanked by *MSB2* sequences. A DNA fragment of 3.8 kb obtained by PCR on genomic DNA (CAF2-1), with primer IPF6003-*Not*I and IPF6003-*Sac*II, was digested by *Not*I and *Sac*II like plasmid pUK21. The fragment of 2.9 kb, issue from pUK21, was ligated to the fragment coming from PCR to form pUK21-6003ns. This plasmid was digested by *Bam*HI and *Kpn*I, like p5921, which contain the URA blaster cassette. Ligation of a 5.3 kb fragment coming from the plasmid pUK21-6003ns and a 4 kb fragment from the p5921 constitute pUK-6003.Ko.Urab.

***IPF4949***. To inactivate this gene, a strategy using the URA blaster cassette is realised. First a 2.9 kb fragment of *IPF4949* gene was amplificated by PCR (primer: ipf4949-3'p and ipf4949-5'proche) on genomic DNA issue from a wild-type strain (CAF2-1) and ligated in pMos-Blue vector (Amersham). This led to the formation of the pMos-*IPF4949* plasmid. Then, the plasmid is digested by *Sna*BI and *Nsi*I like the plasmid p5921 which contains the URA blaster cassette. Fragment of 5.6 kb coming from the plasmid pMos-*IPF4949* and the 4.2 kb fragment containing the Ura blaster were ligated to form plasmid p4949.KO.URAb.

***IPF5005.*** First, *IPF5005* gene was amplified by PCR (1776 bp) with primers 5005-5′ and 5005-3′ on wild-type genomic DNA (CAF2-1), then this fragment was inserted into pMos-Blue vector (Amersham) to obtain pMosBlue-5005. This plasmid was partially digested by *Cla*I and *Xmn*I and p5921, which contain URA blaster sequence, by *Bgl*II and *Pst*I. A DNA fragment of 4.3 kb from pMosBlue-5005 and a 4 kb fragment from plasmid p5921 were purified and their ends were blunt-ended (see 2.6.2). Fragment issue from pMosBlue-5005 is also dephosphorylated (see 2.6.3) to avoid ligation of the plasmid on itself due to the presence of 2 blunt-ends at each end. Ligated together, these fragments constitute p5005.KO.URAb.

pMosBlue-5005 was digested by *Nde*I and *Hin*dIII, and p1367/1 by *Sma*I and *Pst*I, and both fragments were blunt-ended. During ligation, fragment of 1.4 kb coming from p1367/1 containing *URA3* is inserted in front of *IPF5005* homology region to form p5005+URA.

***URA3* complementation**. To integrate a wild-type allele of *URA3* at its own locus, a fragment of 4.3 kb issue from the digestion of pHB-5 by *Xho*I and *Pst*I is required to transform an *ura3* strain.

**2-hybrid**. Identification of protein partner of Msb2p with a classical yeast 2-hybrid occurred by constructing plasmid pGBD-6003-C-tail. For this, DNA encoding C-terminal tail of Msb2p was amplified by primers: 6003-C-term-*Pst*I and 6003-Stop-*Bgl*II. Fragment was digested by *Bgl*II and *Pst*I before ligation with plasmid pGBD-C1 digested with *Bam*HI and *Pst*I. Specific interaction with Cdc42p was obtained with the help of plasmid pGAD-CDC42. A PCR fragment acquired with primers CDC42-Gal4AD-1 and -2 was digested by EcoR*I* and Bgl*II*, like plasmid pGAD-C1. Both fragments were ligated to form the final plasmid.

About split-ubiquitin 2-hybrid, Msb2p was linked to C-terminal part of ubiquitin (CUB) in plasmid p2228-MSB2-Cub. For this, a PCR fragment corresponding to the full length of *MSB2* (primer 6003tot-su1 and 6003tot-su2) was used for a cotransformation in yeast cell with the plasmid pMetYCgate linearised by *Hin*dIII. Plasmid express a chimeric protein with CUB localised at C-terminal tail of Msb2p. Second plasmid pNXgate, to place N-terminal part of ubiquitin (NUB) in C-terminal part of a protein, or pNXgate to place Nub in N-terminal part, were linearised by *Cla*I and cotransformed in yeast cell with PCR fragment corresponding to random genomic sequences. To test a specific interaction, *SHO1* was amplified by PCR using primer: ShoI Cub for and ShoI long Cub rev. Then, these PCR fragments were used to be integrated in plasmid pNXgate and pXNgate by cotransformation in yeast cells. This led to the formation of two chimeric proteins with NUB localised at the N- (p2230-Nub-SHO1) or C-terminal tail (p2229-SHO1-Nub) of Sho1p. Following the same protocol MSB2 sequence was put into pXNgate (p2229-MSB2-Nub) and SHO1 into pMetYCgate (p2228-SHO1-Cub)

## 2.4 Transformation

### 2.4.1 Transformation of E. coli

#### 2.4.1.1 Electrocompetent cells

5 ml of an LB over-night culture of DH5α was used to inoculate 1 L of LB at 37 °C. Once the solution had reached an $OD_{600\ nm}$ between 0.5 and 0.6, it was placed on ice for a few minutes, before being centrifuged at 4000 rpm for 15 min (4 °C). Cells were washed in 1 L of ice-cold $H_2O$ and centrifuged again. After a second washing step the cells were resupended in 20 ml ice-cold 10 % glycerol and centrifuged again. Finally cell pellets were taken in 2 to 3 ml of ice-cold 10 % glycerol and 200 µl aliquots were frozen in liquid nitrogen. Cells were kept at -80 °C.

#### 2.4.1.2 Transformation

40 µl of DH5α electrocompetent frozen cells were thawed on ice and added to 5 µl of ligation mix. The suspension was placed in a special cell for a Biorad Gene pulser, (Gene controller II, Capacitance extender). An electric pulse of 1.4 V (250 µFD, 200 ohms) was

applied to the cells, and then cells were resuspended in 900 µl LB and incubated at 37 °C for 1 h. After centrifugation at 4,000 rpm for 1 min, supernatants were removed and cells were plated on specific selective medium.

### 2.4.2 Transformation of *S. cerevisiae*

Transformations of *S. cerevisiae* with plasmid were done by following the method of Klebe *et al*. (1983), modified by Dohmen *et al*. (1991).

### 2.4.3 Transformation of *C. albicans*

From an overnight culture in YPD, 50 ml of the same medium was inoculated at an $OD_{600\ nm}$ 0.1 and grown to an $OD_{600\ nm}$ of 0.6 at 30 °C; the culture was centrifuged for 5 min at 2,500 rpm and cells were washed in 10 ml $H_2O$, and resuspended in 1 ml of 100mM LiAc in a 1.5 ml-tube. After centrifugation for 1 min at 4,000 rpm, cells were resuspended in 400 to 500 µl LiAc 100 mM. 50 µl of this solution was mixed with 240 µl of PEG (50 % w/v), 36 µl 1 M LiAc, 50 µl SS-DNA (2 mg/ml; previously boiled 10 min at 95 °C) and 0.1 to 10 µg of linearised DNA, in a final volume of 360 µl. After homogenisation, the mixture were placed overnight at 30 °C, then placed at 44 °C for 15 min. Cells were centrifuged for 1 min at 4,000 rpm, resuspended in 200 µl water and plated on selective plates.

## 2.5 Preparation of nucleic acids

### 2.5.1 Extraction of plasmids from *E. coli*

"Mini-preparation" method was used to extract quickly a plasmid from a 5ml over-night culture in LB (Sambrook *et al*., 1989). For a pure plasmid extraction, plasmids were purified from 50 ml LB culture with the help of a column from Qiagen (see protocol: QIAGEN Plasmid Midi kit).

### 2.5.2 Extraction of plasmid from *S. cerevisiae*

Cells were collected from a 5 ml overnight culture by centrifugation (10,000 rpm, 10 min). Pellet was resuspended in 1 ml of QIAGEN P1 buffer containing RNAase, and then 1 ml of P2 buffer and an equivalent volume of 0.8 ml of glass beads were added. Cells were broken by strong agitation on a Vibrax machine (IKA®) 5 min at 4 °C. Suspensions were centrifuged quickly 2 min at 2,000 rpm, and 1 ml of the supernatant was mixed with 0.5 ml of P3 buffer at 4 °C during 10 min. After a 15 min centrifugation step at 10,000 rpm, one volume of isopropanol was added to the supernatant. DNA was precipitated by centrifugation 13,000 rpm for 30 min and washed once with 500 µl of 70 % ethanol. Pellets containing plasmids were resuspended in 20 µl water.

### 2.5.3 Extraction of genomic DNA from *C. albicans*

5 ml of an overnight culture was centrifuged 5 min at 2,500 rpm, and cells were washed once with 5 ml of water. Pellets were resuspended in 400 µl of SCE (1 M sorbitol, 0.1 M Na-citrate, 10 mM EDTA) with 5 mM DTT and 87.5 µg/ml zymolyase (???), then incubated 1 h at 37° C. Cells were collected by centrifugation for 5 min at 4,000 rpm and

resuspended in 500 µl of 50 mM EDTA, 1% SDS and placed at 65 °C for 30 min. Then 200 µl of 5 M KAc (pH 6) was added and the solution incubated 1 h on ice. The supernatant obtained after centrifugation for 15 min at 13,000 rpm/4 °C, was mixed with 900 µl of absolute ethanol. After another centrifugation the pellet was resuspended in 400 µl TE, 60 mM NaAc/pH 5.9, 2 mg/ml RNAase, and incubated 30 min at 37 °C. 400 µl of phenol/chloroform was added to the solution, followed by centrifugation at 13,000 rpm for 2 min. The upper phase was mixed with 800 µl of absolute ethanol and DNA was precipitated overnight at -20 °C. After centrifugation at 13,000 rpm for 15 min the pellet was resupended in 100 µl of TE.

### 2.5.4 Extraction of total RNA from *C. albicans*

Isolation of RNA from *C. albicans* was carried out using a cell culture at $OD_{600}$=0.5, which was centrifuged at 3,500 rpm for 5 min (4 °C). The supernatant was discarded and the pellet was resuspended. Drops of this suspension were frozen in liquid nitrogen. They were stored at -80° C. To break cells, freezing drops were placed in a teflon-vessel with a metal ball (∅ 7 mm) and shaken at 2600 rpm for 2 min in a micro-dismembrator (B. Braun Biotech International GmbH, Melsungen). The powder obtained after this treatment was resuspend in 2 ml Trizol® (Invitrogen) for a 50 ml cell culture or 1 ml for a 14 ml culture and transferred to one or two 1.5 ml tubes. Suspensions were kept 5 min at room temperature to allow dissociation of the nucleoprotein complexes, and centrifuged at 12,000 rpm for 10 min. Supernatants were transferred to a new 1.5 ml tube with addition of 0.4 volumes of chloroform, shaken for 15 sec, kept 10 min at room temperature and centrifuged (5 min, 12,000 rpm). The clear upper phase was transferred to a new tube with 0.5 volume of isopropanol. RNA was precipitated for 15 min at room temperature and harvested by centrifugation (10 min, 12,000 rpm). The RNA pellet was washed by 1 ml of 70 % ethanol and centrifuged identically. The pellet was resuspended in 500 µl of water treated with DEPC (0.1 %); then the RNA was precipitated overnight at -20 °C after addition of 500 µl of LiCl-Buffer (4 M LiCl; 20 mM Tris/HCl pH 7.5; 10 mM EDTA). The RNA-preparation was centrifuged 30 min at 13,000 rpm and the pellet was washed twice with 70 % ethanol. RNA pellets were dried and resuspended in 50 to 100 µl of DEPC-treated water. Incubation at 37 °C for 10 min was used to help the solubilisation of RNA. RNA samples were quantified by spectrophotometry (optical density at 260 nm).

## 2.6 Methods of molecular biology

### 2.6.1 Restriction enzyme

All restriction enzymes were used in agreement with company instructions. Enzymes were provided by NEB or Roche companies.

### 2.6.2 Formation of blunt-ended DNA

To obtain blunt-ended DNA after restriction enzyme digestions, the DNA fragment was incubated in buffer 4 (NEB) with 3 U of Klenow fragment for 3’ overhanging ends. For 5’-overhangs dNTPs were added (0.625 mM final). The reactions were allowed to proceed at 37 °C for 30 min and stopped at 72 °C (15 min).

### 2.6.3 Phosphatase reaction

To avoid ligation of plasmids without inserts a dephosphorylation step was carried out. DNA fragments were incubated in the presence of dephosphorylation buffer and alkaline phosphatase (1.5 U/50µl reaction) (Roche) for 30 to 60 min at 37 °C. DNA fragments were purified on gels to avoid any contamination by alkaline phosphatase.

### 2.6.4. Ligation

Ligations were carried out in a ratio 1/3 (vector/insert), in the presence of the ligation buffer (66 mM Tris-HCl pH 7.6, 5 mM $MgCl_2$, 5 mM DTT, 0.5 mM ATP) and T4 DNA-Ligase (1 U/20 µl final volume). Reactions were allowed to proceed at room temperature for at least 2 h. Salts were removed from the mix before transformation of electro-competent cells. For a mix of 20 µl, 30 µl of distilled water was added, followed by 500 µl of butanol. After mixing the solution was centrifuged at 13,000 rpm for 15 min. Pellets were dried and resuspended in 10 µl of distilled water.

### 2.6.5 Size markers for DNA fragment

To evaluate the size of DNA fragments, restricted DNA of bacteriophage lambda was used for comparison. Lambda DNA (MBI-Fermentas) was digested by *Eco*RI and *Hin*dIII yielding bands of 24756, 21226, 5148, 4973, 4268, 3530, 2027, 1904, 1584, 1375, 947, 831, 564 and 125 bp.

### 2.6.6 Purification of DNA from agarose gels

DNA fragments were isolated and purified from agarose gels after electrophoresis by using the solutions and protocol of the „QiaExII DNA Gel Extraction“-Kits (Qiagen, Hilden).

### 2.6.7 Quantification of nucleic acids by photometry

Nucleic acid concentrations were determined by measuring the absorbance of the solution at 260 nm using the following values: $E_{260}$ = 1 corresponds to 50 µg/ml of double stranded DNA, 40 µg/ml of RNA and 33 µg/ml of single stranded DNA (Müller *et al*., 1993).

### 2.6.8 Southern blot

1.5 µg of genomic DNA was digested by the appropriate restriction enzyme and incubated overnight at the specific temperature in 200 µl total volume. DNA was concentrated to 20 µl after precipitation overnight with 0.1 volume of absolute ethanol/ 2.5 volumes of 4 M LiCl and centrifugation. Samples were placed on an agarose gel (0.8 %) along with a DNA size reference (lambda DNA). The migration occurred in an electric field of 24 V during 12 h.

#### 2.6.8.1 DNA transfer on Nylon membrane

DNA was transferred from the agarose gel to a nylon membrane (Hybond$^{TM}$-N, Amersham). The system contained from bottom to top a permeable screen, a Whatman paper,

an impermeable mask (smaller than the size of the gel) and a nylon membrane (bigger than the size of the gel). Then the gel was placed on the top of nylon membrane. The transfer was allowed to proceed under a vacuum of 40 cm $H_20$. During the initial 5 min a 0.25 M HCl solution was applied on the gel, then this solution was removed and the denaturing buffer (1.5 M NaCl, 0.5 M NaOH) was added for 3 min. It was replaced by the renaturing buffer (3 M NaAc, pH 5.5) for 3 min; then the transfer was carried out with 20x SSC (3 M NaCl, 0.3 M Na-citrate/ pH 7) during 45 min. The nylon membrane was removed from the system and allowed to air-dry before exposure to UV for 3 min to fix DNA on the membrane. Membranes were stored at 4 °C.

#### 2.6.8.2 Labelling of probes

Purified DNA fragments of 0.2 to 2 kb were boiled at 95 °C for 10 min and then placed on ice. 10 ng to 3 µg of DNA were mixed with 2 µl of hexanucleotide mix (Roche), 2 µl dNTP labelling mixture (Roche) and 2 U of Klenow enzyme (Roche), in a final volume of 20 µl. Reactions were placed at 37 °C overnight and stopped by addition of 2 µl EDTA (0.2 M/ pH 8.0). DNA was precipitated by 2 µl of LiCl 4M/50 µl absolute ethanol and exposure to -20° C during 30 min. After 15 min of centrifugation at 13,000 rpm probes were resuspended in 20 µl TE.

#### 2.6.8.3 Staining of blots

After UV fixation the membrane was incubated at 68 °C for 7 h in pre-hybridising buffer (1% blocking solution [Roche]; 5x SSC, 0.02 %SDS, 0.1% lauryl sarcosine). Labelled probes were boiled 10 min and immediately placed on ice, then the probe was incubated at 68° C, overnight, in 5 ml of pre-hybridising buffer with the Nylon membrane; in parallel, a smilarly-prepared bacteriophage lambda-DNA probe was incubated in 2.5 ml of the same buffer with the membrane containing the reference DNA. After the labelling step, the membranes were washed twice for 5 min in NRW1 (2x SSC, 0.1 % SDS), then twice for 15 min in NRW2 (0.1x SSC, 0.1 % SDS) at 68 °C. After 1 min in NRB1 (100 mM maleic acid, 150 mM NaCl, pH 7.6), membranes were blocked in NRB2 (1 % blocking solution [Roche] in NRB1) during 1 h. After one minute in NRB1, membranes were incubated in 20 ml NRB2 with 4 µl of anti-Dig-AP-conjugate (Roche) for 45 min. Then two washes for 15 min in NRB1 and one wash for 2 min in NRB3 (100 mM Tris-HCl, 10 mM NaCl, 50m $MMgCl_2$) was carried out. The colour developed by incubation of membranes in NRB3 with 45 µl NBT (75 mg/ml in 70 % DMF; ICN Biomedicals) and 35 µl X-Phos (50 mg/ml; Roche) in the dark.

### 2.6.9 Polymerase Chain Reaction (PCR)

PCR was used to amplify DNA fragments according to the method of Mullis und Fallona (1987) in a thermocycler (Biometra). Annealing temperatures and elongation times were adjusted depending on the primers used and the size of the DNA fragment to be amplified. PCR fragments were purified by using the „QIAquick PCR-Purification-Kit" from Qiagen.
The "high fidelity polymerase" (Roche) was used to amplify DNA fragments from plasmid or genomic DNA. For amplification with whole cells as sample, the reaction was done with the

Taq polymerase from Eppendorf. To perform colony PCR on *C. albicans* cells, the sample was prepared by inoculating a small amount of colonies in 15 µl 0.02 M NaOH. This solution was treated at 95 °C for 10 min and 1µl was used for the PCR reaction, in a volume of 30 µl.

### 2.6.10 Quantitative real-time RT-PCR (qRT-PCR)

This assay was subdivided in three parts: DNAase-treatment of the RNA, followed by a reverse transcriptase-catalysed reaction and finally the real time-PCR reaction in the presence of SYBR green. All samples and standards were tested in duplicate at the same time, along with a control without reverse transcriptase to verify the absence of DNA contamination.

#### 2.6.10.1 DNAase I treatment

8 µg of RNA (cf. 2.4.4) was incubated with 2 units of DNAase I (Ambion) in the appropriate buffer (10x DNAase buffer: 100 mM Tris pH 7.5; 25 mM $MgCl_2$; 5 mM $CaCl_2$) for 30 min at 37 °C.

#### 2.6.10.2 RNA purification

RNA was purified by using the RNA clean-up kit from (Zymoresearch). 4 volumes of RNA-binding buffer were mixed with the above sample. Then solution was transferred to a column placed on a collection tube and centrifuged at 13,000 rpm for 1 min at room temperature. The column was washed twice with 200 µl of wash buffer. The elution was realised with two additions of 10 µl of RNase-free water to the columns.

#### 2.6.10.3 Reverse transcription

2 µg of RNA was added to 2 µl of oligo(dT) (Ambion) in a final volume of 12 µl of nuclease-free water, and then the solution was heated at 70 °C for 3 min and placed on ice.
For the "No RT"-control, 10 µl of nuclease free water were added to this solution. In the case of the RT reaction, water was replaced by 2 µl of 10x RT buffer, 4 µl dNTP mix, 1 µl RNAase inhibitor and 1 µl reverse transcriptase. Mixtures were incubated at 42 °C for 1 h, then 92 °C for 10 min to inactivate the reverse transcriptase.

#### 2.6.10.4 Polymerase Chain Reaction

For a single reaction, 10 µl of the preceding solution was mixed with 12.5 µl of SYBR green master mix (1.2 ml of SYBR green mix + 5µl ROX), 0.625 µl of forward primer (stock at 20 µM), 0.625 of reverse primer and 1.25 of nuclease free water. The reaction occurred in a final volume of 25 µl, placed in a 96 well-plate, using the Mx3000p Stratagene-system with the following reaction cycle: 10 min at 95 °C, 40 cycles divided in 3 steps (30 seconds at 95 °C, 1 min at 55 °C, 30 seconds at 72 °C), 1 min at 95 °C, 30 seconds at 55 °C and then 30 seconds at 95 °C. Analyses were carried out using the MxPro software from Stratagene. Results are express following the relative transcript level calculation: $e_{ACT1}^{\text{mean Ct } ACT1}$ / $e_{\text{test}}^{\text{mean Ct target}}$ with e, gene's efficiency.

#### 2.6.10.5 Efficiency calculation

Efficiency (e) was estimate by measuring Ct value of 5 dilutions 10 fold diluted between each from a standard RNA solution. Measurements were represented on a log basis graphic. Efficiency is equivalent to 1 + slope value. Primers used for qRT-PCR experiments were: HWP1-L1 and HWP1-R1; IPF16939-L1 and IPF16939-R1; IPF17558-L1 and IPF17558-R1; PRP8-L1 and PRP8-R1; IPF6003RT-for and IPF6003RT-revACT1-for RT and ACT1-rev RT. Estimation of efficiency gave following value: 1.899; 1.96; 1.907; 1.977; 2.11 and 1.986 for respectively *HWP1*, *IPF16939*, *IPF17558*, *PRP8*, *MSB2*, *ACT1*.

### 2.6.11 DNA-microarrays

Two samples of RNA transcripts were compared by DNA-microarray analyses. RNA samples were used to produce cDNA by reverse transcription, thereby producing cDNA labelled by a fluorochrome; one cDNA-sample was labelled with Cy3-, the second one with Cy5-dyes. The two cDNA probes were mixed and hybridized to a DNA-chip (Eurogentech) containing cDNAs-spots in duplicate for almost each gene in the genome of *C. albicans*. After incubation and washing of the chip, results were obtained by scanning the chip at 532 nm (Cy3 excitation) and 640 nm (Cy5 excitation). Signals obtained for each fluorochrome are proportional to the quantity of labelled cDNA, which indicates transcript levels for each gene in the two original RNA samples.

#### 2.6.11.1 cDNA synthesis

RNA used during the reverse transcription was extracted (see 2.4.4) from a 50 ml YPD culture at 37 °C, $OD_{600nm}$=0.5. These cultures were prepared by inoculating YPD medium with an overnight culture of the strain in YPD at 37 °C at $OD_{600nm}$=0.1. Labelling of the cDNA was carried out by incorporating a fluorochrome-modified cytosine (Cy3- or Cy5-dCTP) using the solution described in Table 7. A denaturation step of 5 min at 65 °C was followed by 5 min at 42 °C, to stabilise the RNA-primer complex. 3 µl of RNAsin (Promega) and 3 µl of Superscript II reverse transcriptase (Invitrogen) were added to the mix and incubated 2 h at 42 °C. After 1 h of this incubation, 3 µl of Superscript II RT were added. The reaction was stopped with 15 µl EDTA (50 mM, pH 8.0). 10 µl of NaOH (10 M) were used to degrade RNA at 65 °C during 20 min. Degradation was blocked by addition of 20 µl of acetic acid (5 M). cDNA were purified on columns of the Qia-quick PCR Purification Kit (Qiagen, Hilden) and each sample was split in two portions. In each purification, the elution was carried out in two steps by 50 µl of warm water (42 °C). Eluats were pooled on a Microcon-YM30 column (Millipore) and centrifuged at 13,000 rpm for 14 min. Columns were placed on a new tube up-side down and centrifuged for 1 min at 13,000 rpm. A final volume of 10 µl was obtained.

Tab. 7: Reaction mix for the labelling of cDNA from total RNA

| Product | Volume [µl] |
|---|---|
| 5x concentrated Buffer | 24 |
| *C. albicans* specific primer mix (0.1 pmol/µl) | 3 |

| | |
|---|---|
| AncT mRNA primer (1.5 µg/µl) | 3 |
| Oligo dT18-21 (0.5 µg/µl) | 6 |
| 10 mM dNTP-dCTP | 18 |
| 1 mM dCTP | 3 |
| 1 mM Cy3- or Cy5 dCTP | 4.5 |
| 0.1 M DTT | 12 |
| RNAsin | 3 |
| Total RNA | x µl (30 µg) |
| | $H_2O$ to 120 µl |

### 2.6.11.2 Hybridization and washing of the DNA-microarray.

DNA-microarray slides were provided by the company Eurogentec (Belgium), containing spots of the 6039 PCR fragments representing at least 95 % of each predicted gene encoded in the SC5314 *C. albicans* strain. Each gene was represented twice on the slides. Hybridization between the PCR fragments on the slide and the cDNA-probes was realised under a specific glass cover slip (Erie Scientific Company, USA, Fig. 6). For this purpose, the two labelled probe solutions (10 µl cDNA-Cy3 and 10 µl cDNA-Cy5) were mixed with 10 µl yeast DNA carrier (10 mg/ml, Clontech laboratories) and denaturised at 95 °C for 2 min before cooling on ice. 55 µl of hybridization buffer (Roche) was added to this mix and the solution was inserted in the space between the DNA-microarray slide and the cover-slip. The whole assembly was inserted inside a hybridization chamber (Corning) where previously 10 µl of water were added in the two designated area to keep a constant humidity. Incubation was done at 42 °C for 24 h in a water bath. Then the DNA-microarray slide was washed for 15 min in buffer I (30 mM NaCl, 3 mM citrate, 0.1 % SDS), 10 min in buffer I, 10 min in buffer II (30 mM NaCl, 3 mM citrate) and finally 5 min in buffer II. Slides were dried by centrifuging at 550 rpm for 5 min.

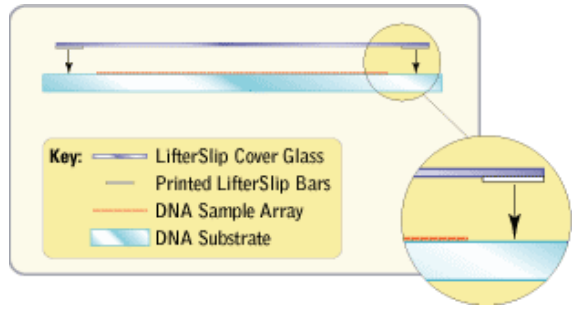


Fig. 6: Schematic representation of the DNA-microarry slide and the cover-slide.

### 2.6.11.3 DNA-microarray scanning

DNA-microarray slide was scanned at a wave length of 532 nm for the Cy 3 signal and at 640 nm for the Cy 5 signal with a Fuji (FLA-8000) scanner. Quantification of each signal was realised with the help of the software AIDA Array Metrix (Raytest).

### 2.6.11.4 Normalization and statistical analysis

The statistical analysis of the raw data was done using the software GeneSpring (Silicon Genetics). For each comparison between two samples (e.g., reference wild-type RNA and mutant RNA), three biological replicates were evaluated. Experimentally, 3 slides corresponding to each replicate were scanned. 2 of the 3 replicates were labelled with Cy3 on

wild-type strain cDNA and one with Cy5, unfortunately no dye-swap was made. Normalisation of all Cy3-/Cy5-ratio were done based on the overall fluorescent intensity, and exported into Excel table. Moreover each gene was twice represented on each slide, which gives 6 signal intensity ratios per genes. To normalise these data, the statistical software SAM (http://www-stat.stanford.edu/~tibs/SAM) was used. In a first step, all ratios were modified in log 2 basis. Then SAM was calculating q-value, which represent the variation amount the 6 value (a low value indicates a low level of variation). To these calculations, a value close to 5% for the predicted minimal false discovery rate (FDR) value was applied for each experiment. Final genes list was obtain by considering only genes regulated with a factor superior to 1.5-fold. Genes with low q-value and a factor of at least 1.5-fold were considered as significantly regulated between the two conditions. A new table with all the normalized values was transfer into GeneSpring for further analysis (cluster analysis, Venn diagram)

## 2.7 Methods of biochemistry

### 2.7.1 Protein analysis

#### 2.7.1.1 Protein extraction

Cells were grown overnight or to a $O.D._{600nm}$ of around 0.8 and harvested by centrifugation at 3500 rpm for 5 min. Cells were washed with 20 ml water and were mixed with 500 µl lyses buffer (50 mM HEPES, 150 mM NaCl, 5 mM EDTA, 1% Triton X-100) and 150 µl glass beads, before breaking them by shaking 2 times for 10 min at 4 °C on a VXR-Vibrax system (IKA®, Germany). After centrifugation for 2 min at 13,000 rpm, 500 µl of the supernatant was placed in a 1.5 ml tube and kept until use at -80 °C.

### 2.7.2 Cell wall composition

#### 2.7.2.1 Isolation of cells walls

Cells were inoculated in 200 ml of SD medium and grown during 20 h at 30 °C. Cells were harvested at an $OD_{600\ nm}$ between 3 and 4 by centrifugation at 3500 rpm for 10 min (4° C). 100 ml of the supernatant was kept at -20 °C for further analysis, the pellet was resuspend in 50 ml of cold PMSF (1mM), and washed 3 times. 3 volumes of glass beads were added to the pellet to break the cells on a vortex (10 to 15 times 1 min per sample). Cells disruptions were checked by microscopy, 90 % of the cells were required to be broken. Glass beads were washed 3 to 4 times by adding 50 ml cold PMSF (1 mM), the supernatant was shacked and collected (clear appearance after last wash). Supernatants were centrifuged at 3,000 rpm for 10 min. Supernatants were kept at -20 °C, while pellets were placed 10 min at 100 °C with 3 volumes of 2 % SDS; then they were centrifuged at 3,000 rpm for 10 min. Supernatants were kept at -20 °C and the pellet was treated the same way as in the preceding step. The pellet was washed with 1 mM PMSF, until the SDS was removed. After the last centrifugation step, the weight of the pellet was measured (wet weight) and resuspend in 1 mM PMSF to adjust the solution at 0.1 g/ml. The solution was kept at -20 °C.

#### 2.7.2.2 Determination of mannoproteins

1 ml of 1 M NaOH was added to 100 mg wet weight of cells walls and incubated 10 min at 100 °C. The solution was centrifuged for 5 min at 12,000 rpm and the supernatant was

transferred to a new tube. Protein determinations were done by the Bradford dye (Bradford, 1976) with a standard curves obtained by BSA measurement from 0 to 15 µg.

#### 2.7.2.3 Determination of chitin

50 mg wet weight of cells walls were lyophilized and transferred with 1 ml 6 N HCl in a sealed glass ampoule, then placed for 17 h at 100 °C. The glass ampoule was opened and placed at 65 °C for evaporation during 2 days. Samples were resuspended in 1 ml of water. To 0.1 ml of this suspension, 0.1 ml of solution A (1.5 N $Na_2CO_3$ in 4 % acetylacetone) was added and incubated for 20 min at 100 °C. Then 0.7 ml of ethanol (96 %) was added and incubated for 1 h at room temperature. Finally 0.1 ml of solution B (1.6 g p-dimethylaminobenzaldehyde in 30 ml of concentrated HCl and 30 ml of ethanol) were added. Once the formation of gas into the solution stopped, samples were placed few minutes at 65 °C until the pellet disappeared. Samples were measured at 520 nm with a standard curve of N-acetylglucosamine (0-200 µg).

#### 2.7.2.4 Determination of mannan

100 mg wet weight of cells walls were treated 1 h at 75 °C with 1 ml of 1 M NaOH, then centrifuged for 5 min at 12,000 rpm. Pellets were kept for glucan determination; 500 µl of Fehling reagent (1 volume of 7 % $CuSO_4$ x 5 $H_20$ and 2 volumes of 3.4 % $C_4H_4KNaO_6$ x 4 $H_2O$ in 10 % NaOH) was added to 500 µl of the supernatant and allowed to precipitate for 45 min at 4 °C, before centrifugation at 12,000 rpm for 5 min. The pellet was resuspended with 0.1 ml 6 N HCl, 0.5 ml water and 2 ml of Fehling reagent. The solution was placed at 4 °C for 2 h and centrifuged for 5 min at 12,000 rpm. The pellet was resuspended in 500 µl of water, 50 µl 6 N HCL and ready to use for carbohydrate determination.

#### 2.7.2.5 Determination of glucan

Pellet obtained previously (2.6.2.4) was treated twice at 75 °C for 1 h with 1M NaOH. The pellet was then washed twice with 1 ml of 100 mM Tris-HCl/pH 7.5 and once with 10 mM Tris-HCl/pH 7.5. The pellet was resuspended in 1 ml 10 mM Tris-HCl/pH 7.5, 1 mg/ml Zymolase 20T and incubated overnight at 37 °C. Insoluble materials were separated by centrifugation (15 min at 13,000 rpm), and 400 µl of supernatant, containing β-1,6-glucan and digested β-1,3-glucan (total glucan fraction), were kept at 4 °C. 600 µl of supernatant were dialysed against water using a dialysis membrane with a size pore membrane of 12-14000 Da, during 2 days with 3 changes of waters. Samples containing β-1,6-glucan were conserved at 4 °C and before carbohydrate determination. Differences between total glucan fraction and purified β-1,6-glucans give concentration of β-1,3-glucans.

#### 2.7.2.6 Carbohydrate determination by the Dubois method

Samples were adjusted to a volume of 2 ml with water. Then 50 µl of 80 % phenol was added, immediately followed by 5 ml of 98 % sulphuric acid. Solutions were carefully mixed and incubated at room temperature for 30 min. Absorbance was measured at 490 nm, and values were compared to a standard curve realised with glucose (0-100 µg). Results were be expressed in µg per 100 mg wet weight or dry weight, or by relative ratios (control strain has value 1).

# 3 Results

Results are divided between two projects: first, the characterisation of a *C. albicans* homologue of the *S. cerevisiae* sensor Msb2p; second, an identification of genes encoding putative sensors in *C. albicans* genome predicted from structures of known sensors and characterisation of four candidates.

## 3.1 *MSB2*

As described in the Introduction (1.4), Msb2p shares some homology of sequence and function with Hkr1p in *S. cerevisiae*. A search for a homologue of these 2 plasma membrane proteins in *C. albicans* led to only one candidate, which is the protein encoded by *orf19.1490*, (alias *CA1345*, *IPF6003* or *MSB2*). The protein of 1410 a.a. presents a predicted topology in agreement with ScMsb2p and ScHkr1p (Fig. 7). Furthermore, Msb2p possesses some characteristic domains of these 2 proteins including a serine-threonine rich region (STR) (a.a. 57 - 1088), an Hkr1-Msb2 homology domain (a.a. 1098 - 1261), one transmembrane domain (a.a. 1298 – 1321) and a relatively short C-terminal tail of 89 a.a. No other domains were identified, but the STR region is reminiscent of certain motifs found in mucin proteins. A mucin domain is highly glycosylated as in ScMsb2p and ScHkr1p. Except mucin, no other protein with identified functions is closely homologous to Msb2p. The mucin family is known to have a role in disease resistance and metastasis development in mammalian cells (Napoletano *et al.*, 2007). In yeast, ScMsb2p and Hkr1p are involved in osmosensing and filamentous growth.

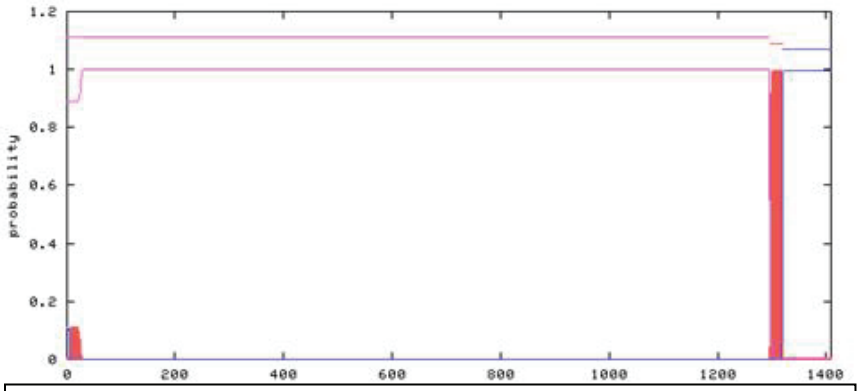


Fig. 7: Predicted topology of Msb2p of *C. albicans*. Best topologic probability is represented on top of the graph. Region turned to the inside of the membrane is in blue, and in purple if turned to the outside of the membrane. Transmembrane (TM) region are drawn as red bars.

### 3.1.1 Gene structure and disruption

The first step to characterize Msb2p in *C. albicans* was the construction of a null mutant. Inactivation of both alleles of *MSB2* was managed by using an Ura blaster cassette (Fonzi *et al.*, 1993). This construction is composed by a 1.3 kb fragment encoding the *URA3* gene flanked by two identical *hisG* sequence of 990 bp from *Salmonella typhimurium*. This cassette has a total size of 4 kb and expresses a functional *URA3* gene. Inactivation had to be done in an auxotrophic strain for uridine (*ura3*) like CAI4 or BWP17 (Wilson *et al.*, 1999). A major advantage of this construct is the possibility to loose *URA3* by homologous recombination between the two *hisG* sequences. Due to this property, both alleles of a gene can be inactivated with the same construct. Towards this aim, plasmid pUK-6003.Ko.Urab was constrcured.

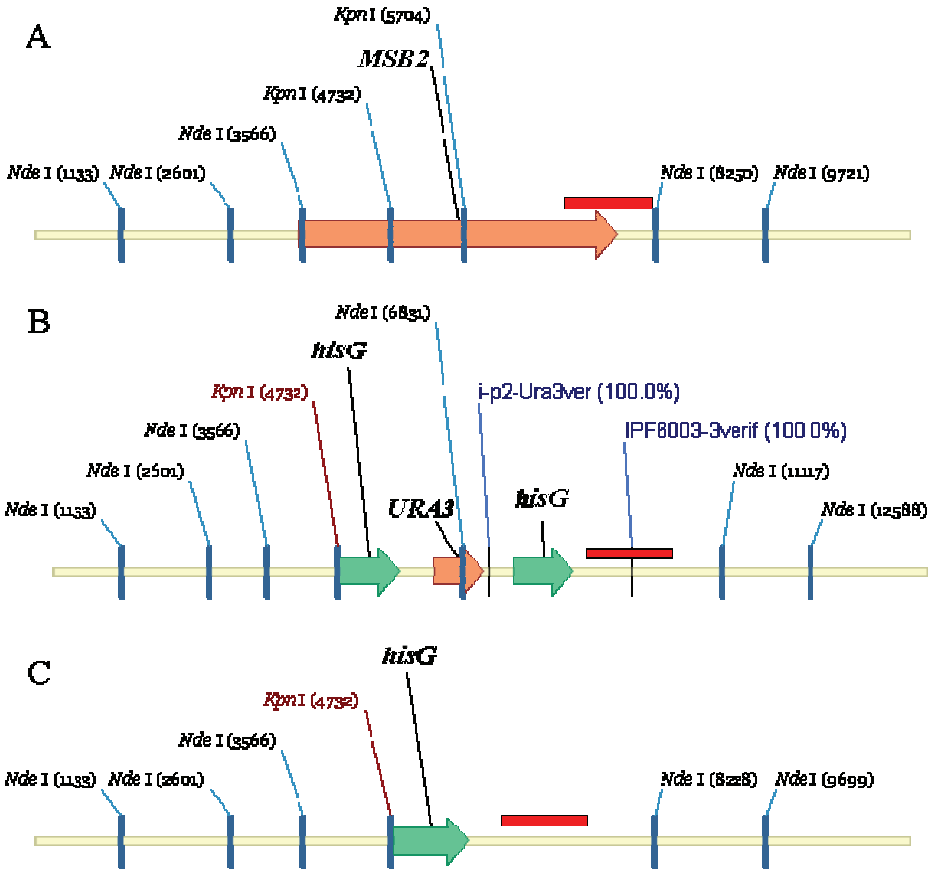


Fig. 8: Scheme of *MSB2* locus during different steps of inactivation. Genome organisation in wild-type strain (A), after replacement of a wild-type allele by URA blaster cassette (B) and after recombination between *his*G sequences (C). The probe used for Southern blot hybridization is indicated by the red box. Scheme obtained by Vector NTI software from Invitrogen.

Digestion of pUK-6003.Ko.Urab by *Not*I and *Sac*II liberated a fragment of 6.6 kb containing the Ura blaster flanked by *MSB2* sequences. This fragment was used to transform strain CAI4. The correct transformant should contain one allele of *MSB2* inactivated by the Ura blaster, which was verified as described below. Correct mutants (FCCa22 and 23) were then plated on agar media containing 5-FOA (5-fluorootic acid), to select for *ura3* mutants. Mutants FCCa24 and 25 indeed contained one disrupted allele of *MSB2* with a single *hisG* repeat. The second allele was removed following the same protocol. Thus, homozygous mutants for *MSB2* and *ura3* were produced (FCCa28 and 29). To obtain a strain that is as close as possible to a wild-type strain, a functional *URA3* gene was reintroduced at its own locus. A 4.3 kb fragment generated by digestion of pHB-5 (Losberger *et al.*, 1989; Prill *et al.*, 2005) with *Xho*I and *Pst*I was used to transform FCCa28 and 29.

Fig. 9: Southern blot of strains at different stages of *MSB2* inactivation. First and last lane are bacteriophage lambda DNA digested, respectively, by *Eco*RI + *Hin*dIII and *Hin*dIII. Sizes are in kb. Tested DNA of strains from second to 9th lane: wild-type (CAF2-1), then FCCa22 to FCCa24 and FCCa28 to FCCa31.

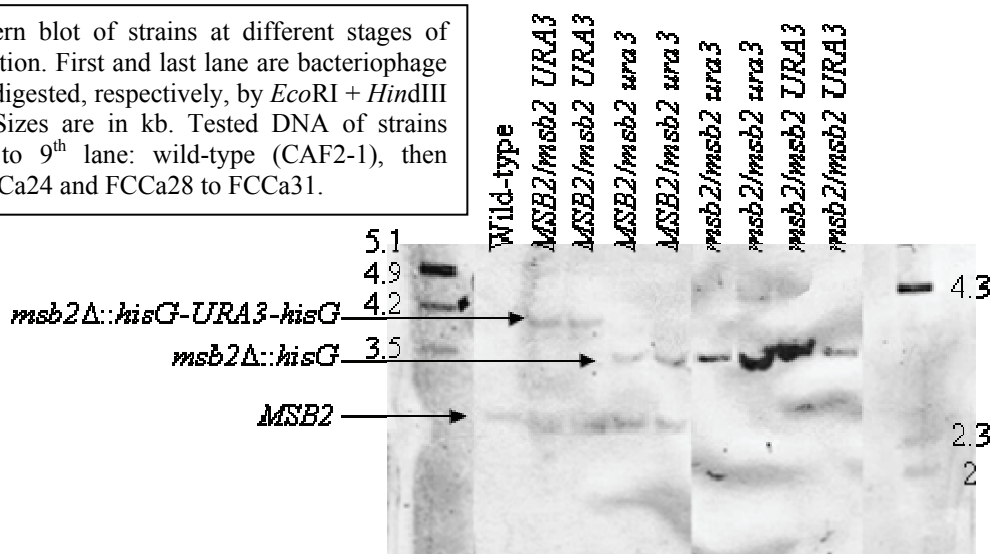

During the process of gene inactivation, the different mutants were checked by PCR to verify if the disruption cassette was located inside the *MSB2* locus (using primers i-p2-Ura3ver and IPF6003-3verif). A band of 2.3 kb was obtained if the construct was introduced correctly. For all strains containing the Ura blaster, an appropriate band was observed (FCCa22, 23, 26 and 27), other mutants, as expected, did not show this band. Southern blots were carried out with DNA of different mutants digested by *Kpn*I and *Nde*I. The organization of the *MSB2* locus in different mutants is shown in Fig. 8. The probe used was a fragment of 779 bp derived from the digestion of pUK21-6003ns by *Bam*HI and *Pst*I. With these conditions, a wild-type allele of *MSB2* produces theoretically a band of 2.5 kb. In Fig. 9, control strain CAF2-1 presents the exact expected band (lane 2). After inactivation of one allele (lanes 3 and 4), alleles were not identical, since introduction of the Ura blaster induced formation of a 4.3 kb band (FCCa22 and 23). Selection on 5-FOA plate led to a recombination between two *hisG* regions and transformed the band at 4.3 kb to 3.5 kb, as observed for FCCa24 and 25 (lanes 5 and 6). Inactivation of the second allele means the replacement of the wild-type band (2.5 kb) by a 4.3 kb band. These homozygous mutants present a band at 3.5 and one at 4.3 kb (FCCa26 and 27). After the loss of *URA3* by 5-FOA selection, both alleles became identical with only one *hisG* repeat at the *MSB2* locus and showed a single band at 3.5 kb (lanes 7 and 8). These *ura3* mutants (FCCa28 and 29) were transformed to introduce a wild-type allele of *URA3* at its wild-type locus, which did not modify the profiles of these strains (lanes 9 and 10). Thus, Southern blots confirmed the exact genomic organisation of all tested strains.

### 3.1.2 Other *msb2* mutant strains

The group of J. Pla (Madrid) constructed in parallel a *MSB2* homozygous mutant in background strain RM100 but used a *SAT1*-flippase cassette (Reuss *et al.*, 2004), which conveys resistance to nourseothricin. Using this cassette, inactivation of *MSB2* was realised in a *sho1* (Roman *et al.*, 2005), *ssk1* (Calera *et al.*, 2000) and *sho1 ssk1* (Roman *et al.*, 2005) mutant background. In collaboration with this group, we characterised the following strains: RM100, *msb2* (REP16), *sho1* (REP3), *ssk1* (CSSK21), *sho1 msb2* (REP21), *ssk1 msb2* (REP25) and *sho1 ssk1 msb2* (REP29). Nomenclature based on inactivated genes, and not strain names, were used for the following strain description.

### 3.1.3 Morphology

First I established that inactivation of *MSB2* does not lead to any growth deficiency. A growth curve in liquid YPD medium was measured for RM100, *sho1*, *msb2*, *sho1 msb2*, *ssk1*, *ssk1 msb2* and *ssk1 sho1 msb2* strains. After inoculation at $OD_{600\ nm}$ 0.1, values were taken during 10 h. During that period all strains have a generation time close to 85 min. Thus, inactivation of these genes did not interfere with cell growth in general.

*Filamentation of msb2 mutant on agar inducing media*

Inactivation of *MSB2* in *S. cerevisiae* leads to defects in filamentous growth and in agar invasion. These mutants were defective in pseudohyphal growth on SLADH (low nitrogen medium) agar to a same degree as a *sho1* mutant (Cullen *et al.*, 2004). For this reason, we wanted to check the influence of Msb2p on morphology in *C. albicans*. Several media are known to induce hypha formation in *C. albicans* but one of the strongest inducing media consists of 5 % of horse serum in water. An *msb2* mutant (FCCa30) on this medium presented the same hypha-forming capacity as the wild-type CAF2-1 (data not shown). Thus, Msb2p appears not to be required for sensing serum signals. No hyphal defects were obtained

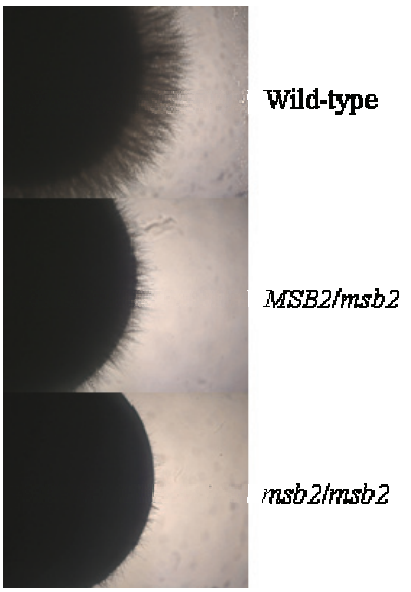


Fig. 10: Hyphal differentiation of strains on YPM-medium at 37 °C. Photographs of wild-type strain CAF2-1, as well as heterozygous (FCCa26) and homozygous (FCCa30) *msb2* mutants were taken after 3 days of growth. Magnification 100x.

on other inducing media including SLADH but also Lee's medium, while on Spider agar an *msb2* mutant presented a hyphal deficit, as compared to the wild-type strain (data not shown). Spider medium contains a concentration of 1 % mannitol and in Lee medium, glucose (2 %) is sometimes replaced by mannitol to stimulate hyphal differentiation (Liu *et al.*, 1994). It is known also that *C. albicans* does not form hyphae on YPD plates even at 37 °C. To explore if Msb2p is required for hyphal growth on mannitol, mutants were plated on YPM agar, which has the same composition as YPD medium except that glucose is replaced by mannitol (2 %). After 3 days of growth at 37 °C, wild-type strains produced hyphae, whereas the heterozygous *msb2* mutant (FCCa26) presented a clear reduction of the number and sizes of hyphae. This phenotype was even stronger in the homozygous mutant (FCCa30). Indeed, in this case only few and short hyphae were observed (Fig. 10). Thus, mannitol is a signal for hyphal induction and Msb2p seems to be required for this input. Removal of mannitol from YPM-medium, or its replacement by glucose, lactose or saccharose did not allow hypha formation. Thus, only mannitol is able to induce hyphae.

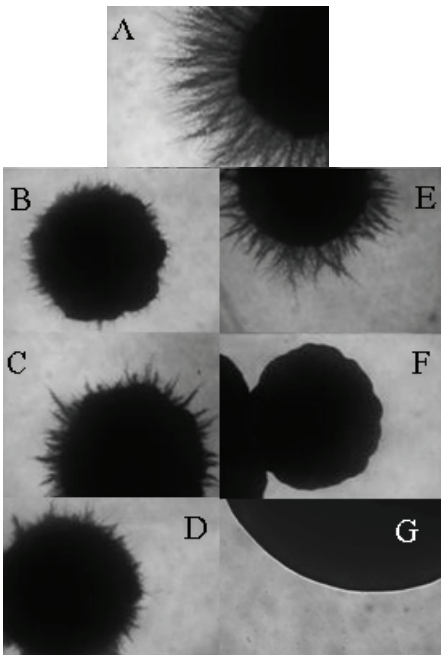


Fig. 11: Hyphal differentiation on YPM-medium at 37 °C. Photographs of RM100 (A), *sho1* (B), *msb2* (C), *sho1 msb2* (D), *ssk1* (E), *ssk1 msb2* (F), *ssk1 sho1 msb2* (G) after 4 days of growth. Magnification 100x

*Filamentation of msb2 double and triple mutants on agar inducing media*

Using the same conditions, mutants obtained from J. Pla were also tested to observe role of Msb2p in *sho1* and *ssk1* background (Fig. 11). After 4 days of growth at 37 °C, a wild-type strain produced abundant long hyphae, while *sho1*, *msb2* and double mutant *sho1 msb2* strains showed a clear decrease in hypha formation. These strains differentiated less and shorter hyphae compared to a wild-type strain. An *ssk1* mutant behaved like a wild-type strain; certain colonies showed even more hyphae than the wild-type strain. The strongest phenotype was obtained for the double mutant *ssk1 msb2*, since, inactivation of *MSB2* in an *ssk1* background led to a complete absence of hyphal differentiation on YPM-medium at 37 °C (Fig. 11 F). A complete absence of filamentation was also observed for the *sho1 ssk1 msb2* triple mutant (Fig. 11 G). Thus, Msb2p is essential for hypha formation on YPM medium in an *ssk1* background.

*Overexpression of genes involved in the PKA pathway*

In *S. cerevisiae*, Msb2p is acting upstream of the filamentous growth (FG) pathway, and activation of downstream elements of this pathway can rescue an *msb2* mutant phenotype (Cullen *et al.*, 2004). Following this hypothesis for *C. albicans*, homozygous *msb2 ura3*

mutant strain FCCa28 was transformed with plasmids over-expressing *EFG1* (p2297UE), *TPK1* (p2297T1) or *TPK2* (p2297T2). These genes are involved in the PKA pathway, inducing the filamentation of *C. albicans* (Stoldt *et al.*, 1997; Sonneborn *et al.*, 2000). *EFG1*, *TPK1* and *TPK2* were expressed under the control of the constitutive *ACT1* promoter. Plasmids were digested with *Bsa*BI in the *LEU2* gene, and linearised plasmids were integrated at the genomic *LEU2* locus by transformation. After 4 days of growth on YPM medium at 37 °C, strains with plasmids overexpressing *EFG1* (FCCa36), *TPK1* (FCCa37) or *TPK2* (FCCa38) gene presented the same hyphal deficiency as the *msb2* mutant (FCCa30). This result suggests that Msb2p acts on hypha formation through a pathway independent of PKA.

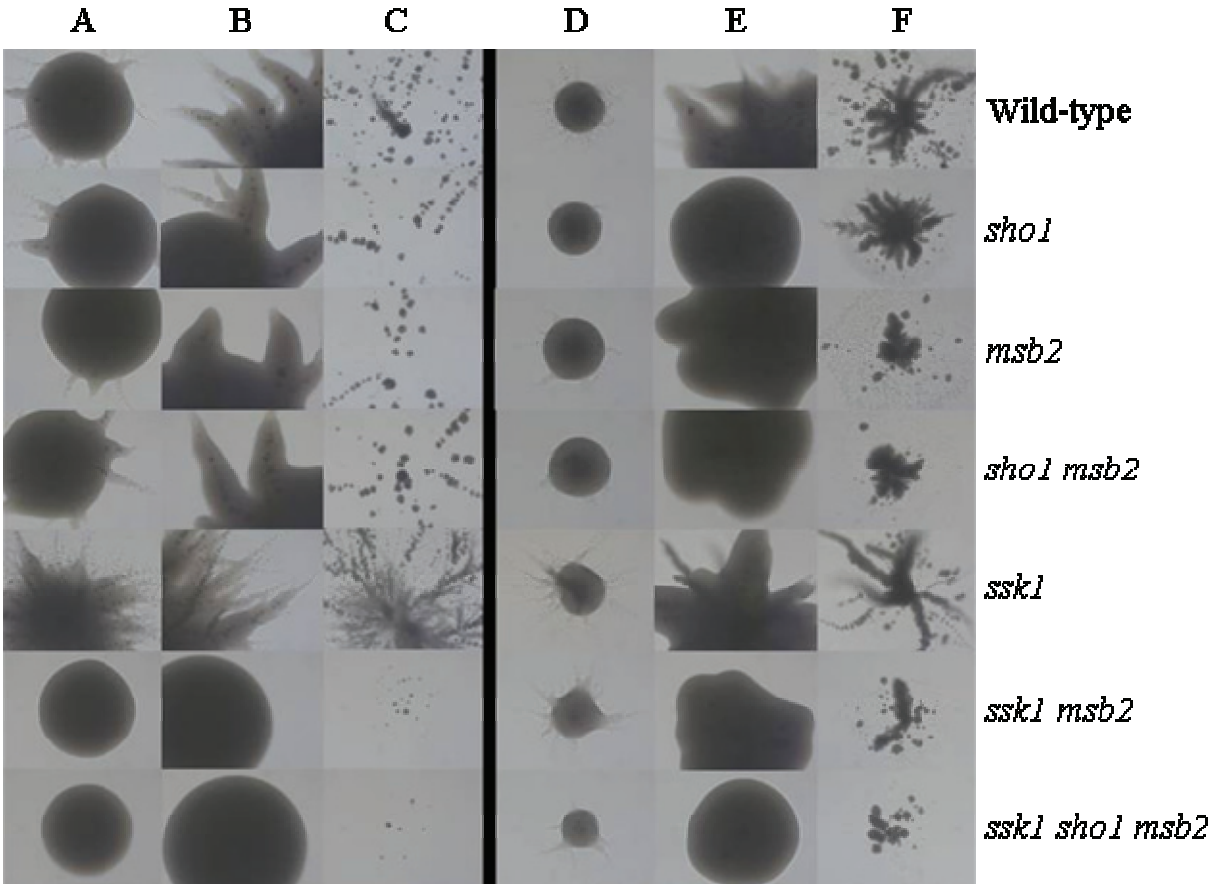


Fig.12: Hypha differentiation in hypoxic conditions on YPS-medium at 30 and 37 °C. Photographs were taken after two (A) or three (B) days of growth at 30 °C, then colonies were washed off by a stream of water (C). Photographs correspond to one (D) or two (E) days of growth at 37 °C before washing (F). Magnification 100x

*msb2 mutant growth in hypoxic condition*

The previous experiments were carried out in normoxic conditions, i.e. air (78 % $N_2$, 20.95 % $O_2$, and 0.038 % $CO_2$). However, *C. albicans* is able to grow not only on skin surfaces, but also in deep tissues and organs, such as kidney and liver, where gas conditions are very different (oxygen is less available and $CO_2$ concentration is increased). Furthermore, Efg1p is known to be an activator of hypha formation in normoxic condition, but has an exact opposite role in hypoxic conditions (i.e. 0.2 % $O_2$, 5 % $CO_2$), where it appears to be a repressor of hypha formation (Setiadi *et al.*, 2006). To estimate if Msb2p is acting in a particular way in hypoxic conditions, mutants were plated on YPS medium (non-inducing medium) and then incubated in a hypoxia workbench to maintain a hypoxic environment (0.2 % $O_2$, 5 % $CO_2$) at 30 or 37 °C during 2 to 3 days. After this period, colonies were washed off

under a stream of water to remove cells on the surface and to reveal the capacity of agar invasion of these mutants (Fig. 12). Strains had the same phenotypes as during normoxia on YPM plates. Indeed, *sho1*, *msb2* single mutants and the *sho1 msb2* double mutant showed a reduction of hypha formation compared to the wild-type strain. This effect was even stronger at 37 °C and not only for the cells on the surface but also for their ability to invade agar. In contrast to normoxia, the *ssk1* mutant showed hyperfilamentation and increased agar invasion in hypoxic conditions particularly at 30 °C compared to the wild-type strain. However, as during normoxia on YPM-medium, inactivation of *MSB2* in an *ssk1* background led to a complete absence of hyphae in hypoxic conditions at 30 °C. An *ssk1 msb2* strain, like the *ssk1 sho1 msb2* triple mutant was not able to produce surface hyphae and was severely defective to invade agar. At 37 °C, after one day of growth, some hyphae were observed and agar invasion occurred after two days, although these two mutants were highly affected in hypha formation compared to the wild-type strain. Interestingly, while *sho1* and *msb2* mutants presented each a slight reduction in hypha formation, inactivation of both genes in a wild-type as well as in an *ssk1* background strain did not lead to a stronger phenotype than a single *msb2* mutation. It appears that in an *msb2* background, *SHO1* is not critical for hypha formation, but *MSB2* plays an important role in hyphal formation during hypoxic conditions in an *ssk1* mutant background, as it was already observed in normoxic conditions.

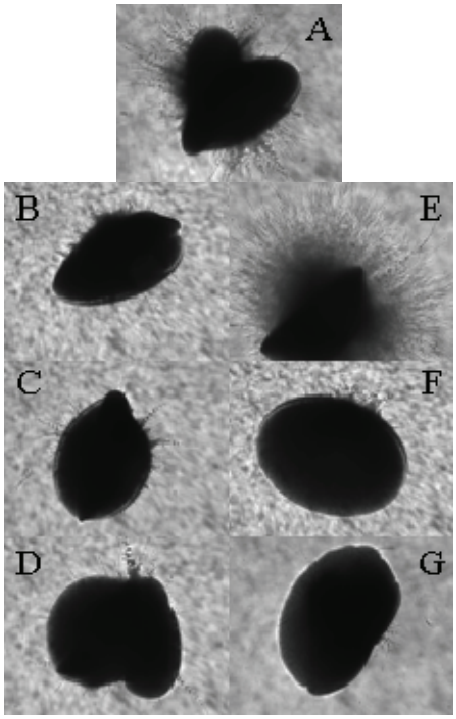


Fig. 13: Hypha differentiation in agar-embedded conditions at 30 °C. Photographs of RM100 (A), *sho1* (B), *msb2* (C), *sho1 msb2* (D), *ssk1* (E), *ssk1 msb2* (F), *ssk1 sho1 msb2* (G) were taken after two days of growth at 30 °C. Magnification 100x

*msb2 mutant growth in agar-embedded condition*

Hypha formation of *C. albicans* has also been studied during agar-embedding (Brown *et al.*, 1999). In this model system, cells are trapped in YPS agar without contact with external air, simulating the conditions of yeast cells embedded in a tissue. For this experiment, cells were mixed with liquid YPS agar (saccharose replacing glucose in YPD medium), and plated between two layers of YPS agar. After 2 days of growth at 30 °C, a wild-type strain produced some hyphae (Fig. 13). Like for the previous conditions, *sho1*, *msb2* single mutants and *sho1 msb2* double mutant strains had a strong deficiency in hypha formation compared to the wild-type. An *ssk1* mutant behaved as during hypoxia showing hyperfilamentation. Inactivation of *MSB2* in this background also led to a decrease in hypha formation. However, compared to hypoxic conditions at 30 °C, where strains where unable to produce hyphae, in embedded condition these mutants were able to differentiate short hyphae. It is important to remember that on YPS agar in normoxic conditions, no hypha were differentiated after 3 days even by the wild-type strain.

Collectively, these results implicate Msb2p in hypha formation in different conditions in contact with agar.

*Liquid induction media*

In its natural environment *C. albicans* is mostly found attached to a surface and less frequently growing in a suspension. Nevertheless, because *C. albicans* can be isolated from blood cultures, it is interesting to explore how mutants react to hyphal induction in liquid. One

of the strongest media to induce hyphae in liquid is 5 % horse serum in YPD at 37 °C. By inoculation at $OD_{600\ nm}$ = 0.2 of this medium by an overnight culture in YPD, it is possible to count numbers of yeast cells differentiating hyphae during a 2 h time period (Fig. 14). All strains previously tested in agar media presented the same ability to produce hyphae in YPD with 5 % serum. At all time points (30, 60, 90 and 120 min), strains showed no significant difference to control strains RM100 and CAF2-1. This result is in agreement with morphogenesis on agar plates with serum, where all strains were behaving as the wild-type strain. Interestingly, when liquid induction was done in YPM liquid, wild-type but also *sho1*, *msb2* single mutant and *sho1 msb2* double mutant strains were identical in hypha formation (around 80 %), while inactivation of *SSK1* induced a reduction of hyphal differentiation. Indeed, mutants *ssk1*, *ssk1 msb2* and *ssk1 sho1 msb2* presented the same profile with only 55 % of yeast cells forming hyphae. Contrary to the situation in YPM agar, inactivation of *MSB2*, even in an *ssk1* background did not induce any particular phenotype. Thus, Msb2p function in morphology seems to be dependent on mannitol and on agar contact.

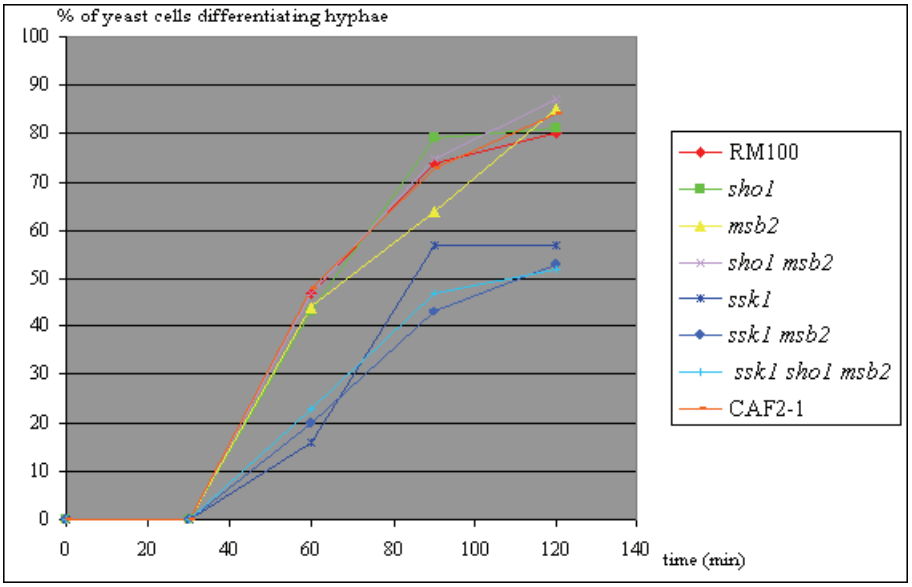


Fig. 14: Hyphal induction in YPM liquid medium at 37 °C. At the indicated times the percentage of yeast cells differentiating hyphae were determined microscopically for control strains RM100 and CAF2-1 and other mutants.

*Thigmotropism*

Morphological responses to a surface or a contact stimulus are called thigmotropism. Recently, this phenomenon well described in fungi like *M. grisea* (Liu *et al.*, 2007) was also discovered in *C. albicans* (Brand *et al.*, 2007). This work showed that in a wild-type strain, when hyphae got in contact with a ridge of 0.79 µm, it induced a reorientation of the hyphal growth axis with a frequency of 60 %, while mutants affected in calcium uptake mainly passed through ridges. To test this phenotype in the above set of mutants, cells were allowed to adhere to glass slide with ridges, and where then placed in a solution with glucose and horse serum during 6 h for hyphal induction. Then each contact between hyphae and ridges were monitored microscopically and categorised in two groups depending on modification or not of the growth axis. For all strains previously tested on agar or in liquid induction media, the response to contact stimuli was the same as for reference strains RM100 and CAF2-1, i.e. around 60 % of hyphae reoriented their growth axis. Thus, Msb2p seems to not be involved in thigmotropism.

*Chlamydospore formation*

A relatively specific and conserved morphological capacity of *C. albicans* is its ability to produce chlamydospores, which are thick-walled enlarged cells. They are assumed to be structures to allow surviving in unfavourable conditions (Cochrane, 1974). Chlamydospore

formation can be induced under nutrient-poor oxygen-limited (microaerophilic) conditions at low temperatures (25 °C). Cells were plated on corn meal agar and a cover-slide was placed on them to assure a microaerophilic environment at room temperature (Nobile *et al.*, 2003). After 15 days, chlamydospores started to appear on hyphae for wild-type (RM100), *sho1*, *msb2* and *sho1 msb2* mutant, while inactivation of *ssk1* led to an absence of them (Fig. 15). However, observations were different between single, double or triple *ssk1* mutants. While, a single *ssk1* mutant produced long hyphae, as it was already observed in hypoxic conditions, it did not form chlamydospores. *ssk1 msb2* and *ssk1 sho1 msb2* mutants, as reported above, did not form hyphae under conditions used for chlamydospore formation. Because chlamydospores are formed on pseudohyphal or hyphal suspensor cells, this defect in filamentation may be the reason of chlamydospore deficiency of these strains. Taken together, Msb2p is not required for chlamydospore formation.

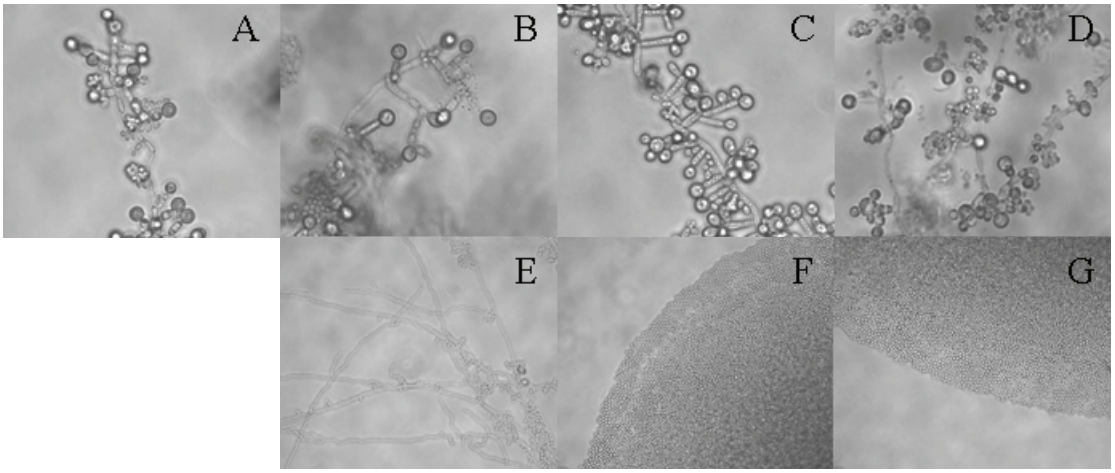


Fig. 15: Chlamydospore induction on corn meal agar. Photographs were taken after 15 days of growth at room temperature in darkness for RM100 (A), *sho1* (B), *msb2* (C), *sho1 msb2* (D), *ssk1* (E), *ssk1 msb2* (F), *ssk1 sho1 msb2* (G). Photographs A to D represent an enlarged detail of the original photograph. Magnification 400x

### 3.1.4 Resistance

Msb2p is clearly involved in morphogenesis on agar induction media in normoxic and hypoxic conditions. We next characterised sensitivities of the *msb2* mutant to different conditions.

*Glycosylation inhibitors*

In *S. cerevisiae*, sensitivities of *msb2* mutants were not established but it was demonstrated that Msb2p is glycosylated (Cullen *et al.*, 2004). Because an anti-Msb2p antibody or a tagged version of Msb2p in *C. albicans* was not available, we could not verify the glycosylation status of Msb2p. However, it was possible to study the impact of *O*- and *N*-glycosylation inhibitors on *msb2* mutant growth (Fig. 16). Mutants were spotted on YPD plates containing an *O*-glycosylation inhibitor (OGT2468 JNG5-24 from Oxford Glycosciences) at a concentration of 2 µM or an *N*-glycosylation inhibitor tunicamycin at 2 µg/ml and placed at 30 °C. All strains grew with the same efficiency as the wild-type strain on plates with or without *O*-glycosylation inhibitor. However, in presence of tunicamycin (Fig. 16 B), all strains including the wild-type were growing slower, except the *sho1* mutant that did not show a growth deficiency. Inactivation of *MSB2* in a *sho1* background led to a higher sensitivity to tunicamycin. It was concluded that Msb2p is not a target of *O*-glycosylation

inhibitor but the resistance of a *sho1* mutant to tunicamycin appears to depend partially on the presence of Msb2p.

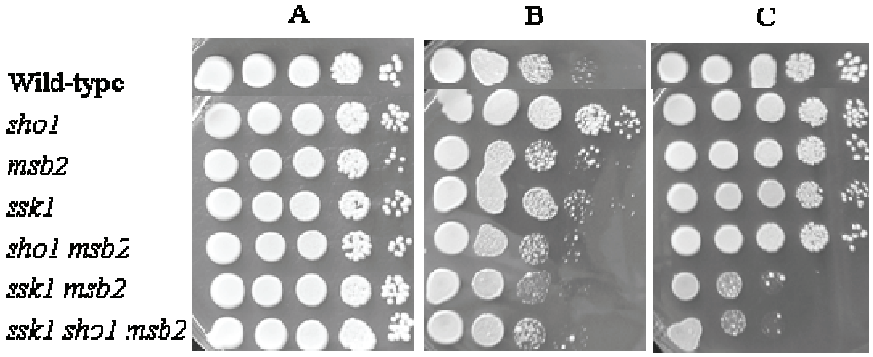


Fig. 16: Sensitivity to tunicamycin and osmotic stress. A series of dilution was spotted on plates. All mutants are represented, on plate, by 5 dilutions corresponding to $10^5$, $10^4$, $10^3$, 100 and 10 cells coming from an overnight culture. Photographs after 2 days of growth at 30 °C on YPD (A) with tunicamycin 2 µg/ml (B) or 0.5 M NaCl (C).

*Antifungal drugs*

Next, I tested the sensitivity of mutants to antifungal drugs. On YPD plates complemented with 200 µg/ml of hygromycin B all mutants grew like the control strain RM100. To test susceptibility to azoles, I used fluconazole, ketoconazole and clotrimazole on YPD agar at 30 °C with respective concentrations of 4 µg/ml, 4 µg/ml and 2 µg/ml. Results for fluconazole (Fig. 17 B) and ketoconazole (Fig. 17 C) were similar for *sho1* and *msb2* single mutants, which had the same sensitivity as the wild-type strain. Inactivation of *MSB2* in a *sho1* background led to a slight increase of the sensitivity. This was also observed in an *ssk1* background, were inactivation of *MSB2* induce a higher sensitivity compared to a single *ssk1* mutant. But it is important to consider that an *ssk1* mutant was more resistant to these two azoles than the wild-type strain. Opposite results were obtained for clotrimazole (Fig. 17 D), to which *ssk1* and *ssk1 msb2* mutants were slightly more sensitive than all other mutants. Thus, *MSB2* has a role in resistance to some but not all azoles (fluconazole and ketoconazole) not in a wild-type background but in an *ssk1* or *sho1* mutant.

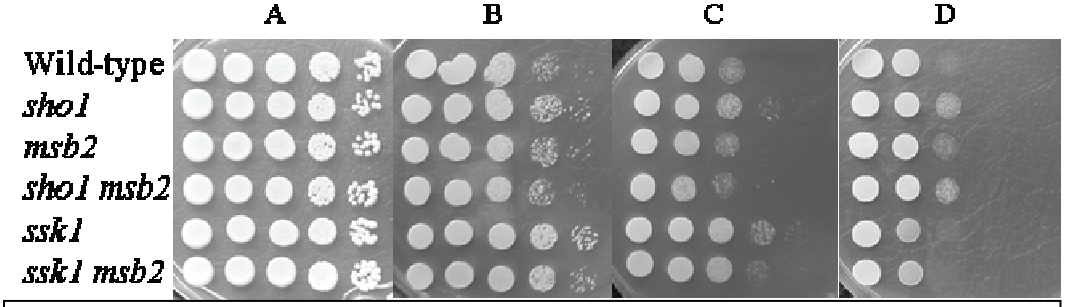


Fig. 17: Sensitivity to azoles. Photographs taken after 2 days of growth at 30 °C on YPD (A) with fluconazole (4 µg/ml) (B), ketoconazole (4 µg/ml) (C) or clotrimazole (2µg/ml) (D).

*Osmotic, oxidative and temperature stresses*

*C. albicans* faces three major stresses in its different environments: osmotic, oxidative and temperature stresses. Sensitivity to oxidative stress was observed by spotting mutants on YPD plates containing 5 mM $H_2O_2$, at 30 °C. After 2 days of growth, all mutants showed the same sensitivity as the wild-type. Thus, Msb2p is probably not involved in oxidative stress response. To test sensitivity to temperature, cells were spotted on YPD and SD, and then placed at 16, 30, 37 and 42 °C or at 30 °C after a treatment at 55 °C during 7 min. In these

conditions, all strain grew at all temperature from 16 to 42 °C with the same efficiency as the wild-type. However, a heat shock at 55 °C presented growth sensitivity of the *msb2* mutant (Fig. 18 E), while the double mutant *sho1 msb2* showed a synthetic effect of both mutations, i.e. a strong sensitivity to heat shock. Interestingly *ssk1* and *ssk1 msb2* mutant presented a high sensitivity to heat shock, but inactivation of *SHO1* in an *ssk1 msb2* mutant induced a higher resistance than single and double *ssk1* mutants.

To determine sensitivities to osmotic stress, cells were spotted on YPD agar containing 0.5 M NaCl (Fig. 16 C). Interestingly *sho1*, *msb2*, *ssk1* and *sho1 msb2* mutants were not sensitive to this stress, but inactivation of *MSB2* in *ssk1* background induced a strong sensitivity. Triple *ssk1 sho1 msb2* mutant presented the same phenotype as *ssk1 msb2* double mutants. These observations are also obtained for stronger osmotic stress (1.5 M NaCl). These results again demonstrate the important function of Msb2p in an *ssk1* background. Msb2p is implicated in resistance to osmotic and heat shock stresses but not to oxidative stress in *C. albicans*.

*Cell wall perturbation*

The sensitivity to osmotic stress raises the question if these mutants are altered in their cell wall. To test this possibility, mutants were spotted on YPD medium complemented with compounds known for their perturbation of the cell wall including: calcofluor white (40 µg/ml), Congo red (125 µg/ml) and caspofungin (125 ng/ml). For these inhibitors, results were similar (Fig. 18), since *sho1* and *msb2* mutants were more sensitive than the wild-type strain and an additive effect was observed for the *sho1 msb2* mutant, which was even more sensitive than the single mutants. Interestingly, *SSK1* inactivation led to a strong increase of resistance to these molecules, but additional inactivation of *SHO1* and/or *MSB2* generated the same phenotypes as both single mutants. Mutant *ssk1 msb2* showed a higher sensitivity than a single *ssk1* mutant, and a triple mutant *ssk1 sho1 msb2* was even more sensitive. Thus, Msb2p is clearly involved in resistance to Congo red, which decreases β-glucan stability (Roncero *et al.*, 1985) and increases the concentration of chitin in the cell wall (Imai *et al.*, 2005), but also in resistance to caspofungin, which inhibits β-1,3-glucan synthesis (Johnson *et al.*, 2003). All these experiments were done at 30 °C, but at 37 °C qualitatively identical phenotypes were observed, although sensitivities of all strain were increased (data not shown). Mutants were also spotted on YPD-medium containing SDS at a concentration of 0.01, 0.02 and 0.05 %. It is interesting to notice that on SDS plates all strains were able to grow as the wild-type strain, except for the *SSK1* inactivated strain, which had a higher resistance (Fig 18 D). Like for hyphal induction in YPM liquid, an *ssk1* mutation led to a specific phenotype which was not modified by *MSB2* inactivation (Fig.14). Results are consistent with a weakness of the cell wall in an *msb2* mutant.

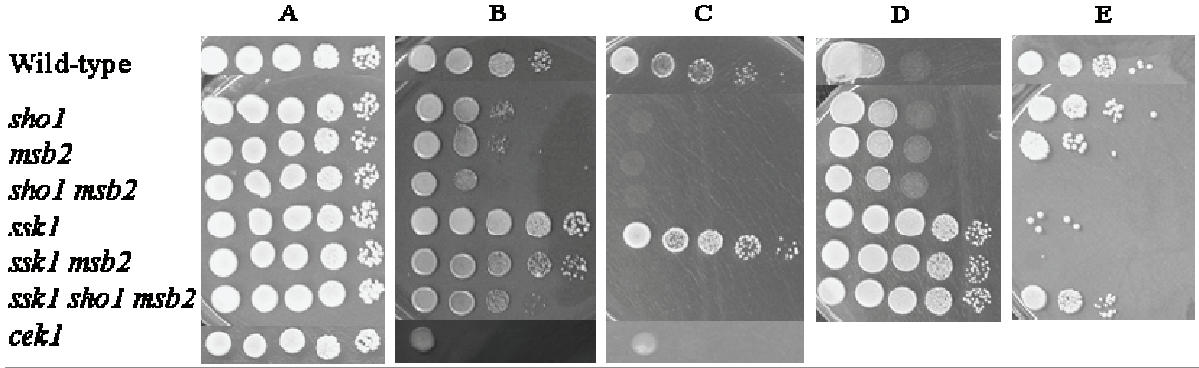


Fig. 18: Sensitivity of mutants to cell wall perturbations. Photographs taken after 2 days of growth at 30 °C on YPD (A) with Congo red (125 µg/ml) (B), caspofungin (125 ng/ml) (C), SDS (0.02 %) (D) and after a heat shock of 55 °C during 7 min (E).

### 3.1.5 *MSB2* inactivation in a *cek1* and *efg1* background

Cek1p is known to be a critical protein involved in Congo red resistance (Eisman *et al.*, 2006). As demonstrated above, Msb2p is also acting is this resistance. The facts that Cek1p is a cytoplasmic protein acting downstream of a MAPK pathway and that Msb2p is predicted to be localised in the plasma membrane suggest that both compounds could act in the same pathway. If this were the case, inactivation of *MSB2* in a *cek1* background should not modify *cek1* phenotypes. To generate a double mutant, a *cek1* strain (CK43B-16L) was transformed with Ura blaster cassette of plasmid pUK-6003.Ko.Urab, to create an *msb2* mutant. After selection on 5-FOA plates, inactivation of both alleles and introduction of a *URA3* wild-type allele at its original locus, strains were verified by Southern blotting to possess no more wild-type allele of *MSB2* (see section 3.1.1). By the same protocols that were previously described, it was possible to confirm inactivation of *MSB2* alleles in *cek1* background. Mutant *cek1* was also transformed with a DNA fragment to reconstitute a wild-type *URA3* allele. This mutant (FCCa32) was used as reference strain.

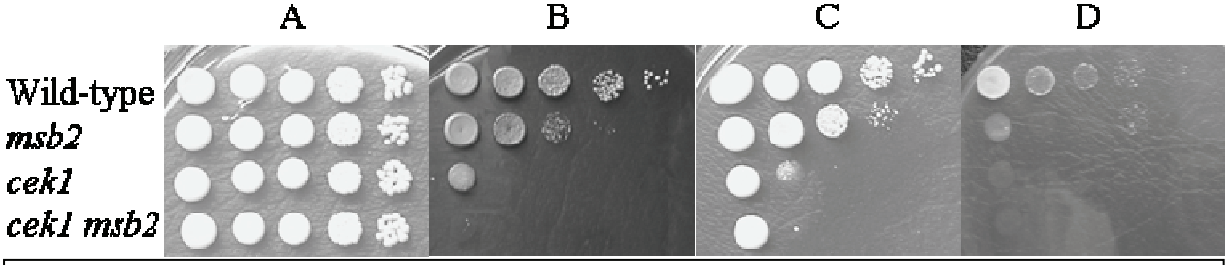


Fig. 23: Sensitivity to cell wall perturbation. Photogtraphs after 2 days of growth at 30 °C on YPD (A) with Congo red (125 µg/ml) (B), calcofluor white (40 µg/ml) (C) or caspofungin (125 ng/ml) (D).

The double mutant *cek1 msb2* (FCCa35) was spotted on YPD medium without (Fig. 23 A) or with Congo red (Fig. 23 B), calcofluor white (Fig. 23 C) or caspofungin (Fig. 23 D). The result indicates that the double mutant is more sensitive to Congo red and calcofluor white than single mutants, particularly to Congo red at 30 or 37 °C. The fact that the double mutant presents a stronger phenotype than single *cek1* mutant suggests that Msb2p is acting on an additional pathway independent of Cek1p, although it is not possible to exclude that Msb2p is also acting in a Cek1p-dependent manner.

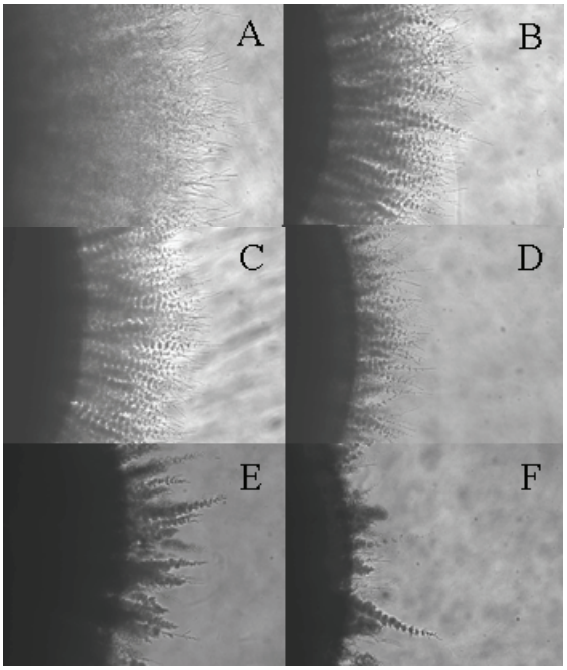


Fig. 24: Hyphal differentiation on YPM-medium at 37 °C. Photographs of CAF2-1 (A), *msb2* : FCCa30 (B), *cek1* (C), *cek1 msb2* (D), *efg1* (E), *efg1 msb2* (F) after 3 days of growth. Magnification 100x

Because, Cek1p is also known to play a role in hyphal formation, this phenotype was also tested for double mutants on YPM medium at 37 °C. After 3 days of growth, colonies of *msb2* and *cek1* presented an identical phenotype, which is a clear reduction in hyphal formation (Fig. 24). But the fact that the *cek1 msb2* mutant presented a stronger phenotype of hyphal differentiation suggests again that Msb2p acts not only in Cek1p pathway. Identical phenotypes were obtained with an *efg1 msb2* mutant. This strain was constructed following the same protocol as the *cek1 msb2* double mutant but using an *efg1* mutant strain as

parental strain (HLC67). Here again, a single *efg1* mutant (HLC52) presented a deficit in hypha formation which worsened when *MSB2* was inactivated (FCCa43). Thus, Msb2p appears to have a function in hyphal formation that is both PKA and MAPK independent or involved in both pathways.

### 3.1.6 Cell wall composition

According to the results of the sensitivity tests, it was possible that *msb2* mutants have an altered cell wall. To establish which component of the cell wall is particularly affected by the *MSB2* gene inactivation, I determined protein, chitin, mannan, β-1,3-glucan and β-1,6-glucan levels of the cell walls in 6 strains: RM100 (wild-type), *sho1*, *msb2*, *sho1 msb2*, *ssk1* and *ssk1 msb2*. Cells were grown at 37 °C in SD medium to an $OD_{600\ nm}$ of around 0.8 and then cell wall fractions were obtained after cell breaking and washing by hot SDS treatments (Martinez *et al.*, 2004). A sample of the cell wall fraction was treated to measure the protein concentration. It appears that the cell wall of all mutants except the *sho1* mutant contained a lower level of proteins than the wild-type strain (Tab. 7). Proteins localized in the cell wall are frequently *O*- and/or *N*-glycosylated. These modifications induce addition of saccharides to proteins, mostly consisting of mannose residues. Thus, the level of manoses is expected to be proportional to the protein level. After purification by precipitation with Fehling reagent, mannan concentration was measured by the Dubois method (Dubois *et al.*, 1956). For *sho1 msb2*, *ssk1* and *ssk1 msb2* mutants the relation between protein and mannan concentration was maintained, since both were decreased in parallel (Tab. 7). However, for the *sho1* and *msb2* mutants, the results were different. A *msb2* strain, which possesses less protein than the wild-type strain, showed a higher content of mannan. A reversed situation was obtained for the *sho1* mutant, but it is important to note that the differences to the wild-type strain were moderate, around 20 %. Results about protein and mannan levels were mainly correlated in the other mutants.

| (%) | Protein | Chitin | Mannan | β-1,6-glucans | β-1,3-glucans |
|---|---|---|---|---|---|
| Wild-type | 100 | 100 | 100 | 100 | 100 |
| *sho1* | 110 | 140 | 89 | 26 | 117 |
| *msb2* | 85 | 107 | 106 | 60 | 112 |
| *sho1 msb2* | 88 | 121 | 60 | 59 | 78 |
| *ssk1* | 73 | 66 | 62 | 114 | 57 |
| *ssk1 msb2* | 58 | 69 | 57 | 55 | 64 |

Tab. 7: Quantification of cell wall compounds. Numbers express percentage levels of the masses in mutant compared to wild-type (RM100) strains.

Chitin is a chain of β-1-4-linked *N*-acetylglucosamine residues implicated in rigidity. Two populations differing with regard to chitin were obtained (Tab. 7). The first group comprised *sho1*, *msb2* and *sho1 msb2* mutants, which presented a higher level of chitin compared to the wild-type strain. The second group consisted of *ssk1* and *ssk1 msb2* mutants, where the level of chitin was lower than in the wild-type strain. It is interesting to notice that strains with a high amount of chitin are sensitive to Congo red, but resistant for strains with a low level of chitin. This is in agreement with observations in *S. cerevisiae*, where relations between sensitivity to Congo red and high amounts of chitin in cell wall were demonstrated (Imai *et al.*, 2005). Thus, inactivation of *SSK1* leads to a decrease of chitin in the cell wall and inactivation of *SHO1* and *MSB2* genes induces an increase of chitin.

The main constituents of the cell wall in *C. albicans* are β-glucans with 50 to 60 % of cell wall mass. These molecules allow anchoring of proteins in the cell wall. Glucans are separated in two categories: β-1,3-glucans that constitute a three-dimensional network and β-1,6-glucans, which are ramifications of β-1,3-glucan structures (Kapteyn *et al.*, 2000). s*ho1* and *msb2* mutants showed similar result with an increase of β-1,3-glucans and a reduction of β-1,6-glucans level compared to the wild-type strain (Tab. 7). Inactivation of both genes simultaneously led to a reduced level of all glucans. This could explain the sensitivity to these strains to caspofungin and Congo red known to target glucans. An *ssk1* and *ssk1 msb2* mutant contains less β-1,3-glucans in the cell wall than a control strain. However, while the level of β-1,6-glucans increased in an *ssk1* mutant, an opposite effect was obtained for inactivation of *MSB2* in the *ssk1* background. The high level of β-1,6-glucans in an *ssk1* strain could explain the high resistance to caspofungin; indeed this glucan appears to compensate for absence of β-1,3-glucans, which are the target of the drug. Thus, composition analysis confirms the weakness of the cell wall in the *msb2* mutant.

### 3.1.7 Gene expression profiles

For *msb2* mutants a clear correlation between sensitivity to cell wall-perturbation agents and cell wall composition was demonstrated. To explore if alterations in cell wall structure are caused by specific gene regulation, a genome-wide transcriptional profile of wild-type (RM100), *msb2*, *sho1* and *sho1 msb2* mutant strains was performed. For this purpose, cells were grown in YPD at 37 °C and collected when suspensions reached an $OD_{600\ nm}$ of 0.5. Each strain was grown in triplicate to allow statistical analysis of results. After RNA extractions and cDNA synthesis, comparisons in each microarray slide were carried out between cDNA of RM100 (Cy3-labelled) and Cy5-labelled cDNA of the 3 mutant strains (*sho1*, *msb2* or *sho1 msb2*). Because all genes are represented twice on each slide, 6 ratios of intensity between Cy3 and Cy5 signal were obtained. To validate reproducibility of replicates, the software SAM (Tusher *et al.*, 2001) was used to analyse the quality of the values. Then a list of genes regulated at least 1.5 fold relative to the wild-type level was established (supplementary data, table 1), i.e. all genes with a ratio greater than 1.5 (for up-regulated genes) or less than 0.666 (for down regulated genes). A new set of 6 tables was obtained with only significantly regulated genes with good reproducibility between the 3 experiments (Tab. 8). These lists were composed of one up-regulated gene (*orf19.9332*) and 13 down-regulated genes in an *msb2* mutant compared to a wild-type strain. These numbers were respectively for *sho1* and *sho1 msb2* comparison: 60 and 21; 106 and 101 (Tab. 8). To visualise

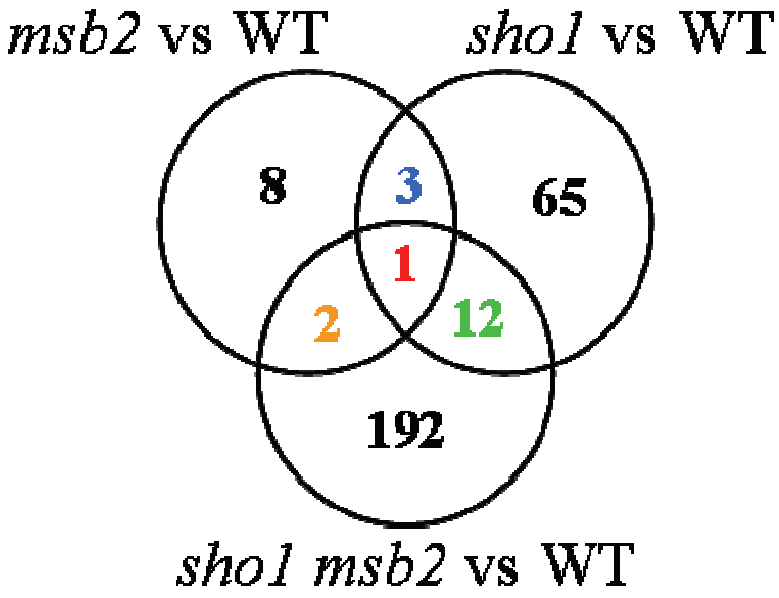


Fig. 19: Venn diagramm of regulated genes between *msb2*, *sho1*, *sho1 msb2* mutants and a wild-type strain (RM100).

| | up-regulated | down-regulated |
|---|---|---|
| *msb2* | *orf19.9332* | *PRP8, orf19.641, orf19.8613, IFL1, orf19.5291, ECE1, LEM3, orf19.3926, orf19.5270, orf19.10861, orf19.1490, orf19.5430, orf19.3376* |
| *sho1* | *ALS10, ECE1, RBT5, HWP1, orf19.5674, orf19.1691, orf19.4035, orf19.5635, SLY1, orf19.4048, GDH3, orf19.11525, ILV3, URA2, orf19.3117, PYC2, orf19.5372, HTS1, orf19.7676, orf19.4045, orf19.4459, GLK1, FRE7, orf19.3198, PHR1, CDC19, FRE5, orf19.4752, PGK1, MUM2, IFR2, MET15, PRP22, RHR2, orf19.675, orf19.6920, orf19.4013, orf19.6586, FBA1, ALP1, RNR1, MET10, IPF407, SCW1, FUN34, orf19.6608, ERG3, CTF18, orf19.5673, FRE30, EFG1, ENO1, YHB3, GPM1, APM1, FRP1, SCS7, TPS3, orf19.9993, TPI1* | *SHO1, URA3, PAP12, PRE6, IFL1, orf19.8613, orf19.997, orf19.10708, FBP1, SUC1, PRP8, orf19.1367, PHO84, orf19.2531, orf19.4222, IPF2268.3, CDC8, orf19.6816, orf19.3618, orf19.1172, orf19.13651* |
| *sho1 msb2* | *orf19.1364, IPF14348.3, SSA4, CPR6, SBA1, IPF11391, orf19.7085, orf19.3396, orf19.4998, orf19.5277, GCD14, KAR2, HSP90, HSP104, STI1, orf19.2260, ALS3, orf19.2770, RPS620B, RPS620A, HSP78.5F, YDJ1, orf19.5409, orf19.7602, NUM11, SSA1, orf19.9405, IPF2268.3, orf19.10345, orf19.5474, orf19.8136, orf19.1445, CDC37, FAA24, SIS1, YAL011, IFT1, orf19.11788, orf19.4424, orf19.7539, SSK2, HWP1, orf19.8332, orf19.304, orf19.320, orf19.7818, IPF4137.3F, CRK1.5F, PRP31, orf19.5469, PEX17, orf19.7492, orf19.5126, ALS10, NUT2, PLC1, orf19.2432, RAD32, NUP49, ALS9.5EOC, PEX14, orf19.6973, CTA24, orf19.1168, GAC1, SGT2, orf19.1341, orf19.7739, CAR2, orf19.11, orf19.6586, orf19.4622, orf19.2238, CTA24.3, orf19.1757, orf19.4492, orf19.3281, CTA241.EXON2, orf19.6688, HSP10.3, CBK1, AQY1, orf19.13252, IPF15772, orf19.6193, GIT1, CGR1, CIN4, HSP78.3F, orf19.7167, orf19.11979, orf19.2989, CDC43, orf19.831, YTA7, IPF6712.3F, orf19.1087, orf19.1091, orf19.6377, orf19.6326, orf19.10868, orf19.3210, orf19.5281, orf19.11626, orf19.3831, HOM3* | *PRE2, orf19.934, orf19.2659, STF2, YHB1, IFE2, EBP1, orf19.7765, SHO1, HRT2, QDR1, MVD1.3, EBP4, orf19.1306, PCK1, orf19.3908, HXT61, orf19.9578, PHO84, FET33, APT1, FAS2.3F, DDR48, HXT5.3F, orf19.7405, GAL7, orf19.6741, LAT1, ATP1.EXON2, FTR2, orf19.7676, PLB1, orf19.2670, GRP3, RNR21, FUM12.53F, RNR22, orf19.5698, orf19.8467, orf19.1387, RPO21, orf19.951, orf19.5343, orf19.2451, orf19.9988, orf19.5459, orf19.5576, MSH3, ADH5, orf19.220, SMF12, GRP4, orf19.3917, SCS7, orf19.1187, ERG13, ERG251, orf19.5193, DIP51.3F, orf19.9332, PIF2, orf19.11525, orf19.3130, orf19.6881, ADH2, HXT62, LSC2.3EOC2, CYT12, ACO2, LAB5, ACS1, ACO1, EBP2, ZRT2, PRP8, orf19.6068, PRS4, SAC7, orf19.5517, ERV14, orf19.7459, IDH1.3, LSC1, orf19.6608, TOM22, orf19.4268, VTC2, orf19.2336, HXK2.3F, COX15, FUN34, TRX1, orf19.10861, FTR1, orf19.5663, PGI1, GRD19, ERG16, HTS1, orf19.6757* |

Tab. 8: Genes differently and significantly regulated between mutants and wild-type strain on YPD at 37 °C. Only genes with a regulation greater than 1.5 fold are listed. Commonly regulated genes are represented in agreement with coloring used on Venn diagram (Fig. 19).

commonly regulated genes between each experiment, a Venn diagram was calculated (Fig. 19). This graphic shows that only few genes were commonly regulated between the three experiments and also that simultaneous inactivation of *SHO1* and *MSB2* results in many alterations in genes regulation. Indeed in an *msb2* mutant, only 14 genes were differently and significantly regulated, compared to the wild-type strain, while this number reached 81 with a

*sho1* mutant, but a value of 207 in a double mutant. This synergetic effect of *sho1* and *msb2* mutation affected several genes and probably pathways. Only one gene is commonly regulated in the 3 experiments, which is *PRP8* (*orf19.6442*), which encodes a homologue of a *S. cerevisiae* protein implicated in RNA splicing. The software Genespring (Agilent Technologies) allows an analysis of all genes regulated in a defined pathway (Table 9). For the *msb2* mutant, no activation or repression of a particular pathway was identified. For the *sho1* mutant, 6 pathways were found to be up-regulated including pathways for amino acid synthesis (methionine, valine leucine and isoleucine biosynthesis), but also glutamate synthesis. The 3 other pathways are particularly interesting because they are significantly up-regulated in the *sho1* mutant but strongly down-regulated in a *sho1 msb2* mutant. These pathways are fatty acid biosynthesis, glycolysis and sphingolipid biosynthesis. The double mutant was also affected in 3 other pathways down-regulated (citric acid cycle, pyruvate metabolism and reductive carboxylate cycle).

| Pathways | *sho1* | *sho1 msb2* |
|---|---|---|
| citrate cycle | | *MDH1, ACO1, FUM12, MDH11* |
| fatty acid biosynthesis | *ACC1, FAS1, FAS2* | *ACC1, FAS1, FAS2* |
| glutamate synthesis | *GDH3, IDH1, PUT2* | |
| glycolysis | *ADH1, CDC19, ENO1, FBA1, GPM1, PFK1, PGI1, PGK1, TPI1* | *ADH1, CDC19, , ENO1, FBA1, GPM1, PGI1, TPI1* |
| methionine biosynthesis | *MET15, MET1, MET2, MET6, MET10, orf19.1159, orf19.2092* | |
| pyruvate metabolism | | *POT14, MDH1, ACC1, MDH11* |
| reductive carboxylate cycle | | *ACO2, MDH1, ACO1, FUM12, MDH11* |
| sphingolipid biosynthesis | *AUR1, SUR2* | *SUR2, orf19.6343* |
| valine leucin and isoleucine biosynthesis | *ILV2, ISW1* | |

Tab. 9: List of regulated genes involved in different metabolic pathway. All genes regulated in *sho1* mutant were up-regulated, contrary to *sho1 msb2* where all genes shown were down-regulated.

The original question of this experiment was to clarify if alterations observed in cell wall composition were also reflected in gene expression. It appears that the *msb2* mutant, which is sensitive to chitin and caspofungin and contains a high amount of chitin and β-1,6-glucan, regulated only three transcripts involved in cell wall construction. Two genes suggested being involved in glucan synthesis, *SCW11* and *orf19.4666*, are respectively, up- and down-regulated. *Orf19.4463* is also down-regulated in the *msb2* mutant; this gene encodes a protein homologous to Pir3p in *S. cerevisiae*, a known protein required for cell wall stability. For the *sho1* mutant, 3 genes involved in chitin synthesis are up-regulated (*CHS1*, *CHS4*, *CHT3*), which correlates with the higher amount of chitin in this mutant compared to the wild-type strain. Other genes involved in cell wall and glucan formation are regulated positively (*KRE6*, *PHR1*, *SCW1*, *PGA10*, *PGA4*, *PGA7*, *orf19.675*, *ENO1*, *ALS3*) or negatively (*orf19.4463*, *YWP1*, *CSP37*). These observations correlate with phenotypes demonstrating the weakness of *sho1* cell walls. The same results were obtained for the double mutant *sho1 msb2*. Indeed genes involved in chitin synthesis are up-regulated (*CHS21* and *CHS24*), while other genes involved in cell wall stability are up-regulated (*SMI1B*, *PHR1*, *EXG2*, *KRE1*, *ALS3*, *ALS9*) or down-regulated (*BIG1*, *BGL2*, *orf19.2336*, *PIR1*, *PGA45*). These gene regulations are in agreement with a higher chitin content and lower glucans level

compared to wild-type. All together, these results confirm observations in the sensitivity tests and the analysis of cell wall composition.

To validate result obtained by DNA microarrays, a series of quantitative RT-PCR experiments was carried out on some selected genes. In these qRT-PCR experiments, the level of expression of a gene in a special condition was compared to a reference transcript (*ACT1*). Expression of *HWP1*, *IPF16939*, *IPF17558* and *PRP8* was measured in RM100, *sho1*, *msb2* and *sho1 msb2* strains compared to the level of *ACT1* in each of these strains. RNA samples used for these experiments are the same that the one for microarrays. It appears that results were not strictly identical to observation of microarray result, but the tendency was conserved. From the precedent results, *HWP1* was predicted to be up-regulated in a *sho1* mutant compared to the wild-type strain, and it is clear that the relative transcript level of this gene was higher in a *sho1* than in RM100 strain (Fig. 20). This conclusion was also possible for *IPF16939* (*orf19.1364*) in the *sho1 msb2* mutant or with *IPF17558* (*orf19.1763*) in the *msb2* mutant. Regarding genes commonly regulated in 3 mutants, *PRP8* was predicted to be down-regulated in all mutants. This phenomenon was confirmed by qRT-PCR (Fig. 20). All together, these results confirmed the regulation obtained by microarray analysis.

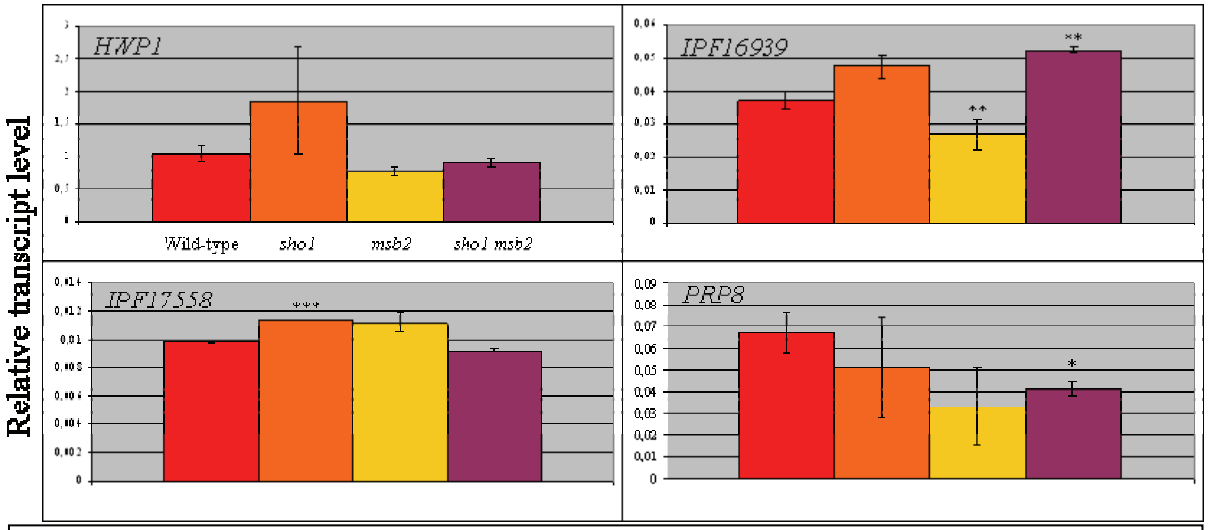


Fig. 20: Relative transcript levels obtained by qRT-PCR in different strains. 4 strains were used: wild-type (RM100) in red, *sho1* in orange, *msb2* in dark yellow and *sho1 msb2* in purple. *HWP1*, *IPF16939*, *IPF17558*, *PRP8* transcripts are expressed relative to *ACT1* transcript. *P < 0.05; **P<0.033; ***P<0.016

### 3.1.8 *MSB2* regulation

Inactivation of *MSB2* induces an altered expression of genes predicted to have a role in cell wall formation. This alteration in gene expression causes an alteration in cell wall composition, which is revealed by sensitivity to different cell wall perturbation compounds like Congo red, caspofungin and calcofluor white. If Msb2p is involved in resistance to Congo red, it is possible that in presence of this compound, wild-type cells up-regulate *MSB2* transcription. To verify this possibility, wild-type cells (CAF2-1) from an overnight culture were inoculated in YPD medium with or without Congo red (125 µg/ml). Strains were grown at 30 °C during 4 hours, before harvesting of cells. 3 different replicates were done and RNA was extracted from each culture. cDNA was produced from RNA and prepared for qRT-PCR. Replicates show relativly identical results, *MSB2* expression was increased in wild-type cells in presence of Congo red compared to the same strain in simple YPD medium. The average ratio of regulation is about 1.39 (Fig. 21). These experiments also reveal the level of

expression of *MSB2* compared to *ACT1*, representing around 0.8 % of *ACT1* transcript. This relatively low value is in agreement with the idea of a regulatory or a sensor function of Msb2p.

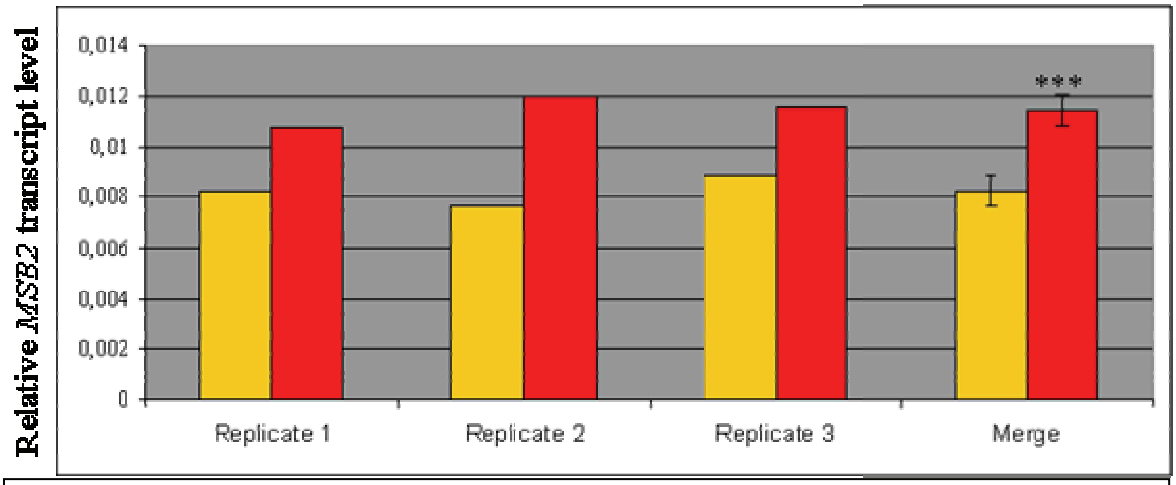


Fig. 21: qRT-PCR result on *MSB2* expression in presence or not of Congo red (125 µg/ml) in CAF-1 strain relative to *ACT1* transcript. Relative transcript levels of wild-type strain without Congo red are represented in orange and with Congo red in red. 3 individual replicates and the merge of them are shown. ***P<0.016

Similar analyses were done with a wild-type strain grown in the presence of an *O*-glycosylation inhibitor (2 µM) or tunicamycin (2 µg/ml). Results are not expressed as relative transcript level as above but as ratio of transcript level between the two conditions (with or without inhibitor). Sensitivity tests on plates had not shown any particular phenotype to these compounds (see section 3.1.4), contrary to Congo red. However, a clear down-regulation of the *MSB2* transcript level was observed after 4 h of growth at 30 °C. Indeed, in presence of both inhibitors, levels of *MSB2* transcript represented 0.6 fold the level as in absence of them (Fig. 22). Thus, defects in *O*- and *N*-glycosylation lower *MSB2* transcript levels.

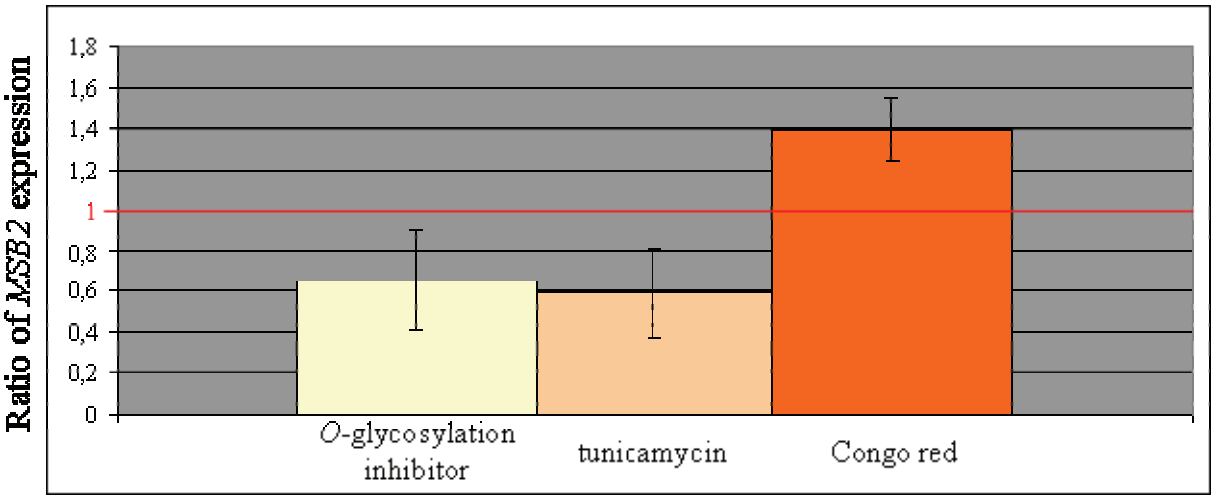


Fig. 22: Ratio of expression between *MSB2* expression in wild-type strain in YPD with or without different molecules. Ratio in presence of *O*-glycosylation inhibitor is shown in beige, of tunicamycin in light orange and with Congo red in orange.

### 3.1.9 Pmt-mediated *O*-glycosylation

ScMsb2p was described to be glycosylated (Cullen *et al.*, 2004). Furthermore, high numbers of serine and threonine residues are conserved between the Msb2p protein in *S.*

*cerevisiae* and *C. albicans* (Fig. 5). It is reasonable to consider that Msb2p in *C. albicans* is also *O*-glycosylated and that this modification is essential for its function. Following this hypothesis, glycosylation could occur by one of 5 PMTs: Pmt1p, Pmt2p, Pmt4p, Pmt5p and Pmt6p (Prill *et al.*, 2005). If a single *pmt* mutant showed identical phenotypes as the *msb2* mutant, this would indicate that this Pmt isoform modifies Msb2p. To test this hypothesis, *pmt* mutants were spotted on YPD agar complemented with Congo red (Fig. 25 B) or caspofungin (Fig. 25 C). An *msb2* mutant presents a moderate sensitivity to Congo red of about 10 fold higher compared to a wild-type strain (CAF2-1). 2 *pmt* mutants, *pmt1* (SPCa2) and *pmt2*/*PMT2* (SPCa4) presented a strong sensitivity to Congo red, while *pmt4* (SPCa6), *pmt5* (SPCa10) and *pmt6* (SPCa8) showed a moderate phenotype closer to an *msb2* mutant. These three last mutants could be candidates to have a role in Msb2p glycosylation. But the *msb2* mutant showed also a drastic sensitivity to caspofungin, and only *pmt2*/*PMT2* and *pmt4* mutants presented such a phenotype. Thus, comparisons of sensitivity tests indicate that Pmt4p is the best candidate to glycosylate Msb2p. A second above described phenotype of *msb2* mutant is the deficit of hypha formation on YPM plates. Again, all *pmt* mutants were plated on YPM and incubated at 37 °C during 3 days (Fig. 26). *pmt1* and *pmt2*/*PMT2* mutants showed a strong phenotype with no hyphae, while *pmt4*, *pmt5* and *pmt6* mutants presented a reduction in their ability to produce hyphae. Again, the *pmt4* mutant, like in sensitivity tests, had a phenotype similar to the *msb2* mutant. These results suggest that functional Msb2p requires *O*-glycosylation by Pmt4p.

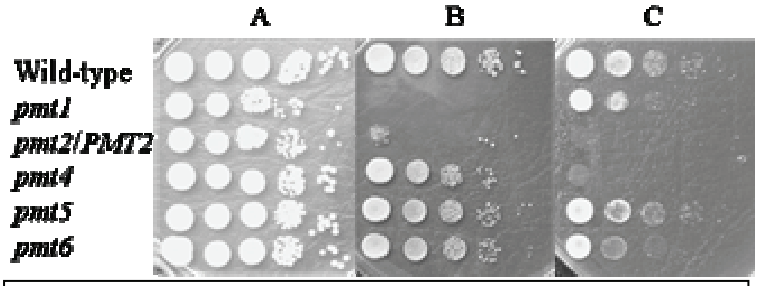


Fig. 25: Sensitivity to cell wall perturbation. Photographs after 2 days of growth at 30 °C on YPD (A) with Congo red (125 µg/ml) (B), caspofungin (125 ng/ml) (C) for wild-type (CAF2-1) and the 5 *pmt* mutant

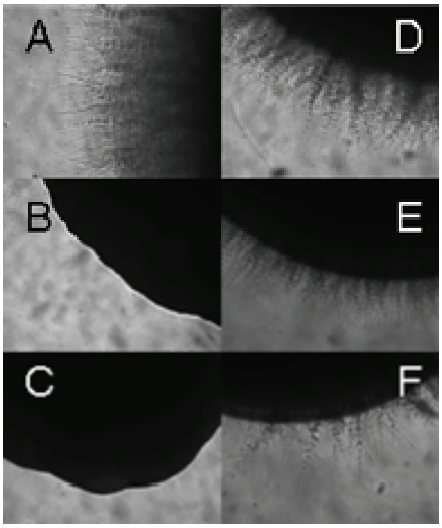


Fig. 26: Hypha differentiation on YPM at 37 °C. Photographs of CAF2-1 (A), *pmt1* (B), *pmt2*/*PMT2* (C), *pmt4* (D), *pmt5* (E), *pmt6* (F) after 3 days of growth. Magnification 100x

### 3.1.10 CaMsb2p protein partners

In *S. cerevisiae*, interaction of Msb2p with Cdc42p was demonstrated by a classical yeast 2-hybrid method and with Sho1p by co-immunoprecipitation (Cullen *et al.*, 2004). To find protein partners of Msb2p in *C. albicans* two strategies were attempted: classical and split-ubiquitin 2-hybrid screening. These methods were also used to test specific interactions between Msb2p and Cdc42p or Sho1p.

For classical 2-hybrid screening (James *et al.*, 1996), a fusion between the binding domain of Gal4p and the C-terminal tail of Msb2p was constructed. Plasmid pGBD-6003-C-tail was co-transformed in a PJ69-4A strain with plasmid pGAD, which contains random DNA fragments of SC5314 strain of *C. albicans*, or a fragment corresponding to the Ca*CDC42* (*orf19.390*) obtained by PCR on genomic DNA. Integration of both plasmids induced prototrophy for tryptophan and leucine due to presence of *TRP1* and *LEU2* on

respectively pGBD and pGAD plasmid. At this step, many transformants were obtained. In case of positive interaction between two proteins linked to the binding or activating domain of Gal4p, a prototrophy for histidine and adenine should occur, since respective genes are under *GAL2* and *GAL1* promoter regulation. Some cells grew in the absence of these 4 amino acids on minimal medium (MM), but unfortunately, after purification and re-introduction of plasmids extract from these strains, cells were not able any more to grow on minimal medium lacking histidine and adenine. For the *CaCDC42* construct (pGAD-CDC42), no positive interaction was identified. The fact that Msb2p is a plasma membrane protein can explain the absence of a protein partner isolate by a classical 2-hybrid approach. For this reason, only the soluble C-terminal part of Msb2p was used which not reflects all interactions resulting from transmembrane or extra-cellular domains.

The split ubiquitin 2-hybrid assay was developed for protein interaction between proteins localised in membranes (Johnsson *et al.*, 1994; Obrdlik *et al.*, 2004; Iyer *et al.*, 2005). Here again, the association of 2 proteins is essential to liberate a transcriptional factor, which activates promoters of reporter genes. This transcriptional factor is linked to C-terminal part of ubiquitin (CUB), this association is itself used to tag a protein. Second, the protein used to test interaction is tagged with the N-terminal part of ubiquitin (NUB). When CUB and NUB are associated, which occurs in case of interaction between the two proteins tested, the transcriptional factor is released by proteolytic cleavage. This leads to activation of the 3 reporter genes: *lacZ*, *ADE2* and *HIS3* genes. Strains prototrophic for tryptophan and leucine indicate the presence of both plasmids, because plasmids with NUB or CUB fragments contain, respectively, *TRP1* and *LEU2* genes. Furthermore, if the strain is also prototroph for adenine and histine, a probable interaction between the proteins fused to NUB or CUB tags exists. Plasmid containing *MSB2* fused to CUB (p2228-MSB2-Cub) was used to transform strain THY.AP4 (*MAT*a), while all plasmids encoding a NUB fusion were used for THY.AP5 (*MAT*α) transformation. THY.AP4 and THY.AP5 transformants were mixed on YPD medium to induce mating. During this step, formation of diploid cells occurred, which contained both plasmids. Then cells were replicated on minimal medium without leucine, tryptophane, adenine and histidine to identify positive interaction. Only strains with both plasmids and with a positive interaction between the two chimeric proteins can grow. Unfortunately, like for the classical 2-hybrid analyses, only false positives were found. Use of plasmids p2229-SHO1-Nub and p2230-Nub-SHO1 for specific interaction between Sho1p and Msb2p did not produce any positive strain able to grow on selective minimal medium lacking histidine and adenine. Even by inverting NUB and CUB positions between Msb2p and Sho1p (p2229-MSB2-Nub and p2228-SHO1-Cub) results were similar. Thus, no protein partners were identified for Msb2p in *C. albicans*.

## 3.2 Bioinformatics approach

In *S. cerevisiae* and *C. albicans*, sensors localised in the plasma membrane and partially involved in morphogenesis were previously described. These proteins present some common characteristics, since they possess more than 1 transmembrane (TM) domain and an extended cytoplasmic tail, which in some cases was demonstrated to interact with cytoplasmic proteins important for signal transduction. To identify new putative sensors in *C. albicans*, we used these common properties to identify candidate genes. The *C. albicans* genome is predicted to comprise 6114 genes and almost half of them (3362) are actually without a clear function or homologue. Among such genes we attempted to identify genes encoding new sensors. Only 350 genes were encoding a protein with at least 3 TM domains. The second selection was the presence of an N- or C-terminal cytoplasmic tail with a length of at least 30 a.a., which would increase the chance of interactions with other protein. With this second parameter, a final list of 166 candidate genes was obtained (Supplementary data, table 2).

From this list, 2 genes were picked for analysis. *IPF4949* (*orf19.7670*) is predicted to encode a protein with some characteristics of transceptors containing 12 TM and a long cytoplamic tail such as Gpa1p, Csy1p, Hgt4p, Ngt1p. *IPF5005* (*orf19.6650*) encodes a smaller protein but without any identified homologue. *NGT1* and *HGT1* are two candidate genes not present in the final list, but predicted also to encode membrane proteins.

### 3.2.1 *IPF4949*

#### 3.2.1.1 Gene structure and disruption

*IPF4949,* alias *orf19.7670* or *CA6053*, is a gene of 2772 bp and is predicted to encode a 924 a.a. protein containing 12 transmembrane domains and a N-terminal tail of 241 a.a. located at the inside of a membrane (prediction programmes: http://www.enzim.hu/hmmtop/ and http://www.cbs.dtu.dk/services/TMHMM-2.0/) (Fig. 27). This protein possesses between its 500$^{th}$ and 900$^{th}$ a.a. some domains found in $Na^+/Ca^{2+}$ and $Ca^{2+}/H^+$ antiporters. The complete search of homologous proteins (http://www.ncbi.nlm.nih.gov/BLAST/) yielded proteins localised in the membrane with a $Ca^{2+}$ transporter function or with proteins not yet characterised.

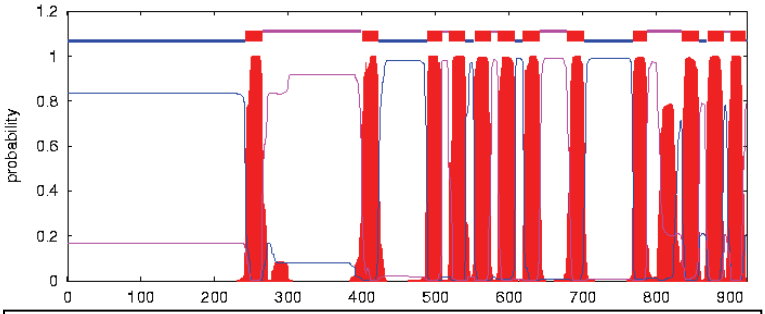


Fig. 27: Predicted topology of Ipf4949p. Best probability for the topology is draw on top of the graph. The region turned to the inside of the membrane is in blue, and in purple if turned to the outside of the membrane. TM domains are drawn as red bars.

Inactivation of the first allele of *IPF4949* was realised following the same strategy as for the *MSB2* gene. Cells from CAI4 strain were transformed by the DNA fragment of 7 kb derived from digestion of p4949.KO.URAb by *Xma*I and *Hin*dIII. Correct mutants (FCCa1) were then plated on medium with 5-FOA to select cells, in which recombination between the two *hisG* sequences had generated the loss of the *URA3* gene present in the Ura blaster cassette (resulting strains: FCCa2 and 3). The second allele was inactivated following the same strategy (resulting strains: FCCa4 to 7). Then a reintroduction of a *URA3* gene at the wild-type locus was realised by transforming the homozygous mutant strain obtained after 5-FOA selection (strains: FCCa6 and 7) with a DNA fragment containing the *URA3* gene (strains: FCCa8 and 9).

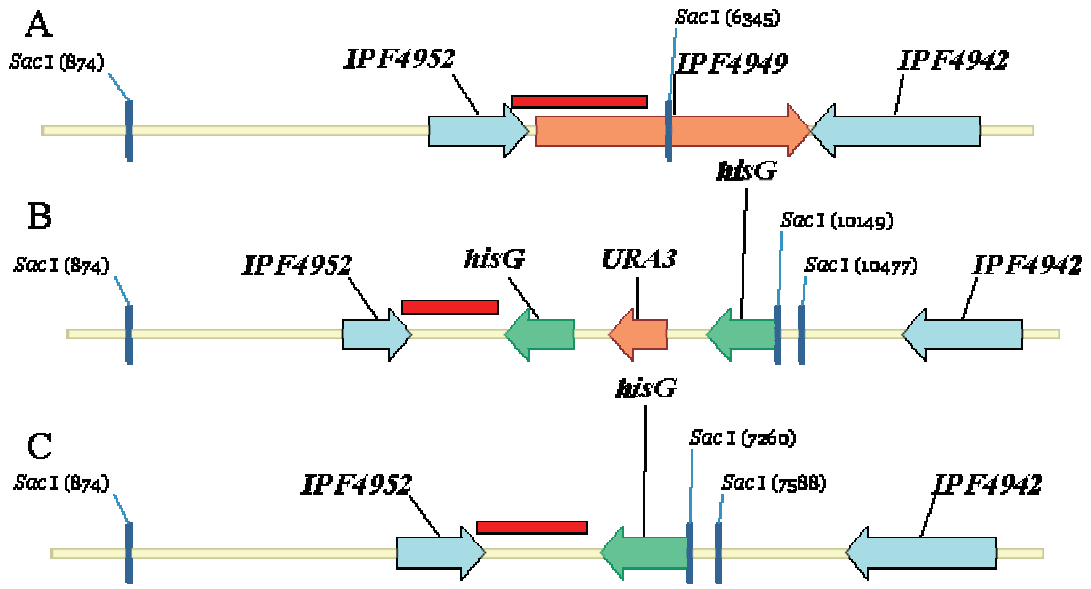


Fig. 28: Scheme of *IPF4949* locus during different steps of inactivation. Genome organisation in wild-type strain (A), after replacement of a wild-type allele by the URA blaster cassette (B) and after recombination between 2 *hisG* sequences (C). The probe used for Southern blot hybridization is indicated by the red box.

To validate all mutant strains obtained for the genomic deletions of *IPF4949* and the *URA3*-complemented strains (FCCa8 and 9), DNA of these strains were extracted and digested by *Sac*I for a Southern blot. For this a DIG-labelled probe consisting of a 1.5 kb DNA fragment obtained by *Hin*dIII and *Nsi*I digestion of pMos-*IPF4949* was produced, which hybridized in the 5′ region of the gene as shown in Fig. 28. After the first inactivation (lane 3) we expected a band at 5.4 kb (wild-type) and one at 9.2 kb (Ura blaster insertion) (Fig. 29). Selection on 5-FOA for loss of *URA3* modified the band at 9.2 kb to a band at 6.3 kb (lanes 4 and 5), containing only one repeat of *hisG*. Homozygous mutant strains (lanes 6 and 7) showed a band at 6.3 kb (*hisG*) and 9.2 kb (Ura blaster insertion) that after 5-FOA selection, presented only one band at 6.3 kb (lanes 8 to 9). The two strains (FCCa8 and 9) with a *URA3* functional allele at its wild-type locus, which were verified by PCR (data not shown) presented the same profile on this Southern blot as the homozygous strains FCCa6 and 7, as expected.

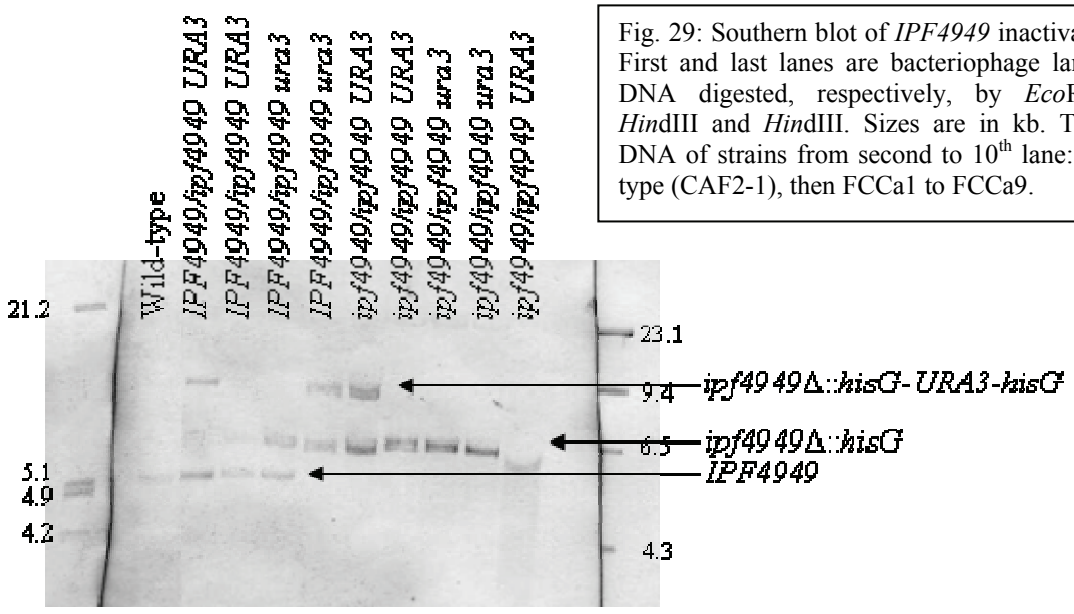


Fig. 29: Southern blot of *IPF4949* inactivation. First and last lanes are bacteriophage lambda DNA digested, respectively, by *Eco*RI + *Hin*dIII and *Hin*dIII. Sizes are in kb. Tested DNA of strains from second to 10th lane: wild type (CAF2-1), then FCCa1 to FCCa9.

### 3.2.1.2 Phenotypic analyses

The function of *IPF4949* in *C. albicans* was characterised by phenotypic analyses of null mutants. First, in liquid YPD or SD medium, inactivation of *IPF4949* demonstrated no significant growth phenotypes (Fig. 30). For this test, the $OD_{600\ nm}$ was measured at different time points for a wild-type strain, a heterozygous mutant (FCCa4) and two independent homozygous mutant strains (FCCa8 and 9) of *IPF4949*. All strains possess one functional *URA3* allele. The generation time for all strains was around 85 min at 30 °C in YPD. The experiment was done at 30 and 37 °C, but no significant differences between wild-type, heterozygous and homozygous mutant strains were observed.

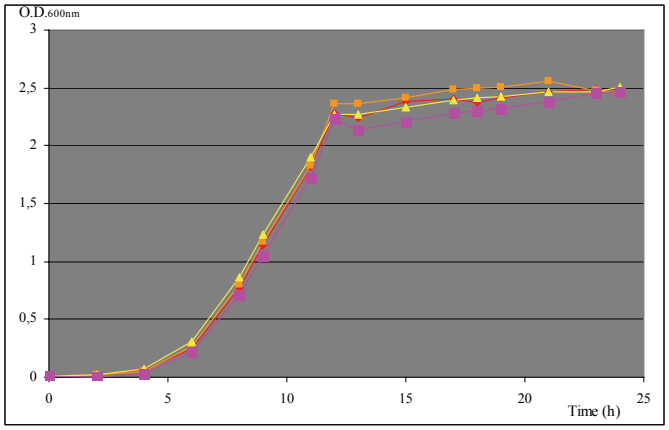


Fig. 30: Growth curve on YPD at 30 °C. Wild-type (CAF2-1) is represented in red, heterozygous mutant (FCCa4) in orange, homozygous *ipf4949* (FCCa8 and 9) respectively in purple and yellow.

To pursue characterisation of the *ipf4949* mutant (FCCa8 and 9), these strains were spotted on media containing various drug: azoles (fluconazole, ketoconazole, clotrimazole 5 µg/ml), hygromycin B (200 µg/ml), caspofungin (125 ng/ml), nourseothricin (200 mg/ml), phloxin B (5 µg/ml), SDS (0.01 - 0.05 %), Congo red (125 µg/ml), calcofluor white (20 and 40 µg/ml), *O*- (2 µM) and *N*-glycosylation (tunicamycin 2 µg/ml) inhibitor (Fig. 31). Furthermore, growth in high osmolarity (0.5 and 0.7 LiCl, 0.5 – 1.5 M NaCl), oxidative stress (5 mM $H_2O_2$), cold and heat shock (16 °C, 42 °C) was tested. In all these conditions, heterozygous and homozygous mutants presented the same sensitivity as the wild-type strain. All tests were done at 30 °C and some tests were repeated at 37 °C, but no particular sensitivity was described. Ipf4949p seems to not be involved in any of the stress condition tested.

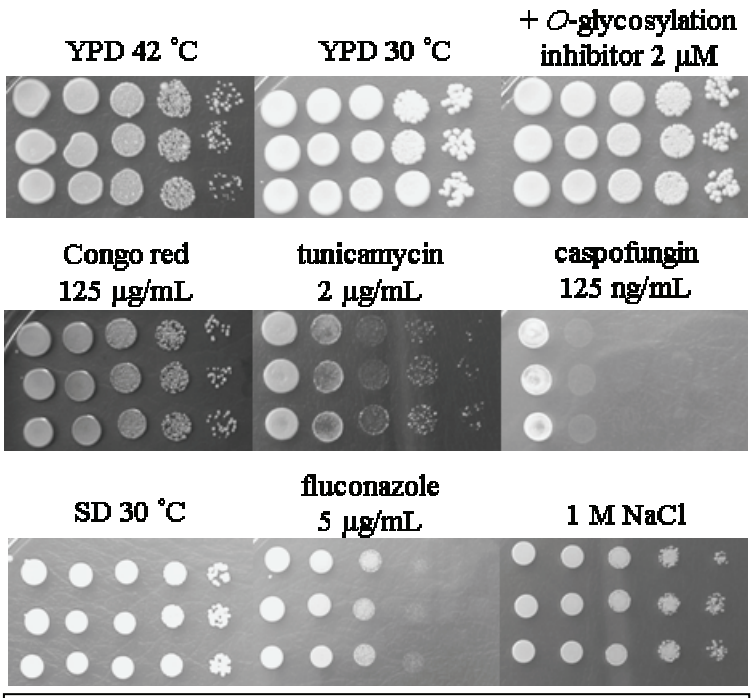


Fig. 31: Sensitivity test of *ipf4949* mutants. Several dilutions (5 µl) of $4x10^7$ to $4x10^3$ cells/ml were spotted on different media. Photographs were taken after 2 days of growth at 30 °C. From top to bottom of each photographs: CAF2-1, and two homozygous mutant (FCCa8 and 9).

The ability of mutants to differentiate hyphae in liquid was estimated by counting percentages of yeast cells able to develop a germ tube during 2 h in liquid induction media. It appears that mutants possess the same capacity as wild-type cells to differentiate germ tubes in YPD + 5 % serum, in Lee (Lee *et al.*, 1975) and Spider (Liu *et al.*, 1994) media. Indeed, all strains had a final

percentage of around 100 % of yeast cells differentiating a hypha.

The strains were also plated on the same induction medium but containing agar. Mutants showed the same ability of hyphal differentiation as the wild-type strain on an agar plate with 5 % serum at 37 °C. This was observed on YPM medium (37 °C), in embedded and hypoxia condition (30 and 37 °C). Only on Spider and Lee's medium (containing mannitol instead of glucose), *ipf4949* mutants showed after 4 days of growth at 37 °C a clear deficit in hypha formation compared to the wild-type strain (Fig. 32). However, after 7 days on these media, *ipf4949* mutants started to differentiate hyphae, but in lower amounts than the wild-type strain. This result suggested a contribution of Ipf4949p for differentiation of hyphae on solid medium.

Our hypothesis is that Ipf4949p is a receptor localised on the plasma membrane, which activates a pathway to induce hyphae formation. Following this model, it is possible that constitutive activation of downstream elements of the pathways could complement the defective phenotype due to the absence of sensor. Two important transcription factors, localised down-stream in hyphal induction pathway are known: Cph1p (see 1.2.1) and Efg1p (see 1.2.2). To rescue the *ipf4949* hyphal deficit, plasmids containing *EFG1* and *CPH1* under the control of strong promoters, respectively *PCK1* and *ADH1* promoters, were introduced in *ipf4949* background. Strain FCCa8 and FCCa9 (homozygous mutants) were transformed with plasmid pBI-HAHYD for *EFG1* expression and pLJ19 for *CPH1* expression. These plasmids possess an auto-replicating sequence (*ARS*) for *C. albicans*, which means that they do not need to be integrated in the genome. After PCR-verification of plasmid in each strain, cells were plated on induction agar. On Spider and Lee (with mannitol) medium, *ipf4949* strain transformed with over-expression plasmids presented the same hyphal deficiencies as the *ipf4949* mutant. Thus, no evidence for involvement of Efg1p and Cph1p in the pathway defective in the *ipf4949* mutant was observed.

Due to the presence of a $Ca^{2+}$ antiporter motif in the Ipf4949p sequence and to its partial role in hyphal induction, we studied the impact of an *IPF4949* mutation on thigmotropism. This morphological response to surface stimulus was shown to require calcium uptake systems such as Mid1p and Cch1p (see 1.3.8). After observation of the behaviour of *ipf4949* mutant to contact with ridges, no significant differences were noted in comparison to wild-type strain CAF2-1. Chlamydopore formation, another morphogenesis capacity of *C. albicans*, was also tested with this set of strain, but the *ipf4949* mutant showed the same ability as wild-type cells to differentiate chlamydospores.

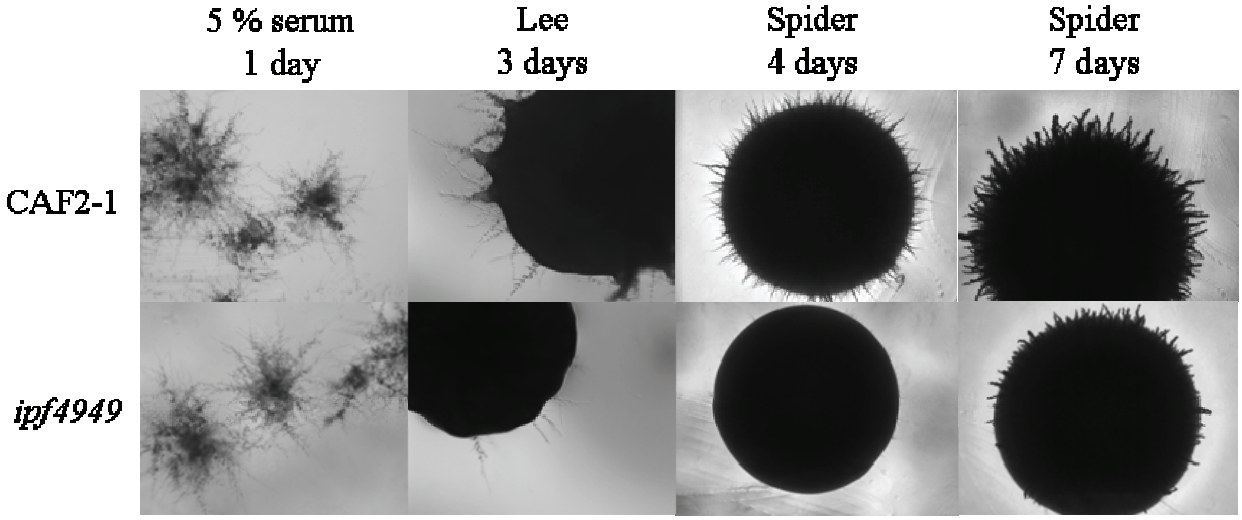


Fig. 32: Hyphal induction on agar media. Photographs taken of colonies of wild-type (CAF2-1) and *ipf4949* mutant (FCCa8) strain. Cells were grown at 37 °C, for the indicated times. Magnification 100x.

Overall, the morphogenetic defects on agar induction media and its similarity with transceptors make Ipf4949p a possible candidate for a morphological sensor in growth on solid surfaces. But absence of phenotypes in liquid induction media and its transitory effects suggest that it is not a dominant element of *C. albicans* morphogenesis.

### 3.2.2 *IPF5005*

#### 3.2.2.1 Gene structure and disruption

*IPF5005*, alias *orf19.6650* or *CA4091*, is a gene of 576 bp predicted to encode a 3 TM region protein of 192 a.a with an N-terminal tail of 73 a.a. turned to the inside of membrane (http://genolist.pasteur.fr/CandidaDB/tmhmm/CA4091.prt.html) (Fig. 33). Interestingly, Ipf5005p does not possess a strong homologue in *S. cerevisiae* or any other ascomycetous fungi. Some species contain a protein with weak homology (*Lodderomyces elongisporus*, *Pichia stipitis*, *Debaryomyces hansenii*) but none of these proteins have an identified function.

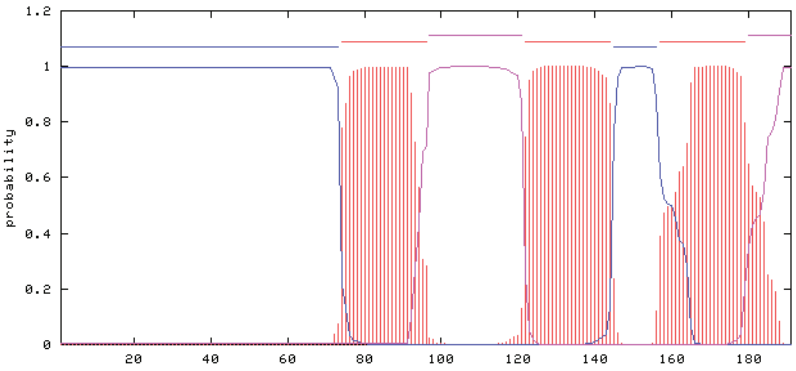


Fig. 33: Predicted topology of Ipf5005p. The best topologic probability is draw on top of the graph. Regions turned to the inside of the membrane are in blue, and in purple if turned to the outside of the membrane. TM regions are drawn as red bars.

Inactivation of *IPF5005* was realised following the same strategy as for *IPF4949*, i.e. disruption by the Ura blaster. Inactivation of the first *IPF5005* allele in CAI4 strain was done by transformation of this strain with a 5.5 kb fragment derived from the digestion of p5005.KO.URAb by *Kpn*I and *Hin*dIII. Heterozygous mutant strains (FCCa10 and 11) obtained by the preceding transformation were then plated on

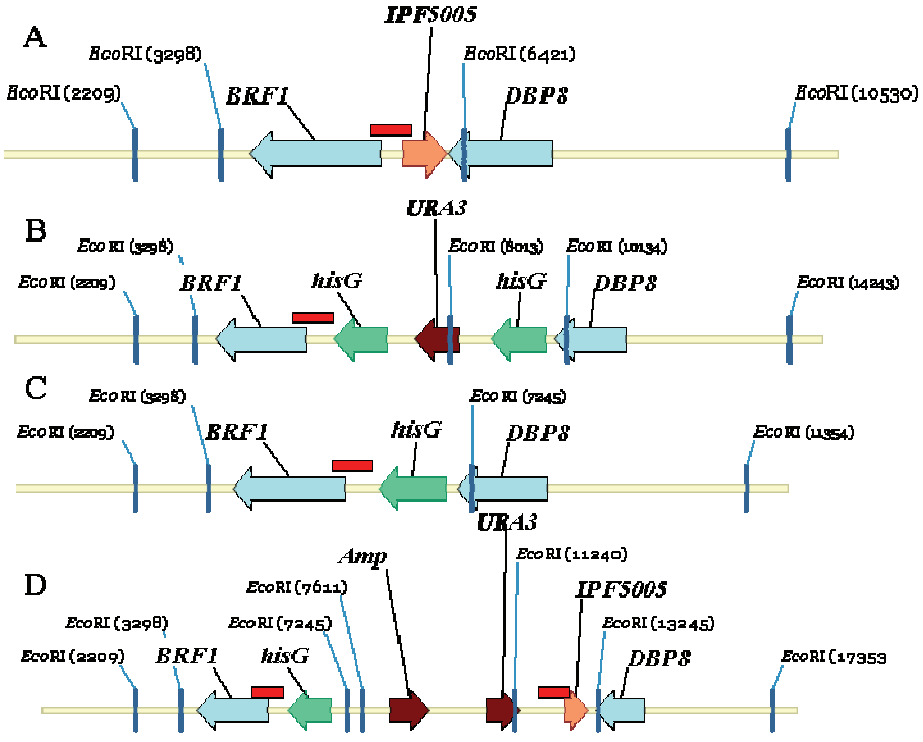


Fig. 34: Scheme of *IPF5005* locus during different steps of inactivation. Genome organisation in wild-type strain (A), after replacement of a wild-type allele by URA blaster cassette (B), after recombination between 2 *hisG* sequences (C), after introduction of an *IPF5005* wild-type allele (D). The probe used for Southern blot hybridization is indicated by the red box area.

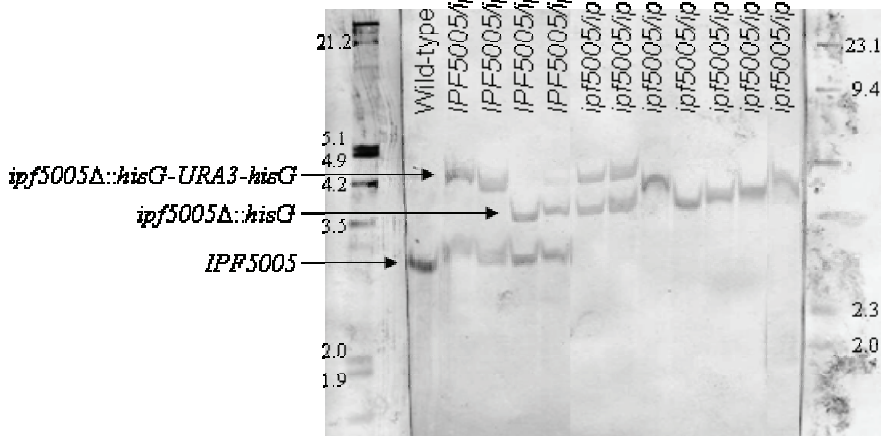


Fig. 35: Southern blot of *IPF5005* inactivation. First and last lanes are bacteriophage Lambda DNA digested respectively by *Eco*RI + *Hin*dIII and *Hin*dIII. Sizes are in Kb. Tested DNA of strain from second to 12th lane: wild-type (CAF2-1), then FCCa10 to FCCa20.

medium containing 5-FOA to select for recombination between the two *hisG* sequences of the Ura blaster and thus loss of *URA3* gene. Inactivation of the second allele was done by the same procedure. This led to construction of a *ipf5005* homozygous mutant strain, where each allele of *IPF5005* contains only a *hisG* repeat (FCCa16 and 17). A functional *URA3* gene was reconstituted in these *ipf5005* strains by transformation with a 4.3 kb fragment derived from the digestion of plasmid pHB-5 by *Xho*I and *Pst*I. To reintroduce an *IPF5005* allele, a plasmid containing a wild-type ORF of *IPF5005* and flanking regions to maintain its regulation, but also a selection marker (*URA3*) was used. Digestion of plasmid p5005+URA by the single cut restriction enzyme *Xho*I, localised in the 3' region of *IPF5005* and transformation of *ipf5005* mutant FCCa17, led to insertion of a wild-type *IPF5005* gene at its own locus. These transformants express a wild-type *URA3* gene which is not located at its wild-type locus in this case but at the *IPF5005* locus.

Like previously for *IPF4949*, validation of *IPF5005* allele inactivation was obtained by Southern blotting. DNA of the different strains was digested by *Eco*RI and probed using a 763 bp fragment coming from the digestion of pMosBlue-5005 by *Hin*dIII and *Xmn*I. The labelled probe hybridized in the 5' region of *IPF5005* (Fig. 34). Results from the Southern blot (Fig. 35) are in agreement with the expected sizes (Fig. 34). After the first *IPF5005* inactivation (lanes 3 and 4), a 3.1 kb and a 4.7 kb bands corresponding, respectively, to a wild-type allele and introduction of the Ura blaster cassette into the *IPF5005* locus were observed. The band at 4.7 kb changes to a size of 3.9 kb for strains selected on 5-FOA (lanes 5 and 6). With inactivation of the second allele (FCCa14 and 15), a band of 3.9 kb corresponding to the first inactivated allele and a band at 4.7 kb were expected and obtained (lanes 7 and 8). Finally homozygous *ipf5005* mutants with *URA3* reintroduction (lanes 11 and 12) or without (lanes 9 and 10) presented a single band at 3.9 kb. Reconstruction of a functional *URA3* gene was verified by PCR (data not show). Integration of a wild-type *IPF5005* allele in an *ipf5005* background led to the appearance of 2 bands for the added allele: 3.9 and 2 kb. The second allele of this strain contained a *hisG* repeat, resulting in a band at 3.9 kb (Lane 13); band at 2 kb is present, even if not clearly visible on the photograph (Fig. 35). Thus, heterozygous, homozygous and *IPF5005*-complemented strains present expected profiles, and can be used for phenotypic characterisations.

### 3.2.2.2 Phenotypic analyses

During the inactivation of the second allele of *IPF5005*, I observed that the growth capacity of transformants was reduced compared to the first *IPF4949* inactivation. Once a full set of transformants was obtained (heterozygous, homozygous and complemented strain), growth curves of these mutants were determined in YPD and SD liquid media. Measurements of $OD_{600\ nm}$ (Fig. 36) during the first 9 hours after inoculation revealed a clear reduction of growth of the *ipf5005* strain (FCCa18 and 19), while heterozygous (FCCa14) and complemented strain (FCCa20) behaved like the wild-type strain (CAF2-1). The fact that the *IPF5005*-complemented strain presented the same growth ability as the wild-type strain proved the functionality of the introduced *IPF5005* allele. The generation times in YPD for wild-type, heterozygous and complemented strains were respectively, 1.31, 1.35 and 1.28 h (78.6, 81 and 76.8 min). As expected, the *ipf5005* mutant has the longest generation time of 2.15 h or 129 min, 2.27 h or 136.2 min in isolates FCCa19 and FCCa18. In SD liquid the wild-type strain had a generation time of about 1.5 h (90.2 min), while these values increased for the homozygous mutant to 2.4 h (144.68 min). In both conditions, the ratio between generation times of the *ipf5005* mutant and the wild-type resulted in a value of around 1.6. Thus, complete inactivation of both *IPF5005* alleles increased generation times 1.6 fold.

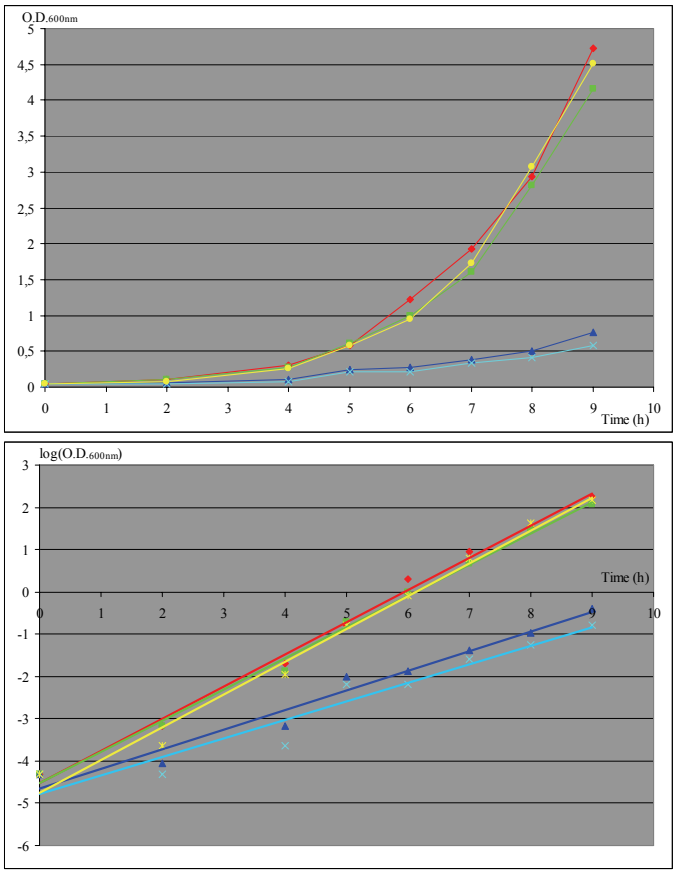


Fig. 36: Growth curve in YPD at 30 °C represented in linear (top) or logarithmic scale (bottom). Wild-type (CAF2-1) is represented in red, heterozygous mutant (FCCa14) in green, homozygous *ipf5005* (FCCa18 and 19), respectively, in dark and light blue, reconstituted strain (FCCa20) in yellow.

Keeping in mind that homozygous mutants do not have the same growth rate as the control strain, sensitivities of these strains to different conditions were explored. Wild-type, *ipf5005* mutant and reconstituted strain were thus spotted on different media (Fig. 37) previously described for sensitivities of *IPF4949* mutant (Fig. 31). In all these conditions, the homozygous mutant FCCa19 presented slower growth compared to the wild-type but inactivation of *IPF5005* did not lead to any particular sensitivity to any condition. Thus, the homozygous mutant shows the same sensitivities as the wild-type strain.

Regarding morphogenesis, inactivations of *IPF5005* led to hypha formation similar to a wild-type strain in liquid induction medium like YPM or YPD + 5 % serum at 37 °C during 2 h of induction. Indeed, only measurements at 60 and 90 min showed a lower number of hyphae, of approximately 20 %,compared to the wild-type (CAF2-1), heterozygous (FCca21) or complemented strain (FCca20). But this difference did not occur after 120 min, where all strains present around 80 % of hyphae. A similar behaviour was observed on solid induction media. After 2 or 3 days on YPM in normoxic conditions (Fig. 38 A) or YPS medium in

embedded conditions (Fig. 38 B), *ipf5005* mutants showed a clear hyphal deficiency compared to the control strain. But the same strain observed after 6 days (Fig. 38 C) presented a number of hyphae equivalent to the wild-type strain. Due to the delay of growth, hyphae were shorter in *ipf5005* mutant. These observations also occurred in hypoxic conditions, but on 5 % serum agar, no particular phenotypes were noticed. As for the *ipf4949* mutant, the impact of *IPF5005* inactivation on thigmotropism was evaluated. It appears that *ipf5005* mutant reacted with the same efficiency as the wild-type strain during contact with ridges. Finally, chlamydospore-formation ability was evaluated, and all *IPF5005* mutants were able to produce chlamydospores like wild-type strain.

All results obtained with the *ipf5005* mutant indicate that this gene is involved in growth but no specific medium was found to reveal a role of this gene in resistance to any stress tested or in morphogenesis.

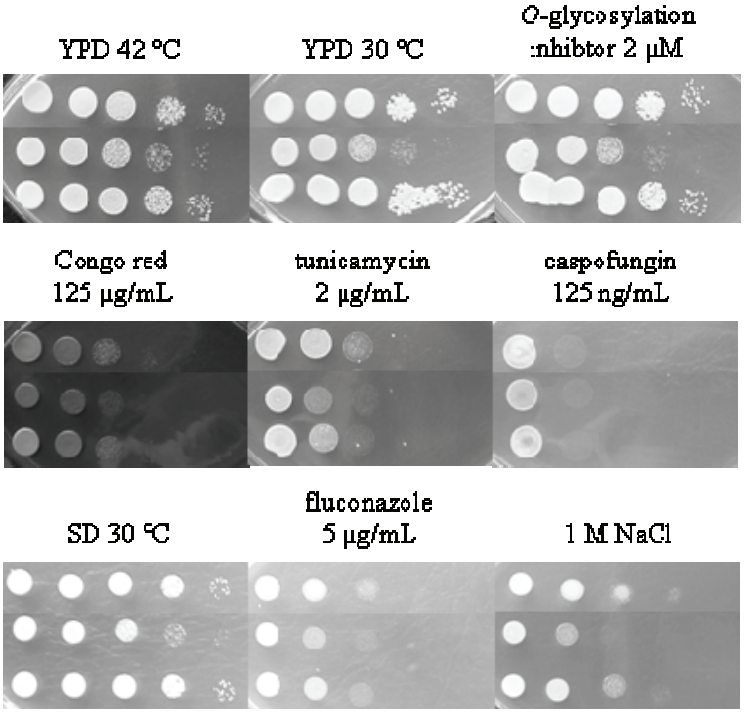


Fig. 37: Sensitivity test of *ipf5005* mutants. Ten fold dilutions (5 µl) of $4x10^7$ to $4x10^3$ cells/ml were spotted on different media. Photographs were taken after 2 days of growth at 30 °C. From top to bottom of each photograph: CAF2-1, homozygous mutant (FCCa19) and complemented strain (FCCa20).

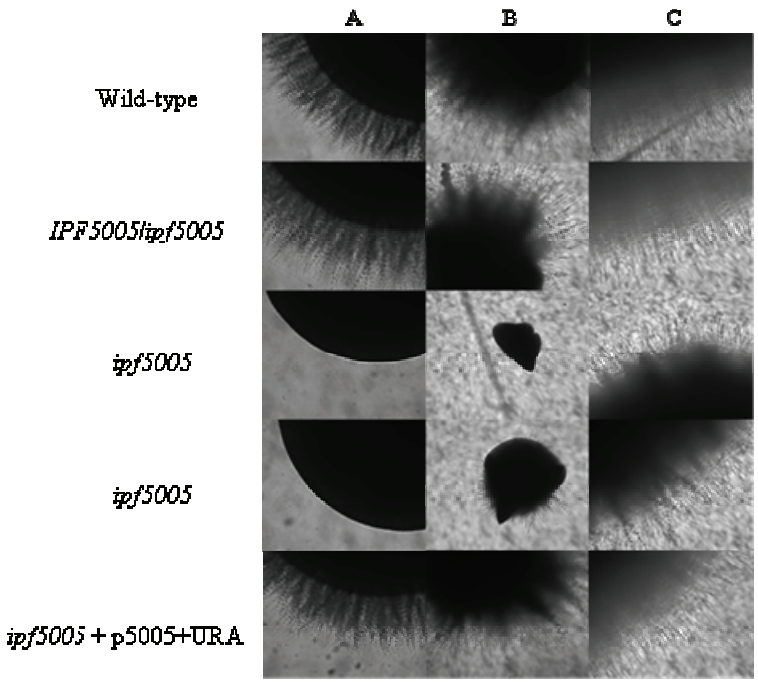


Fig. 38: Morphology of the *ipf5005* mutant in solid induction media. From top to bottom are shown CAF2-1, heterozygous (FCCa21), homozygous (FCCa 18 and 19), and complemented strain (FCCa20) on YPM-medium after 3 days of growth at 37 °C (A), embedded condition after 2 (B) and 6 days of growth (C). Magnification 100x.

### 3.2.3 *NHS1* and *HGT1*

Nhs1p and Hgt1p are two membrane protein of unidentified function, which were discovered previously in our group (S. Delbrück, M. Gerads and J.F. Ernst, unpublished results). Disruption mutants had been produced, but no significant phenotype were described. These mutants were re-analysed in the current work for potential function as environmental sensors.

*NHS1* or *orf19.827* is predicted to encode a protein of 218 a.a. with 1 TM region and a C-terminal cytoplasmic tail of 123 a.a. (Fig. 39). No particular structural domain was identified, and the protein presented no homologue in *S. cerevisiae*, but some in other saccharomycetous species (*Lodderomyces elongisporus*, *Pichia stipitis* or *Debaryomyces hansenii*), in which a function was not identified. *NHS1* was inactivated by the above described Ura blaster cassette. This work and all verification steps were done by M. Gerads (unpublished results) and produced a homozygous mutant: NHSF. This strain was spotted on identical media (Fig. 41) as for sensitivity tests of *ipf4949* and *ipf5005* mutants. Tests were done only at 30 °C during 2 days. After that period, the mutant showed same sensitivities to all drugs as the wild-type strain (CAF2-1). *NHS1* appears not to be involved in temperature, osmotic and oxidative stress or cell wall composition and drug resistance. Hyphal morphogenesis was tested in liquid and on solid induction media including serum, Spider or YPM at 37 °C. Inactivation of *NHS1* did not induce a significant alteration of hyphal formation compared to the wild-type strain (CAF2-1).

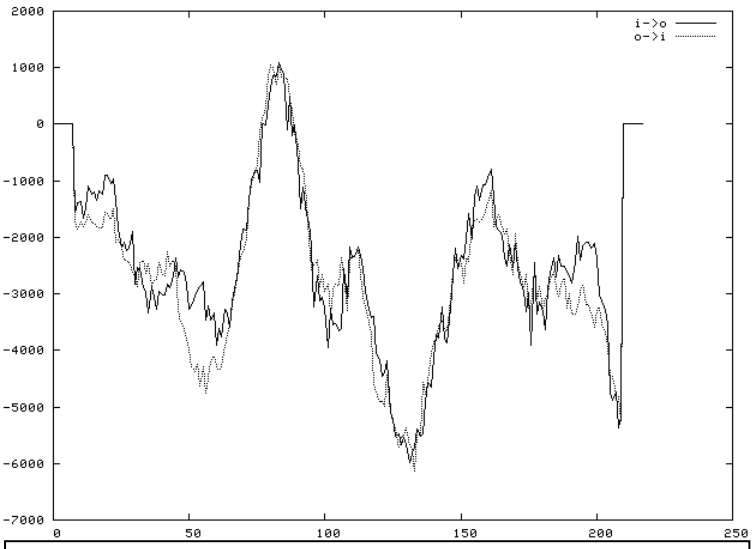


Fig. 39: Topology of Nhs1p of *C. albicans* by prediction plot obtained on Tmpred (http://www.ch.embnet.org/software/TMPRED_form.html). TM domain is represented by area with a value superior to 0 on the graphic.

*HGT1* or *orf19.4527* encodes a 12 TM domain protein of 545 a.a., with a C-terminal cytoplasmic tail of 66 a.a. (Fig. 40). Motifs of sugar transporters were identified in this protein, which agrees with the fact that it is the homologue of the glucose transporter *HXT11* of *S. cerevisiae*, localised in plasma membrane. Like for *NHS1*, inactivation of *HGT1* by Ura blaster cassette was realised by M. Gerads (unpublished results) to produce a homozygous mutant: 1HB3G. The same media as for *NHS1* characterisation were used to evaluate the drug sensitivities of an *hgt1* mutant. This mutant presented identical

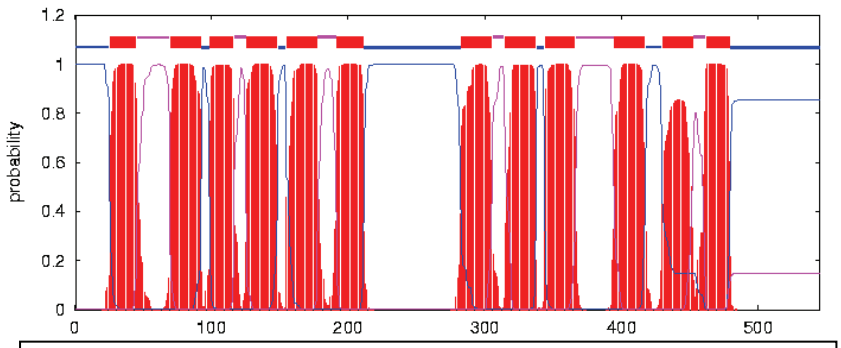


Fig. 40: Predicted topology of Hgt1p of *C. albicans*. Best topologic probability is represented on top of the graph. Region turned to the inside of the membrane is in blue, and in purple if turned to the outside of the membrane. Transmembrane (TM) region are drawn as red bars.

phenotypes as the wild-type strain (CAF2-1) (Fig. 41). *HGT1* seems not to be involved in all stress conditions tested. The capacity to differentiate hyphae was tested on liquid and on solid induction media including serum, Spider or YPM at 37 °C. Similar to sensitivity tests, an *hgt1* mutant induced no significant alterations of hyphal formation compared to the wild-type strain (CAF2-1). Thus, until now, no condition tested revealed a significantly role of *NHS1* and *HGT1*.

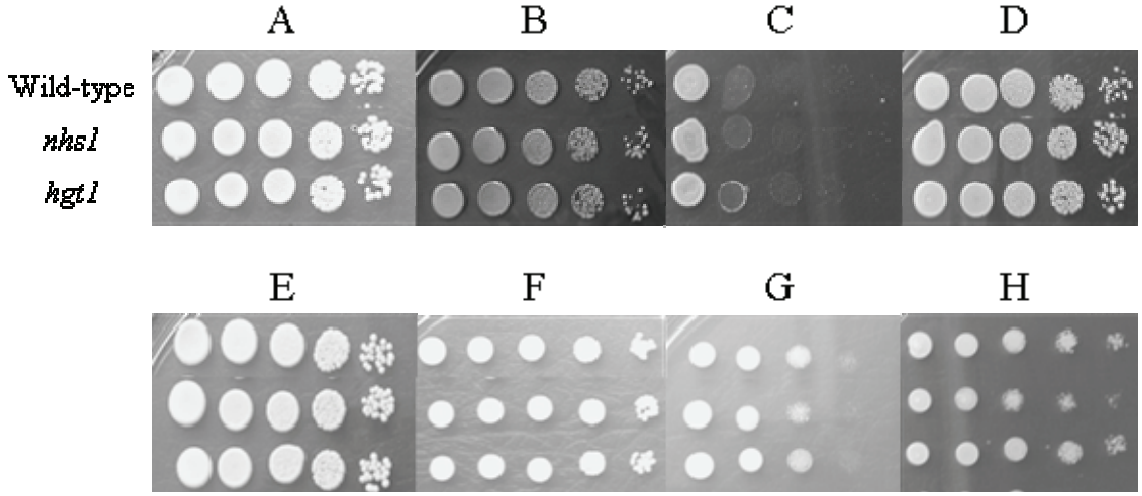


Fig. 41: Sensitivity test of *nsh1* and *hgt1* mutants. Several dilutions (5 µl) of suspension $4x10^7$ to $4x10^3$ cells/ml were spotted on different media: YPD (A) with Congo red 125 µg/ml (B), caspofungin 125 ng/ml (C), tunicamycin 2 µg/ml (D), *O*-glycosylation inhibitor 2 µM (E) or SD (F) containing fluconazole 5µg/ml (G), NaCl 1 M (H). Photographs were taken after 2 days of growth at 30 °C.

# 4. Discussion

## 4.1 *MSB2*

*MSB2* in *S. cerevisiae* was identified by different screening protocols for suppressors of a temperature-sensitive (ts-) *cdc24* mutation (Bender *et al.*, 1992), cross-talk with osmotic stress pathway activation (O'Rourke *et al.*, 2002) and filamentation depending of Ste12p (Cullen *et al.*, 2004). Furthermore, its role in an osmotic stress signalling pathway including Hkr1p was described (Tatebayashi *et al.*, 2007). By protein sequence comparisons it appeared that Msb2p but also Hkr1p possess a unique homologue in *C. albicans*, which is the protein encoded by *orf19.1490*. From all screenings realised in *C. albicans* (transcriptional analyses), this gene had been found to be regulated in only one condition: the *CaMSB2* transcript level was 3.4-fold down-regulated in a *rim101* mutant relative to a wild-type strain at 30 °C in YPD and a pH of 7.4 (Lotz *et al.*, 2004).

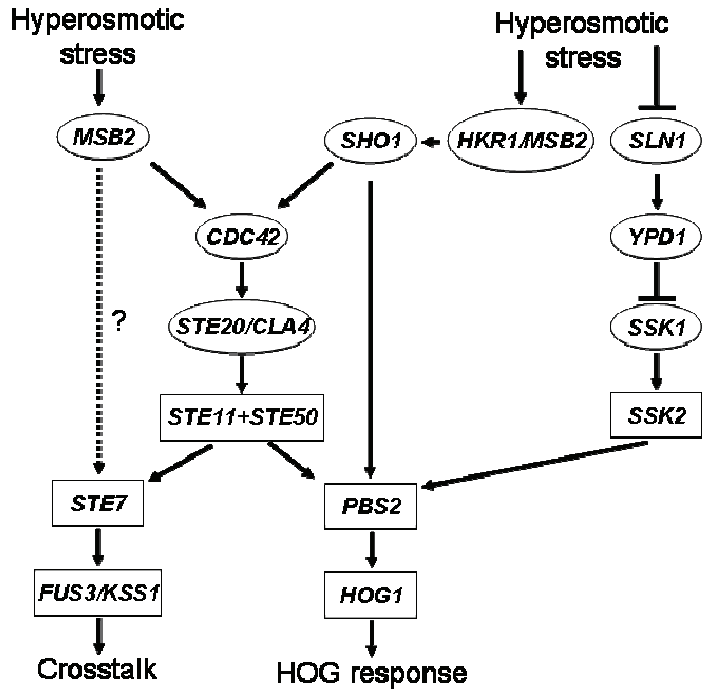


Fig. 42: Scheme of Msb2p function in HOG and crosstalk pathways in *S. cerevisiae*. Based on model from Tatebayashi *et al.* (2007).

Models of ScMsb2p function in osmotic sensing (Fig. 42) show that this protein is also acting in parallel of the main Hog pathway, by its role on Pbs2p activation through Ste11p. This explains why this gene did not appear in some screenings in a wild-type strain. Indeed, *msb2* mutants will express a significant phenotype only, if the main Hog pathway dependent on Sln1p is inactivated. To investigate if these functions are conserved in *C. albicans*, *MSB2* was inactivated by the Ura blaster or SAT-flippase cassettes. The set of mutants produced with the Ura blaster was reconstituted by integration of the *URA3* wild-type allele at its own locus. This avoids any secondary phenotypes due to an abnormal level of *URA3* gene expression, which is known to be dependent on its genomic environment (Staab *et al.*, 2003). It is important to notice that during the process of inactivation, use of 5-FOA is not neutral because it can induce genomic alterations (Wellington *et al.*, 2006). Therefore, analyses were done on 2 independent homozygous mutants and similar phenotypes obtained strongly suggested that no other genomic alterations than *MSB2* inactivation were present. Reintroduction of a wild-type allele in the *msb2* homozygous mutant failed for unknown reasons.

*Morphogenesis*

ScMsb2p was clearly described as an osmosensor, but it also plays a role in morphogenesis (Cullen *et al.*, 2004). In case of *C. albicans*, dimorphism is critical for virulence (Mitchell, 1998). It appeared that inactivation of *MSB2* leads to a decrease in hypha formation but only on certain solid induction media. The importance of Msb2p in

filamentation was evident in hypoxic or embedded conditions, when $O_2$ availability is low, and on Spider and YPM agar in normoxic conditions, which contain mannitol as the signal inducing hyphal differentiation. The fact that YPD or YP agar did not induce hypha formation of wild-type strains, while morphogenesis was possible on YPM agar reveals a role of mannitol in hyphal differentiation. Although the impact of Msb2p on morphogenesis was clear on agar, it was completely absent in liquid induction media. At least two hypotheses may explain this fact: (1) Msb2p function depends on contact with the agar surface, (2) high density of cells after 3 to 4 days of growth on agar, which locally may alter medium composition. Until now, the exact function of Msb2p in morphogenesis is not solved.

Interestingly, when *MSB2* was inactivated in a wild-type or *sho1* background, the hyphal deficiency was similar, but in a *ssk1* background (which alone led to hyperfilamentation), inactivation of *MSB2* result in complete absence of hyphae. To explain these results, we can use the previous model of MAPK activation (Fig. 2) and hypothesize that Msb2p function is closely linked to Sho1p. Following this hypothesis, Msb2p is implicated in the Cek1p pathway. Furthermore, Ssk1p is known to be implicated in Hog1p activation which is a repressor of hypha filamentation (Eisman *et al.*, 2006). Hyperfilamentation obtained in an *ssk1* mutant is due to the fact that the repression of Hog1p on morphogenesis is removed. A single *hog1* mutant is also hyperfilamentous (Eisman *et al.*, 2006). All previous result can be summarise in a model (Fig. 43), where Sho1p and Msb2p are acting positively on Cek1p pathway but also repressing Hog1p activation. In this condition, inactivation of *MSB2* and/or *SHO1* leads to a decrease in Cek1p activation but also in Hog1p repression, which induces a reduction in hyphae formation. Regarding the *ssk1* mutant, in this strain Hog1p residual activatity is strongly repressed by Msb2p and Sho1p, its repression on morphogenesis is removed and induces a stronger hyphal differentiation. To explain the total absence of hyphae in a triple mutant *ssk1 sho1 msb2*, an activation of Hog1p through a Ssk1p-independent pathway or a basal activity are hypothesised, like it is the case for the osmotic stress response, which is for a part Ssk1p-independent (Chauhan *et al.*, 2003). This basal activity of Hog1p repression and the absence of Cek1p activation pathway leads to a non-filamentous strain.

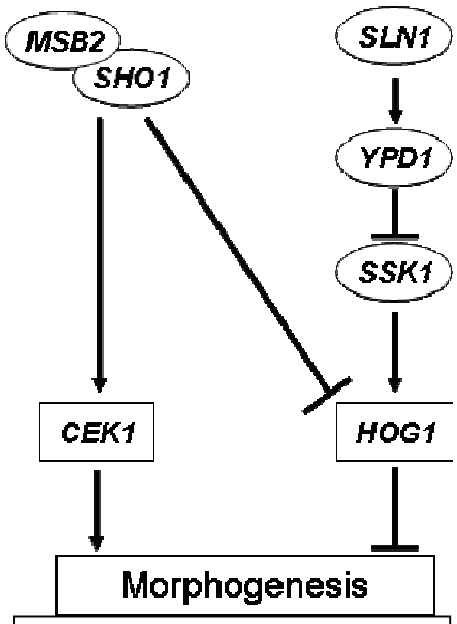


Fig. 43: Schematic model of morphogenesis regulation in *C. albicans*.

Nevertheless, this model presents some incoherence as it predicts that a *cek1 hog1* mutant should present a deficiency in hypha formation. This is not known, however, a *cph1 hog1* mutant has a phenotype close to a single *hog1* mutant (Eisman *et al.*, 2006), while a *cph1* mutant present a decrease in hypha formation, like for a *cek1* mutant. This phenotype is understable by the fact that Cph1p is downstream of Cek1p in the same pathway. These results suggest that another pathway is involved in hypha formation, which is independent of Cph1p and Hog1p. To incorporate these results a new model was conceived (Fig. 44), where Sho1p and Msb2p activate Cek1p during morphogenesis, while inactivation of one or both of these genes leads to a decrease in Cek1p phosphorylation and in hypha formation. However, *sho1*, *msb2* or *sho1 msb2* mutants are still able to form hyphae, although with reduced efficiencies suggesting the presence of a second pathway ("X" in model). Msb2p and Ssk1p are probably both involved in activation of a pathway that is Cek1p- and Hog1- independent.

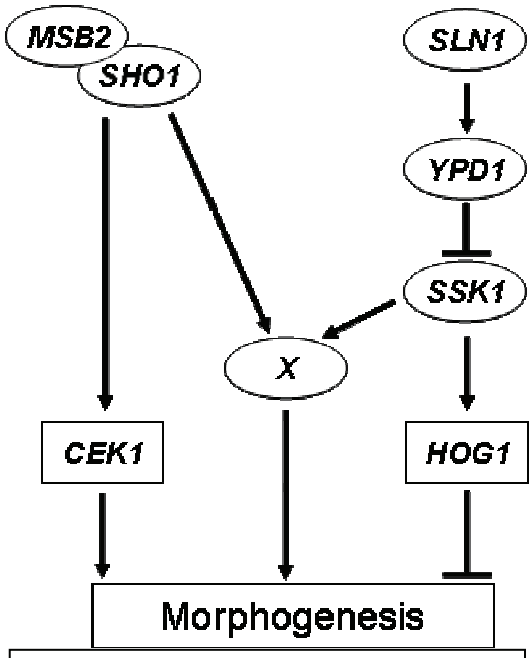


Fig. 44: Alternative model of morphogenesis regulation in *C. albicans*.

This hypothesis can explain the residual hypha formation of a *msb2* mutant, due to residual activation of the second pathway by Ssk1p. The complete absence of hyphae in a *ssk1 msb2* mutant can be understood by the fact that the Cek1p pathway and the second pathway (X) are inactivated.

This model explains results obtained in normoxic, hypoxic and agar-embedded condition on plates. But it raises also the question on the identity of the second pathway implicated in hypha formation. The PKA pathway acting through Efg1p (Tebarth *et al.*, 2003) could have contributed to this second pathway. But introduction of plasmid over-expressing *EFG1*, *TPK1* or *TPK2* genes did not complement the hyphal deficit of an *msb2* mutant strain. A second series of experiments showed that on YPM agar, an *efg1* mutant presented strong hyphal deficiencies and that this effect was even stronger when *MSB2* was inactivated in this background. These results implied PKA pathway in filamentation on YPM medium. A *cek1 msb2* mutant presented a stronger deficit in hypha formation than a single *cek1* mutant strain, which confirms that Msb2p, in agreement with our model (Fig. 44), is not only acting in Cek1p pathway but also in a second pathway. Furthermore, inactivation of both MAPK and PKA pathways as in an *efg1 cph1* mutant leads to the total absence of hypha on different media (Lo *et al.*, 1997) as observed for a *ssk1 msb2* mutant. This observation also confirms our model, where Msb2p is acting on MAPK and on a second pathway which may be identified as the PKA pathway. This model explains results obtained on YPM agar in normoxic conditions or embedded and hypoxic conditions, but not the results in liquid induction, which involved propably other proteins. As previously described, Msb2p is not involved in liquid induction.

Regarding other aspects of morphology in these mutants, absence of particular phenotypes regarding thigmotropism is in agreement with current knowledge. Indeed, only mutants affected in $Ca^{2+}$ uptake were demonstrated to have a different response to contact stimuli (Brand *et al.*, 2007), and Msb2p, Sho1p and Ssk1p are not known to have any function in calcium transport.

For chlamydospore formation, while Msb2p appears to not be involved, the *SSK1* gene showed a critical role, since its inactivation induced the complete absence of chlamydospores. But this phenotype results from different reasons in single or double *ssk1* mutant. Indeed, single *ssk1* mutant led to the absence of chlamydospores on hypha suspensor cells like for a *hog1* mutant (Eisman *et al.*, 2006), while *ssk1 msb2* and *ssk1 sho1 msb2* mutant were unable to produce chlamydospores probably due to the fact that these mutants were altered in the differentiation of hyphal suspensor cells. Indeed, as discussed above double and triple *ssk1* mutants were non-filamentous in hypoxic conditions and chlamydospore induction uses a microaerophilic environment. In this condition *ssk1 msb2* and *ssk1 sho1 msb2* strains do not differenciate hyphae, which induce an absence of chlamydospore.

*Resistance*

Msb2p was shown to be implicated in morphogenesis, which is a particularly important process in pathogenicity (Roman *et al.*, 2007). In addition, it was interesting to establish the role of Msb2p in drug sensitivities. Results in sensitivity tests obtained for azoles (ergosterol inhibitor; Borgers, 1980), or hygromycin B (protein synthesis inhibitor; McGuire *et al.*, 1953) revealed no or only a limited role of Msb2p in resistance. While a single *msb2* mutant did not present particular sensitivity, inactivation of this gene in *sho1* or *ssk1* background led to a weak increase of the sensitivity to certain azole compared, respectively, to *sho1* and *ssk1* mutant.

Responses to temperature and oxidative stresses did not require Msb2p, since mutants behaved like the wild-type strain. Results on oxidative stress, presence of 5 mM $H_2O_2$, were confirmed by the study of Hog1p phosphorylation in different *msb2* mutants (Roman *et al.*, submitted paper). In this experiment, Hog1p phosphorylation was not altered in an *msb2* mutant in presence of hydrogen peroxide, while this occurs in an *ssk1* mutant. Furthermore, no growth deficiencies were observed at any temperature described between 16 and 42 °C.

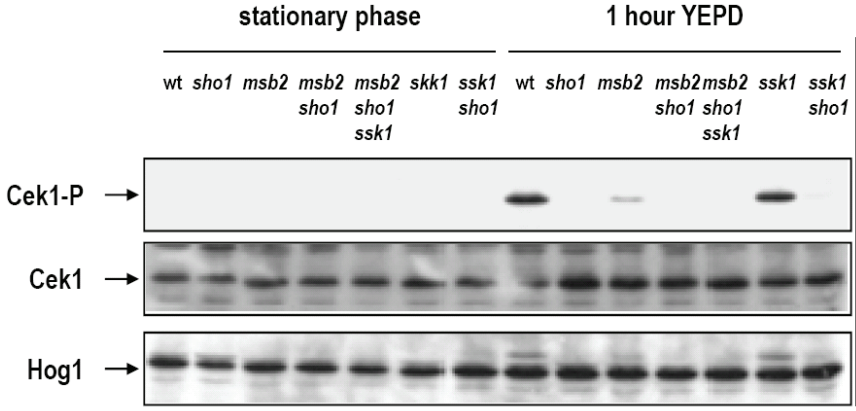


Fig. 45: Cek1p phosphorylation during resumption of growth of the indicated strains. Cek1p and Cek1p phosphorylated forms were detected by blotting the membranes respectively against anti-CaCek1 and anti-phospho-p44/42 antibody. From E. Roman.

Regarding cell wall composition, Msb2p appears to play a significant role. Indeed, inactivation of *MSB2*, in wild-type, *sho1* or *ssk1* backgrounds induced an increase of sensitivity, in all tested conditions leading to cell wall perturbation, as induced by addition of Congo red, calcofluor white, caspofungin or after a 55 °C heat shock. Following previous models, where Msb2p is involved in the Cek1p pathway (Fig. 44), our result on Congo red sensitivity correlates with sensitivity of a *cek1* mutant to Congo red (Eisman *et al.*, 2060). The facts that *cek1*, *msb2* and *sho1* mutants presented significant sensitivities to Congo red suggest that they are implicated in the same process. Furthermore, *sho1 msb2* double mutants show a higher sensitivity than single mutants, which implies both Sho1p and Msb2p in an activation pathway of Cek1p to induce Congo red resistance. Regarding the *ssk1* mutant, this strain is more resistant to Congo red than a wild-type strain, which implies that Cek1p is more activated. This observation indicates that, in a wild-type strain, Ssk1p acts a repressor on Cek1p. This regulation is probably not direct, but mediated through Hog1p, which was demonstrated to repress Cek1p (Eisman *et al.*, 2006). Until recently, only genetic evidence existed for the role of Sho1p and Msb2p in Cek1p activation. Latlely, it was demonstrated that these two proteins are involved directly in Cek1p phosphorylation (Roman *et al.*, submitted paper). A simple test to evaluate this effect is to study Cek1p phosphorylation during resumption of growth from an overnight-culture to a fresh medium. In this condition, Cek1p is known to be phosphorylated, but in the absence of Sho1p or Msb2p a clear decrease of phosphorylation was observed (Fig. 45), while an increase was observed for *ssk1* or *hog1* mutant (Eisman *et al.*, 2006). These results permit to define a model of regulation of Cek1p

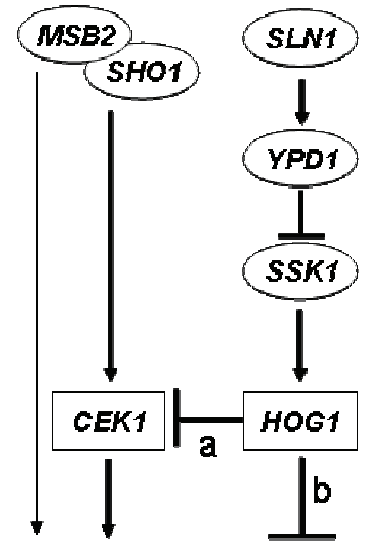


Fig. 46: Schematic model of cell wall biosynthesis regulation in *C. albicans*.

phosphorylation regarding cell wall biosynthesis (Fig. 46). The role of Hog1p was demonstrated in Cek1p phosphorylation during resumption of growth (Eisman *et al.*, 2006). This effect could also occur in cell wall resistance (way "a" on Fig. 46) or not (way "b on Fig. 46) to explain higher resistance of *ssk1* and *hog1* mutants to Congo red.

Other results also implicated an *msb2* mutation with Congo red sensitivity. Following our hypothesis, Msb2p is acting up-stream of Cek1p and inactivation of *MSB2* in a *cek1* background should not lead to additional phenotypes compared to a single *cek1* mutant. However, a double mutant *msb2 cek1* actually showed a stronger sensitivity than single mutants (Fig. 23). Two hypotheses can be formulated to explain this result: the first implies Msb2p in activation of a second pathway acting in Congo red sensitivity (thin ligne on Fig. 46); the second that Msb2p is by itself a structural compound of the cell wall and not just a sensor. It is known that Msb2p in *S. cerevisiae* is localised in the plasma membrane and that its external domain possibly forms a huge structure. In such a case, in *C. albicans* Msb2p could function in cell wall stability. To discriminate, which hypothesis is the most relevant, a construction expressing Msb2p without C-terminal tail could be introduced in a *cek1 msb2* background. Restoration of a *cek1* single mutant phenotype will reveal the structural function of Msb2p in the cell wall. This hypothesis can correlate results from mucine Muc1p of mammalian cells, where the C-terminal part can be cleaved and addressed to the nucleus for binding to transcription factor (Cullen, 2007). In such a case for Msb2p, we could imagine a model where the C-terminal part of Msb2p is essential for transducing the signal, while the extracytoplasmic domain is used for cell wall stability.

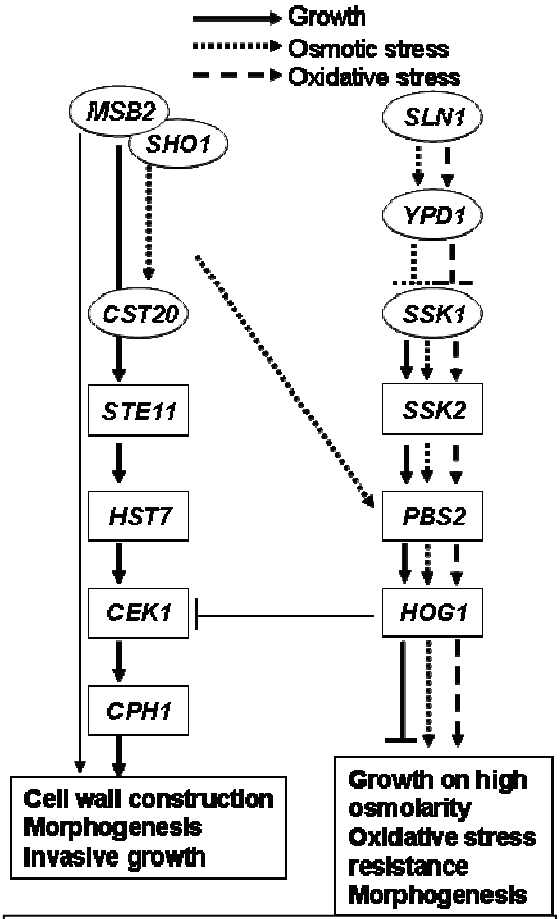


Fig. 47: Schematic model of Msb2p function in *C. albicans* pathway.

*msb2* mutation also affected sensitivity to osmotic stress. Indeed, inactivation of *MSB2* in a *ssk1* background led to strong sensitivity to 0.5 M NaCl. It had already been described that Sho1p, as a member of the Cek1p pathway, was also acting on Hog1p pathway, in a *ssk1* background, during an osmotic stress (Roman *et al.*, 2005), in agreement with the model proposed for the role of Msb2p in *S. cerevisiae* (Fig. 42) and from our model in *C. albicans*. Results obtained by the group of J. Pla about the role of Sho1p in Hog1p activation pathway are summarised in Fig. 2. However, in this model, Sho1p activates Hog1p through the interaction between Ste11p and Pbs2p, while in a recent paper (Cheetham *et al.*,

2007) it was demonstrated that Ste11p is not involved in Pbs2p activation, which seems to be exclusively activated by Ssk2p. This observation implies that Sho1p acts on the Hog1p pathway through compounds up-stream of Ste11p, but also down-stream of Ssk1p. If this were not the case, then a *ssk1 msb2* or *ssk1 sho1* mutant would not present identical phenotype as a single *ssk1* mutant. These considerations led us to design a new model of interaction between Cek1p and Hog1p pathways (Fig. 47) including all previous results. For reason of clarity, the second pathway implicated in hyphal differentiation (Call X on Fig. 44) and activated by Msb2p and Ssk1p is not represented on this scheme. This model summarises all results regarding morphogenesis, oxidative stress, as well as osmotic and cell wall sensitivities. It appears that Msb2p is not involved in oxidative stress, but plays a role in morphogenesis and osmotic stress. How Msb2p senses osmotic stress is unknown, but in *S. cerevisiae* it is hypothesised that a highly glycosylated STR domain could form a kind of organic polymer gel (Tatebayashi *et al.*, 2007), which is sensitive to osmotic conditions (Tanaka *et al.*, 1980). This reaction could lead to a structural modification of the protein and transduce a signal through other proteins. The fact that STR domain is relatively conserved in *C. albicans* suggests a similar way of action for Msb2p.

*Altered cell wall composition*

Cell wall weakness was clearly identified in different *msb2* mutants. Results from cell wall composition show that inactivation of *MSB2* induced an increase of chitin level as for the *sho1* mutant, while additional inactivation of *SSK1* led to a decrease compared to wild-type strain. These levels of chitin were in agreement with sensitivity to Congo red, because a higher level of chitin has been linked to a higher sensitivity to Congo red (Imai *et al.*, 2005). Furthermore, in *sho1* and *sho1 msb2* mutants, different genes for chitin synthases were up-regulated. Interestingly, a *msb2* mutant did not show any gene implicated in chitin synthesis that was significantly regulated, although a clear phenotype of sensitivity to Congo red was observed. One hypothesis is that some genes regulated in the *msb2* mutant compared to the wild-type strain and without identified functions (*orf19.5270*, *orf19.3376*) could be involved in chitin synthesis.

Regarding glucans, β-1,3- and β-1,6-glucans were oppositely regulated. Inactivation of *SHO1* or *MSB2* led to an increase of β-1,3-glucan to the detriment of β-1,6-glucan, while the exact inverse observations were obtained during *SSK1* inactivation. The high sensitivity of *sho1* and *msb2* mutants to caspofungin could be due to the fact that β-1,3-glucans are inhibited and that β-1,6-glucan level is to a low to rescue the loss of the β-1,3-glucan network. Increase of β-1,6-glucan in a *ssk1* mutant lead to resistance to caspofungin. Results obtained by microarray transcriptional analysis regarding genes involved in glucan synthesis were more difficult to interpret because of a high number of regulated genes. Nevertheless, these data shows clearly that the glucan pathway regulation is altered compared to a wild-type.

Mannoproteins were in all mutants, except the *sho1* mutant, less represented than in a wild-type strain. Results of protein and mannan levels were correlated and in accord with the fact that some genes encoding protein localised in the cell wall were down-regulated. Collectively, results between cell wall composition, sensitivities and genes regulation are demonstrating a weakness of cell wall formation in *msb2* mutants. The process of Msb2p action on gene regulation is not known at present, but my experiments suggest that this regulation could occur through the Cek1p pathway.

*Gene regulation*

In addition to regulated genes implicated in cell wall synthesis, microarray data showed other pathways significantly regulated in *sho1* and *sho1 msb2* mutant. Even if these regulations are difficult to understand with phenotypes that were described until now, it

appeared anyway that inactivation of *MSB2* in a *sho1* background significantly altered overall gene regulation, while single *msb2* mutation affected few genes. According to our model, Sho1p and Msb2p are collaborating in the same pathway. Thus, we can hypothesise that inactivation of one of these 2 genes is partially rescued by the presence of the second. But in the case of a *sho1 msb2* double mutant, an entire pathway of activation of Cek1p pathway is completely lost and in such a case, a complete reorganisation of gene regulation is understandable. This observation indirectly proves the roles of Sho1p and Msb2p in a common pathway.

Regarding microarray validity, the qRT-PCR results realised on 4 gene transcripts confirm the regulation ratio. Values for ratios of regulation were not strictly identical, but microarray results are used to give a tendency more than a quantitative value, which is the aim of a qRT-PCR experiment. Furthermore, the fact that Cy3 and Cy5 are not incorporated equally in cDNA is a source of variation (Yang *et al.*, 2002).

Msb2p was shown to be involved in Congo red resistance and to be implicated in Cek1p pathway activation. The hypothesis of positive regulation of *MSB2* by the presence of Congo red was confirmed by qRT-PCR. We found that the *MSB2* transcript level was 1.4 fold higher in a strain grew with Congo red than without. This regulation is moderate, but it is in agreement with the idea of Msb2p acting as sensor. Furthermore, another result supporting this idea was the level of the *MSB2* transcript, which represented only 0.8 % of the level of *ACT1*. Sensors are supposed to not be major components of the plasma membrane, therefore such a low level of expression is in agreement with a protein needed in sensing but not in major tasks for structure and function. If we expect from a sensor not to be strongly regulated, this need not be the case for downstream elements which have to amplify the initial signal. Thus, we found that the expression level of *CEK1* was 3 fold up-regulated in the wild-type strain in the presence of Congo red compared to a standard YPD culture (data not shown). These results confirm a role of both Msb2p and Cek1p in Congo red resistance.

*Protein partner*

By classical and split ubiquitin 2-hybrid screenings, it was not possible to identify any protein partners of Msb2p. Specific interaction between Cdc42p and the C-terminal part of Msb2p, or Sho1p and Msb2p were also negative, while direct links were found in *S. cerevisiae* (Cullen *et al.*, 2004). As in yeast, co-immunoprecipitation has helped to identify Msb2p partner proteins. But until now labelling of Msb2p in *C. albicans* with HA or GFP tag at the C-terminus appeared to produce a non-functional protein, as has been observed for *S. cerevisae* (Cullen *et al.*, 2004). Therefore, insertion of a tag inside the extracytoplasmic domain should be done. Such construction will help to establish which of the 5 Pmt isoforms is involved in Msb2p glycosylation. By phenotypic similarites in YPM induction medium or similar Congo red and caspofungin sensitivities between *msb2* and *pmt* mutants, it appears that the best candidate for Msb2p glycosylation is Pmt4p (Prill *et al.*, 2005). Interestingly, while no particular sensitivity for *msb2* mutants was observed to *O*- or *N*-glycosylation inhibitors, regulation of *MSB2* in a wild-type strain in presence of these drugs showed a significant down-regulation of 0.6 fold. This result inducates that the level of glycosylation is important for *MSB2* regulation, as it was shown in *S. cerevisiae* (Tatebayashi *et al.*, 2007). A decrease in the glycosylation level of Msb2p could induce an increase of its activity, and a down-regulation in the presence of *O*- or *N*-glycosylation inhibitor is understable, because cells need less protein for an equivalent activity. Such hypothesis implies that in a *pmt4* mutant, phenotypes should be opposite to those of a *msb2* mutant, due to the hperactivity of Msb2p. But this did not occur and we can hypothesise that the function and regulation of *MSB2* are separate, maybe by interaction with specific partner.

In conclusion, Msb2p in *C. albicans* appears to be involved in cell wall formation and in morphogenesis by activating the Cek1p pathway. In an *in vivo* model of infection (mouse), inactivation of *MSB2* in a wild-type background did not lead to a different virulence than control strains, while a *msb2* mutation in a *ssk1* or *sho1* background increase the virulence (Roman *et al.*, submitted paper). These observations were not expected due to the facts that in these background, inactivation of *MSB2* leads to a decrease in hypha formation and weaknesses of the cell wall compared to the single mutant, which are two phenotypes involved in pathogenicity (Mitchell, 1998; Norice *et al.*, 2007). Nevertheless, we demonstrate that inactivation of *MSB2* in a *sho1* mutant altered significantly gene regulation *in vitro* and an identical situation could occur *in vivo* to activate pathways involved in pathogenicity like adhesion. It was demonstrated that Als3p and Als9p, which are upregulated in *sho1 msb2* mutants, play a role in adhesion and biofilm formation (Phan *et al.*, 2007; Zhao *et al.*, 2007).

## 4.2 Bioinformatics approach

The research of putative sensor by a bioinformatics approach was based on the structure of identified sensor (several TM domains, cytoplasmic C-terminal tail). Following these hypothesis, we defined a list of candidates and produce homozygous mutant for some of them. As described below, only one protein presents phenotypic similarity with sensors. This reveals that our first assumptions where not suffisant to characterise a sensor, and that a better definition of a sensor is needed. The example of Msb2p shows that a sensor can present another topology that what we used in our bioinformatics approach.

*IPF4949*

This candidate issue from the list of putative sensor was selected for its common characteristic with transceptors, consisting of 12 TM domains and a long cytoplasmic C-terminal tail. Other candidates presented identical profiles, but *IPF4949* was predicted to encode the longest C-terminal tail. Even if this gene presented no overall homology to any other known protein, it appeared to share specific homologies with domains of $Ca^{2+}/H^{+}$ antiporters. This gene is fungal-specific. After inactivation of both alleles, mutants showed aberrant phenotypes in only two conditions, i.e. defective morphology in Spider and Lee's medium. These phenotypes appeared during the first day of incubation, but during longer time hypha were also differentiated. This may be due to the fact that after several days on agar plate, the local medium is altered and other mechanisms of hypha formation can be used. Ipf4949p could play a role during the initial steps of colonisation. The fact that in liquid induction media, no particular phenotype of the *ipf4949* mutant was observed indicates that Ipf4949p is required on solid media. The absence of sensitivity to any drugs and the mutant phenotype in certain hypha induction media describe Ipf4949p as a putative specific sensor for morphogenesis.

*IPF5005*

*IPF5005* was selected for its absence of homology with other yeast genes and seems to be specific to *C. albicans*. Recently this gene was characterised as possible false ORF (CGD, http://www.candidagenome.org/). But inactivation and introduction of a wild-type allele to complement a homozygous mutant strain described here proved the existence of a functional protein encoded by the *IPF5005* gene. In fact, the function of Ipf5005p appears required for cell growth. Until now, all media tested with or without drug showed a decrease of growth rates of a *ipf5005* mutant. Gene inactivation induced an increase of the generation time of 1.6 fold compared to the wild-type strain. These results are in agreement with data implicating

*IPF5005* as an up-regulated gene during resumption of growth at 30 and 37 °C (Enjalbert *et al.*, 2005).

Slowed growth induced some apparents sensitivities to different drugs, but taking into accound the growth deficiency, no particular sensitivity was observed on any medium. The same conclusions were possible for morphogenesis experiments. Thus, delay in morphogenesis appears related to slower growth compared to the wild-type strain. These results lead to the conclusion that Ipf5005p is not a sensor.

*NHS1 and HGT1*

*NHS1* and *HGT1* were already inactivated in other context in our group the presence of, respectively, 1 and 12 TM domains in their predicted sequence made them candidates to be localised in a membrane. Furthermore, they presented a cytoplasmic C-terminus of 123 and 66 a.a. Our characterisations did not provide significant phenotype for each mutant. *nhs1* and *hgt1* mutants were re-analysed for a sensing function, but no medium used during our studies showed a particular sensitivity or morphogenesis phenotype. We can conclude that none of these 2 candidates are sensors.

# 5. Summary

The high capacity of *Candida albicans* to adapt to various environments requires sensors detecting multiple environmental signals. Because few sensors are known, we used two strategies to identify new sensors. First, we characterised a homologue of a recently described membrane sensor in the yeast *Saccharomyces cerevisiae*, Msb2p, which stimulates filamentation by interaction with the Sho1 protein. Second, we studied four candidates of sensors predicted by a bioinformatics approach.

In *C. albicans* the formation of hyphae requires activation of the MAP kinase Cek1p via a Sho1p-dependent pathway, while another MAP kinase, Hog1p, represses filamentation and mediates osmotic protection upon activation by the Ssk1p protein kinase. Inactivation of both *MSB2* alleles in *C. albicans* led to defective hypha formation on mannitol-containing agar, in normoxic, hypoxic or embedded conditions. Such phenotypes worsened in a *msb2 sho1* double mutant, while an *msb2 ssk1* double and a *msb2 sho1 ssk1* triple mutant showed a complete absence of hyphae. These results suggested that in the absence of Ssk1p signalling, both Msb2p and Sho1p proteins control hypha formation not only via Cek1p, but also by the Hog1p pathway. In agreement of such cross-talk between both MAP kinase pathways activated by Msb2p, a *msb2 cek1* double mutant was more defective in hypha formation than the corresponding single mutants. Furthermore, while a *msb2* mutant was not osmosensitive, a *msb2 ssk1* double mutant showed increased sensitivity compared to a *ssk1* mutant, again implicating Msb2p in activation of Hog1p. *MSB2* disruption also led to higher sensitivities to cell wall-damaging compounds, including Congo red, calcofluor and caspofungin. These results match cell wall alterations in a *msb2* mutant, which contained increased levels of chitin and β-1,3-glucan but lower levels of β-1,6-glucan. Furthermore, transcriptomal analyses revealed several genes involved in glucan and chitin biosynthesis regulated jointly by Msb2p and Sho1p proteins. Thus, Msb2p appears to represent an important environmental sensor in *C. albicans* grown on solid surfaces, leading to increased filamentation, osmotic resistance and maintenance of normal cell wall structure.

Known sensors contain several transmembrane regions and extended cytoplasmic tails. By a bioinformatics approach the theoretical genome-wide proteome of *C. albicans* was searched for genes encoding putative sensor proteins and four genes were selected and analyzed (*orf19.7670*/*IPF4949*, *orf19.6650*/*IPF5005*, *orf19.827*/*NHS1*, *orf19.4527*/*HGT1*). Deletion of *IPF4949* alleles showed a delayed hyphal morphogenesis on certain solid induction media, suggesting that the encoded protein contributes to morphogenesis by a yet unknown mechanism. Deletion of *IPF5005* did not show particular phenotypes except a significant retardation of growth, while deletions of *NHS1* and *HGT1* appeared normal with respect to all phenotypes. It is concluded that known structural features of sensors are not sufficient to identify novel sensors by a bioinformatics approach.

# 6. Thanks

First of all,

I would like to thank Prof. Joachim Ernst to have trusted me and for all his advice during my PhD. I'm particularly thankful to Dr. Christophe d'Enfert who helped me with my Masters degree and also to find a place for my PhD work. From the same laboratory, I want to thank Dr. Sophie Goyard for her support and all her ideas. My tutor Prof. Alistair Brown was also a really good support by his advices and optimism about my results.

I want to thank also all the members of the Galar Fungail 2 consortium: Prof. Bernhard Hube and Abigail Mavor, Prof. Frans Klis and Grazina Sozinska, Prof. Claude Gaillardin and Michael Weyler, Emilia Moreno-Ruiz, Prof. Rafael Sentandreu, Prof. Anna Vieccharelli and Franck Skrzypek, Prof. Angel Dominguez and Rita Rodrigues.

But this list would not be complete without the two other members of the French group, with whom I had always fun everywhere in the world. To all our pictures, drinks, jokes and travels a special thanks to Brice «Berserker» Enjalbert and Samuel «Hellspirit» Gelis.

For technical, administration support and a lot more, I want to give my thanks to Christine Noffz and Sven Kluge. For their help during my experiments, Inga Schmidt, Klaus Lengeler, Eleonora Setiadi, Pilar Cantero and Christian Lengsfeld have to be thanked. I don't forget all the others: the "big" Sven, Michael, Jessica, Catrin, Marina, Stephan, Carsten, Nico. A special thanks to "my" students: Eva, Theresia and Dagmar, who almost drove me crazy with their questions and presentations, but it was a really good time.

I should switch to Spanish for the next thanks, unfortunately I'm still not good enough, but I want to thank Prof. Jesus Pla for our collaboration on Msb2p and even more particularly Elvira Roman, even if she never answered quickly to my mail, our work together continued to be intense. Inmaculada Moreno was a pearl of patience with me in Valencia to explain how to do a cell wall characterisation. For this good time in Valencia and Düsseldorf, Gracias!

I will not forget my sister, all my family and friends; I want to thank my parents for their unconditional support during these 8 years of university study and also before. It's obvious that without them I would have never succeeded to write these lines. MERCI !

Thanks, Merci, Danke and Gracias to all of you.

# 7. References

Alonso-Monge R, Navarro-Garcia F, Molero G, Diez-Orejas R, Gustin M, Pla J, Sanchez M, Nombela C. (1999) Role of the mitogen-activated protein kinase Hog1p in morphogenesis and virulence of *Candida albicans*. *J Bacteriol* **181:** 3058-68

Alvarez FJ, Konopka JB. (2007) Identification of an N-acetylglucosamine transporter that mediates hyphal induction in *Candida albicans*. *Mol Biol Cell* **18:** 965-75

Andreasson C, Heessen S, Ljungdahl PO. (2006) Regulation of transcription factor latency by receptor-activated proteolysis. *Genes Dev* **20:** 1563-8

Bahn YS, Sundstrom P. (2001) CAP1, an adenylate cyclase-associated protein gene, regulates bud-hypha transitions, filamentous growth, and cyclic AMP levels and is required for virulence of *Candida albicans*. *J Bacteriol* **183:** 3211-23

Bassilana M, Blyth J, Arkowitz RA. (2003) Cdc24, the GDP-GTP exchange factor for Cdc42, is required for invasive hyphal growth of *Candida albicans*. *Eukaryot Cell* **2:** 9-18

Bender A, Pringle JR. (1992) A Ser/Thr-rich multicopy suppressor of a cdc24 bud emergence defect. *Yeast* **8:** 315-23

Bennett RJ, Uhl MA, Miller MG, Johnson AD. (2003) Identification and characterization of a *Candida albicans* mating pheromone. *Mol Cell Biol* **23:** 8189-201

Bennett RJ, Johnson AD. (2005) Mating in Candida albicans and the search for a sexual cycle. *Annu Rev Microbiol* **59:** 233-55

Berkhout CM. (1923). De Schimmelgeslachten *Monilia, Oidium, Oospora* en *Torula*. Thesis, Rijksuniversiteit te Utrecht

Berman J, Sudbery PE. (2002) *Candida Albicans*: a molecular revolution built on lessons from budding yeast. *Nat Rev Genet* **3:** 918-30

Biswas S, Roy M, Datta A. (2003) N-acetylglucosamine-inducible CaGAP1 encodes a general amino acid permease which co-ordinates external nitrogen source response and morphogenesis in *Candida albicans*. *Microbiology* **149:** 2597-608

Biswas S, Van Dijck P, Datta (2007) A. Environmental sensing and signal transduction pathways regulating morphopathogenic determinants of *Candida albicans*. *Microbiol Mol Biol Rev* **71:** 348-76

Bockmühl, Dirk P., Krishnamurthy, Shankarling, Gerads, Michaela, Sonneborn, Anja & Ernst, Joachim F. (2001) Distinct and redundant roles of the two protein kinase A isoforms Tpk1p and Tpk2p in morphogenesis and growth of *Candida albicans*. *Molecular Microbiology* **42:** 1243-1257

Borgers M. (1980) Mechanism of action of antifungal drugs, with special reference to the imidazole derivatives. *Rev Infect Dis* **2:** 520-34

Bradford, M. 1976 "A Rapid and Sensitive Method for the Quantitation of Microgram Quantities of Protein Utilizing the Principle of Protein-Dye Binding" *Anal. Biochem* **72:** 248-254

Brand A, Shanks S, Duncan VM, Yang M, Mackenzie K, Gow NA. (2007) Hyphal orientation of *Candida albicans* is regulated by a calcium-dependent mechanism. *Curr Biol* **17:** 347-52

Braun BR, Johnson AD. (1997) Control of filament formation in *Candida albicans* by the transcriptional repressor TUP1. *Science* **277:** 105-9

Brewster JL, de Valoir T, Dwyer ND, Winter E, Gustin MC. (1993) An osmosensing signal transduction pathway in yeast. *Science* **259:** 1760-3

Brown D.H., Giusani A.D., Chen X. and Kumamoto C.A. (1999) Filamentous growth of *Candida albicans* in response to physical environmental cues and its regulation by the unique *CZF1* gene. *Mol Microbiol* **34:** 651–662

Brown V, Sexton JA, Johnston M. (2006) A glucose sensor in *Candida albicans*. *Eukaryot Cell* **5:** 1726-37

Calera, J. A., X. J. Zhao, and R. Calderone. 2000. Defective hyphal development and avirulence caused by a deletion of the *SSK1* response regulator gene in *Candida albicans*. *Infect. Immun* **68:** 518-525

Cantero PD, Lengsfeld C, Prill SK, Subanovic M, Roman E, Pla J, Ernst JF. (2007) Transcriptional and physiological adaptation to defective protein-O-mannosylation in *Candida albicans*. *Mol Microbiol* **64:** 1115-28

Cassola A, Parrot M, Silberstein S, Magee BB, Passeron S, Giasson L, Cantore ML. (2004) *Candida albicans* lacking the gene encoding the regulatory subunit of protein kinase A displays a defect in hyphal formation and an altered localization of the catalytic subunit. *Eukaryot Cell* **3:** 190-9

Chabasse, D., Bouchara, J. P., de Gentile, L. & Chennebault, J. M. (1988). Chlamydospores de *Candida albicans* observees in vivo chez un patient attaint de SIDA. *Ann Biol Clin (Paris)* **46:** 817–818

Chauhan N, Inglis D, Roman E, Pla J, Li D, Calera JA, Calderone R. (2003) *Candida albicans* response regulator gene SSK1 regulates a subset of genes whose functions are associated with cell wall biosynthesis and adaptation to oxidative stress. *Eukaryot Cell* **2:** 1018-24

Cheetham J, Smith DA, da Silva Dantas A, Doris KS, Patterson MJ, Bruce CR, Quinn J. (2007) A Single MAPKKK Regulates the Hog1 MAPK Pathway in the Pathogenic Fungus *Candida albicans*. *Mol Biol Cell* **18:** 4603-14

Chen D, Toone WM, Mata J, Lyne R, Burns G, Kivinen K, Brazma A, Jones N, Bahler J. (2003) Global transcriptional responses of fission yeast to environmental stress. *Mol Biol Cell* **14:** 214-29

Cochrane V.W. Dormancy in Spores of Fungi (1974) *Transactions of the American Microscopical Society* **93:** 599-609

Costanzo MC, Arnaud MB, Skrzypek MS, Binkley G, Lane C, Miyasato SR, Sherlock G. (2006) The Candida Genome Database: facilitating research on *Candida albicans* molecular biology. *FEMS Yeast Res* **6:** 671-84

Csank C, Schroppel K, Leberer E, Harcus D, Mohamed O, Meloche S, Thomas DY, Whiteway M. (1998) Roles of the *Candida albicans* mitogen-activated protein kinase homolog, Cek1p, in hyphal development and systemic candidiasis. *Infect Immun* **66:** 2713-21

Csank C, Makris C, Meloche S, Schroppel K, Rollinghoff M, Dignard D, Thomas DY, Whiteway M. (1997) Derepressed hyphal growth and reduced virulence in a VH1 family-related protein phosphatase mutant of the human pathogen *Candida albicans*. *Mol Biol Cell* **8:** 2539-51

Cullen PJ, Sprague GF Jr. (2000) Glucose depletion causes haploid invasive growth in yeast. *Proc Natl Acad Sci U S A* **97:** 13619-24

Cullen PJ, Sabbagh W Jr, Graham E, Irick MM, van Olden EK, Neal C, Delrow J, Bardwell L, Sprague GF Jr. (2004) A signaling mucin at the head of the Cdc42- and MAPK-dependent filamentous growth pathway in yeast. *Genes Dev* **18:** 1695-708

Cullen PJ (2007) Signaling Mucins: The New Kids on the MAPK Block. *Crit Rev Eukaryot Gene Expr* **17:** 241-57

d'Enfert C. (2006) Biofilms and their role in the resistance of pathogenic *Candida* to antifungal agents. *Curr Drug Targets* **7:** 465-70

Dignard D, El-Naggar AL, Logue ME, Butler G, Whiteway M. (2007) Identification and characterization of MFA1, the gene encoding *Candida albicans* a-factor pheromone. *Eukaryot Cell* **6:** 487-94

Doedt T, Krishnamurthy S, Bockmuhl DP, Tebarth B, Stempel C, Russell CL, Brown AJ, Ernst JF. (2004) APSES proteins regulate morphogenesis and metabolism in *Candida albicans*. *Mol Biol Cell* **15:** 3167-80

Dubois, M, Gilles, K A, Hamilton, J K, Rebers, P A and Smith, F (1956) Colorimetric method for determination of sugars and related substances. *Anal Chem* **28:** 350–356

Eisman B, Alonso-Monge R, Roman E, Arana D, Nombela C, Pla J. (2006) The Cek1 and Hog1 mitogen-activated protein kinases play complementary roles in cell wall biogenesis and chlamydospore formation in the fungal pathogen *Candida albicans*. *Eukaryot Cell* **5:** 347-58

Enjalbert B, Nantel A, Whiteway M. (2003) Stress-induced gene expression in *Candida albicans*: absence of a general stress response. *Mol Biol Cell* **14:** 1460-7

Enjalbert B and Whiteway M (2005) Release from Quorum-Sensing Molecules Triggers Hyphal Formation during *Candida albicans* Resumption of Growth. *Eukaryotic Cell* **4:** 1203-1210

Enjalbert B, Smith DA, Cornell MJ, Alam I, Nicholls S, Brown AJ, Quinn J. (2006) Role of the Hog1 stress-activated protein kinase in the global transcriptional response to stress in the fungal pathogen *Candida albicans*. *Mol Biol Cell* **17:** 1018-32

Enloe, B., Diamond A. and Mitchell A.P. (2000) A single-transformation gene function test in diploid *Candida albicans*. *J. Bacteriol* **182:** 5730–5736

Fang HM, Wang Y. RA (2006) domain-mediated interaction of Cdc35 with Ras1 is essential for increasing cellular cAMP level for *Candida albicans* hyphal development. *Mol Microbiol* **61:** 484-96

Flick J S and Johnston M (1990) Two systems of glucose repression of the GAL1 promoter in *Saccharomyces cerevisiae*. *Mol Cell Biol* **10:** 4757-4769

Fonzi, W. und Irwin, Y. (1993) Isogenec strain construction and gene mapping in *Candida albicans. Genetics* **134:** 717-728

Forsberg H, Ljungdahl PO. (2001) Sensors of extracellular nutrients in *Saccharomyces cerevisiae*. *Curr Genet* **40:** 91-109

Garcia-Rodriguez LJ, Valle R, Duran A, Roncero C. (2005) Cell integrity signaling activation in response to hyperosmotic shock in yeast. *FEBS Lett* **579:** 6186-90

Gimeno CJ, Fink GR (1994) Induction of pseudohyphal growth by overexpression of *PHD1*, a *Saccharomyces cerevisiae* gene related to transcriptional regulators of fungal development. *Mol Biol Cell* **14:** 2100–2112

Giusani AD, Vinces M, Kumamoto CA. (2002) Invasive filamentous growth of *Candida albicans* is promoted by Czf1p-dependent relief of Efg1p-mediated repression. *Genetics* **160:** 1749-53

Hanahan, D. (1983) Studies on transformation of *Escherichia coli* with plasmids. *J. Mol. Biol* **166:** 557-580

Imai K, Noda Y, Adachi H, Yoda K. (2005) A novel endoplasmic reticulum membrane protein Rcr1 regulates chitin deposition in the cell wall of *Saccharomyces cerevisiae*. *J Biol Chem* **280:** 8275-84

Iyer K, Burkle L, Auerbach D, Thaminy S, Dinkel M, Engels K, Stagljar I. (2005) Utilizing the split-ubiquitin membrane yeast two-hybrid system to identify protein-protein interactions of integral membrane proteins. *Sci STKE* **275:** l3

Huang LS, Doherty HK, Herskowitz I. (2005) The Smk1p MAP kinase negatively regulates Gsc2p, a 1,3-beta-glucan synthase, during spore wall morphogenesis in *Saccharomyces cerevisiae*. *Proc Natl Acad Sci U S A* **102:** 12431-6

Hollingworth, M.A. and Swanson, B.J. 2004. Mucins in cancer: Protection and control at the cell surface. *Nat. Rev. Cancer* **4:** 45-59

James, P., Halladay, J. und Craig, E.A. (1996) Genomic libraries and a host strain designed for highly efficient Two-Hybrid selection in yeast. *Genetics* **144:** 1425-36

Johnson, M. D. and J. R. Perfect. 2003. Caspofungin: first approved agent in a new class of antifungals. *Expert. Opin. Pharmacother* **4:** 807-823

Johnsson N, Varshavsky A. (1994) Split ubiquitin as a sensor of protein interactions in vivo. *Proc Natl Acad Sci U S A* **91:** 10340-4

Jung WH, Warn P, Ragni E, Popolo L, Nunn CD, Turner MP, Stateva L. (2005) Deletion of PDE2, the gene encoding the high-affinity cAMP phosphodiesterase, results in changes of the cell wall and membrane in *Candida albicans*. *Yeast* **22:** 285-94

Kapteyn JC, Hoyer LL, Hecht JE, Muller WH, Andel A, Verkleij AJ, Makarow M, Van Den Ende H, Klis FM. (2000) The cell wall architecture of Candida albicans wild-type cells and cell wall-defective mutants. *Mol Microbiol* **35:** 601-11

Klengel T, Liang WJ, Chaloupka J, Ruoff C, Schröppel K, Naglik JR, Eckert SE, Mogensen EG, Haynes K, Tuite MF, Levin LR, Buck J, Mühlschlegel FA. (2005) Fungal adenylyl cyclase integrates CO2 sensing with cAMP signaling and virulence. *Curr Biol* **15:** 2021-6

Klepser ME. (2006) *Candida* resistance and its clinical relevance. *Pharmacotherapy* **26:** 68S-75S

Kronstad J, De Maria AD, Funnell D, Laidlaw RD, Lee N, de Sa MM, Ramesh M. (1998) Signaling via cAMP in fungi: interconnections with mitogen-activated protein kinase pathways. *Arch Microbiol* **170:** 395-404

Kruppa M, Calderone R. (2006) Two-component signal transduction in human fungal pathogens. *FEMS Yeast Res* **6:** 149-59

Kurtz MB, Kirsch DR, Kelly R. (1998) The molecular genetics of *Candida albicans*. *Microbiol Sci* **5:** 58-63

Lawrence CL, Botting CH, Antrobus R, Coote PJ. (2004) Evidence of a new role for the high-osmolarity glycerol mitogen-activated protein kinase pathway in yeast: regulating adaptation to citric acid stress. *Mol Cell Biol* **24:** 3307-23

Leberer, E., Harcus, D., Dignard, D., Johnson, L., Ushinsky, S., Thomas, D.Y., and Schröppel, L. (2001) Ras links cellular morphogenesis to virulence by regulation of the MAP kinase and cAMP signalling pathways in the pathogenic fungus *Candida albicans*. *Mol Microbiol* **42:** 673–687

Lee BN and Elion EA (1999), The MAPKKK Ste11 regulates vegetative growth through a kinase cascade of shared signaling components. *Proc. Natl. Acad. Sci. USA* **96:** 12679–12684

Lee KL, Buckley HR, Campbell CC. (1975) An amino acid liquid synthetic medium for the development of mycelial and yeast forms of *Candida albicans*. *Sabouraudia* **13:** 148-53

Leng P, Lee PR, Wu H, Brown AJ. (2001) Efg1, a morphogenetic regulator in *Candida albicans*, is a sequence-specific DNA binding protein. *J Bacteriol* **183:** 4090-3

Liu H, Kohler J, Fink GR. (1994) Suppression of hyphal formation in *Candida albicans* by mutation of a STE12 homolog. *Science* **266:** 1723-6

Liu H, Suresh A, Willard FS, Siderovski DP, Lu S, Naqvi NI. (2007) Rgs1 regulates multiple Galpha subunits in *Magnaporthe* pathogenesis, asexual growth and thigmotropism. *EMBO J* **26:** 690-700

Lo HJ, Köhler JR, DiDomenico B, Loebenberg D, Cacciapuoti A, Fink GR. (1997) Nonfilamentous *C. albicans* mutants are avirulent. *Cell* **90:** 939-49

Losberger, C. und Ernst, J.F. (1989) Sequence and transcript analysis of the *C. albicans* gene (*URA3*) encoding orotidine-5'-phosphate decarboxylase. *Curr. Genet* **16:** 153-157

Lotz H, Sohn K, Brunner H, Muhlschlegel FA, Rupp S. (2004) RBR1, a novel pH-regulated cell wall gene of *Candida albicans*, is repressed by RIM101 and activated by NRG1. *Eukaryot Cell* **3:** 776-84

Maidan MM, De Rop L, Serneels J, Exler S, Rupp S, Tournu H, Thevelein JM, Van Dijck P. (2005) The G protein-coupled receptor Gpr1 and the Galpha protein Gpa2 act through the cAMP-protein kinase A pathway to induce morphogenesis in *Candida albicans*. *Mol Biol Cell* **16:** 1971-86

Martin H, Flandez M, Nombela C, Molina M. (2005) Protein phosphatases in MAPK signalling: we keep learning from yeast. *Mol Microbiol* **58:** 6-16

Martinez AI, Castillo L, Garcera A, Elorza MV, Valentin E, Sentandreu R. (2004) Role of Pir1 in the construction of the *Candida albicans* cell wall. *Microbiology* **150:** 3151-61

Martínez P, Ljungdahl PO (2005) Divergence of Stp1 and Stp2 transcription factors in *Candida albicans* places virulence factors required for proper nutrient acquisition under amino acid control. *Mol Cell Biol* **25:** 9435-46

McGuire, Pettinger (1953), Hygromycin I. Preliminary studies on the production and biological activity of a new antibiotic, *Antibiot. Chemother* **3:** 1268-1278

Mitchell A.P. (1998) Dimorphism and virulence in *Candida albicans*. *Current Opinion in Microbiology* **1:** 687-692

Mouillon JM, Persson BL. (2006) New aspects on phosphate sensing and signalling in *Saccharomyces cerevisiae*. *FEMS Yeast Res* **6:** 171-6

Napoletano C, Rughetti A, Agervig Tarp MP, Coleman J, Bennett EP, Picco G, Sale P, Denda-Nagai K, Irimura T, Mandel U, Clausen H, Frati L, Taylor-Papadimitriou J, Burchell J, Nuti M. (2007) Tumor-associated Tn-MUC1 glycoform is internalized through the

macrophage galactose-type C-type lectin and delivered to the HLA class I and II compartments in dendritic cells. *Cancer Res* **67:** 8358-67

Negredo, A., L. Monteoliva, C. Gil, J. Pla, and C. Nombela. 1997. Cloning, analysis and one-step disruption of the *ARG5,6* gene of *Candida albicans*. *Microbiol* **143:** 297-302.

Nobile CJ, Bruno VM, Richard ML, Davis DA, Mitchell AP. (2003) Genetic control of chlamydospore formation in *Candida albicans*. *Microbiology* **149:** 3629-37

Norice CT, Smith FJ Jr, Solis N, Filler SG, Mitchell AP. (2007) Requirement for *Candida albicans* Sun41 in Biofilm Formation and Virulence. *Eukaryot Cell* **6:** 2046-55.

O'Rourke SM, Herskowitz I. (2002) A third osmosensing branch in *Saccharomyces cerevisiae* requires the Msb2 protein and functions in parallel with the Sho1 branch. *Mol Cell Biol* **22:** 4739-49

Obrdlik, P., M. El-Bakkoury, T. Hamacher, C. Cappellaro, C. Vilarinoet al., (2004) K+ channel interactions detected by a genetic system optimized for systematic studies of membrane protein interactions. *Proc. Natl. Acad. Sci. USA* **101:** 12242–12247

Phan QT, Myers CL, Fu Y, Sheppard DC, Yeaman MR, Welch WH, Ibrahim AS, Edwards JE Jr, Filler SG. (2007) Als3 is a Candida albicans invasin that binds to cadherins and induces endocytosis by host cells. *PLoS Biol*. **5:** 64

Phizicky, E. M., Schwartz, R. C., and Abelson, J. (1986) *Saccharomyces cerevisiae* tRNA ligase. Purification of the protein and isolation of the structural gene*J. Biol. Chem* **261:** 2978-2986

Prill, S.K.-H. , Klinkert, B. , Timpel, C. , Gale, C.A. , Schröppel, K. , and Ernst, J.F. (2005) *PMT* family of *Candida albicans*: five protein mannosyltransferase isoforms affect growth, morphogenesis and antifungal resistance. *Mol Microbiol* **55:** 546– 560

Ram AF, Arentshorst M, Damveld RA, vanKuyk PA, Klis FM, van den Hondel CA. (2004) The cell wall stress response in *Aspergillus niger* involves increased expression of the glutamine: fructose-6-phosphate amidotransferase-encoding gene (gfaA) and increased deposition of chitin in the cell wall. *Microbiology* **150:** 3315-26

Roberts, R.L., Fink, G.R. (1994) Elements of a single MAP kinase cascade in *Saccharomyces cerevisiae* mediate two developmental programs in the same cell type: mating and invasive growth. *Genes Dev* **8:** 2974–2985.

Reuss O, Vik A, Kolter R, Morschhauser J. (2004) The SAT1 flipper, an optimized tool for gene disruption in *Candida albicans*. *Gene* **27:** 341:119-27

Roman E., Nombela C., Pla J. (2005) The Sho1 adaptor protein links oxidative stress to morphogenesis and cell wall biosynthesis in the fungal pathogen *Candida albicans*. *Mol Cell Biol* **25:** 10611-27

Román E, Arana DM, Nombela C, Alonso-Monge R, Pla J. (2007) MAP kinase pathways as regulators of fungal virulence. *Trends Microbiol* **15:** 181-90

Roman E., Cottier F., Ernst J.F., Pla J. Msb2 is an upstream mediator of the Cek1 pathway in the fungal pathogen *Candida albicans*.

Roncero, C. and A. Duran. 1985. Effect of Calcofluor white and Congo red on fungal cell wall morphogenesis: in vivo activation of chitin polymerization. *J. Bacteriol* **163:** 1180-1185

Sabie FT, Gadd GM. (1992) Effect of nucleosides and nucleotides and the relationship between cellular adenosine 3':5'-cyclic monophosphate (cyclic AMP) and germ tube formation in *Candida albicans*. *Mycopathologia* **119:** 147-56

Sanglard D, Ischer F, Marchetti O, Entenza J, Bille J. (2003) Calcineurin A of *Candida albicans*: involvement in antifungal tolerance, cell morphogenesis and virulence. *Mol Microbiol* **48:** 959-76

Santos MA, Tuite MF. (1995) The CUG codon is decoded in vivo as serine and not leucine in *Candida albicans*. *Nucleic Acids Res* **23:** 1481-6

Schweizer A, Rupp S, Taylor BN, Rollinghoff M, Schroppel K. (2000) The TEA/ATTS transcription factor CaTec1p regulates hyphal development and virulence in *Candida albicans*. *Mol Microbiol* **38:** 435-45

Setiadi ER, Doedt T, Cottier F, Noffz C, Ernst JF. (2006) Transcriptional response of *Candida albicans* to hypoxia: linkage of oxygen sensing and Efg1p-regulatory networks. *J Mol Biol* **361:** 399-411

Singh KK. (2000) The *Saccharomyces cerevisiae* Sln1p-Ssk1p two-component system mediates response to oxidative stress and in an oxidant-specific fashion. *Free Radic Biol Med* **29:** 1043-50

Soll DR. (2002) *Candida* commensalism and virulence: the evolution of phenotypic plasticity. *Acta Tro* **81:** 101-10

Soll DR. (2004) Mating-type locus homozygosis, phenotypic switching and mating: a unique sequence of dependencies in *Candida albicans*. *Bioessays* **26:** 10-20

Sonneborn A, Bockmuhl DP, Ernst JF. (1999) Chlamydospore formation in *Candida albicans* requires the Efg1p morphogenetic regulator. *Infect Immun* **67:** 5514-7

Sonneborn A, Bockmuhl DP, Gerads M, Kurpanek K, Sanglard D, Ernst JF. (2000) Protein kinase A encoded by TPK2 regulates dimorphism of *Candida albicans*. *Mol Microbiol* **35:** 386-96

Staab JF, Sundstrom P. (2003) URA3 as a selectable marker for disruption and virulence assessment of *Candida albicans* genes. *Trends Microbiol* **11:** 69-73

Stoldt, V.R., Sonneborn, A., Leuker, C., Ernst, J.F. (1997) Efg1, an essential regulator of morphogenesis of the human pathogen *Candida albicans*, is a member of a conserved class of bHLH proteins regulating morphogenetic processes in fungi. *EMBO J* **16:** 1982–1991

Tanaka T, Fillmore D, Sun ST, Nishio I, Swislow G, Shah A (1980) Phase transitions in ionic gels. *Phys. Rev. Lett* **45:** 1636-1639

Tatebayashi K, Tanaka K, Yang HY, Yamamoto K, Matsushita Y, Tomida T, Imai M, Saito H. (2007) Transmembrane mucins Hkr1 and Msb2 are putative osmosensors in the SHO1 branch of yeast HOG pathway. *EMBO J* **26:** 3521-33

Tebarth B, Doedt T, Krishnamurthy S, Weide M, Monterola F, Dominguez A, Ernst JF. (2003) Adaptation of the Efg1p morphogenetic pathway in *Candida albicans* by negative autoregulation and PKA-dependent repression of the EFG1 gene. *J Mol Biol* **20:** 949-62

Tusher VG, Tibshirani R, Chu G. (2001) Significance analysis of microarrays applied to the ionizing radiation response. *Proc Natl Acad Sci U S A* **98:** 5116-21

Versele M, Lemaire K, Thevelein JM. (2001) Sex and sugar in yeast: two distinct GPCR systems. *EMBO Rep* **2:** 574-9

Viera, J. und Messing, J. (1991) New pUC-derived cloning vectors with different selectable markers and DNA replication origins. *Gene* **100:** 189-194

Vinces MD, Haas C, Kumamoto CA. (2006) Expression of the *Candida albicans* morphogenesis regulator gene CZF1 and its regulation by Efg1p and Czf1p. *Eukaryot Cell* **5:** 825-35

Wang, Y., Dohlman, H.G. (2004) Pheromone signaling mechanisms in yeast: a prototypical sex machine. *Science* **306:** 1508–1509

Wellington M, Kabir MA, Rustchenko E. (2006) 5-fluoro-orotic acid induces chromosome alterations in genetically manipulated strains of *Candida albicans*. *Mycologia* **98:** 393-8.

Wilson D, Tutulan-Cunita A, Jung W, Hauser NC, Hernandez R, Williamson T, Piekarska K, Rupp S, Young T, Stateva L. (2007) Deletion of the high-affinity cAMP phosphodiesterase encoded by PDE2 affects stress responses and virulence in *Candida albicans*. *Mol Microbiol* **65:** 841-56

Wilson RB, Davis D, Mitchell AP. (1999) Rapid hypothesis testing with *Candida albicans* through gene disruption with short homology regions. *J Bacteriol* **181:** 1868-1874

Wilson RB, Davis D, Enloe BM, Mitchell AP. (2000) A recyclable *Candida albicans* URA3 cassette for PCR product-directed gene disruptions. *Yeast* **16:** 65-70

Winkler A, Arkind C, Mattison CP, Burkholder A, Knoche K, Ota I. (2002) Heat stress activates the yeast high-osmolarity glycerol mitogen-activated protein kinase pathway, and protein tyrosine phosphatases are essential under heat stress. *Eukaryot Cell* **1:** 163-73

Wisplinghoff, H., T. Bischoff, S. M. Tallent, H. Seifert, R. P. Wenzel, and M. B. Edmond. (2004). Nosocomial bloodstream infections in US hospitals: analysis of 24,179 cases from a prospective nationwide surveillance study. *Clin. Infect. Dis* **39:**309-317.

Xue Y, Batlle M, Hirsch J. (1998) GPR1 encodes a putative G protein-coupled receptor that associates with the Gpa2p Galpha subunit and functions in a Ras-independent pathway. *EMBO J* **17:** 1996-2007

Yang, Y. H., Buckley, M. J., Dudoit, S., Speed, T. P. (2002) Comparison of methods for image analysis on cDNA microarray data. *J. Comp. Graph. Stat* **11:** 1-29.

Yanish-Perron, C., Vieira, J. und Messing, J. (1985) Improved M13 phage cloning vectors and host strains: nucleotide sequences of M13mp18 and pUC19 vectors. *Gene* **33:** 103-119

Zhao X, Oh SH, Hoyer LL. (2007) Unequal contribution of ALS9 alleles to adhesion between Candida albicans and human vascular endothelial cells. *Microbiology* **153:** 2342-50

# 8. Abbreviations

| | |
|---|---|
| °C | degree Celsius |
| 5-FOA | 5-fluoroorotic acid |
| a.a. | amino acid |
| AIDS | acquired immune deficiency syndrome |
| Amp | ampicilin |
| bHLH | basic helix-loop-helix |
| BSA | bovine serum albumin |
| BSI | bloodstream infections |
| *C. albicans* | *Candida albicans* |
| $C_4H_4KNaO_6.4H_2O$ | potassium sodium tartrate tetrahydrate |
| $CaCl_2$: | calcium chloride |
| cAMP | cyclic adenosine monophosphate |
| cDNA | complementary DNA |
| $CuSO_4.5H_2O$ | Copper(II) sulfate pentahydrate |
| DEPC | diethylpyrocarbonat |
| DNA | deoxyribonucleic acid |
| DMF | dimethylformamide |
| DTT | dithiothreitol |
| *E. coli* | *Escherichia coli* |
| EDTA | ethylenediamine tetraacetic acid |
| FDR | false discovery rate |
| FG | filamentation growth |
| Fig. | figure |
| GFP | green fluorescent protein |
| GlcNAc | N-acetylglucosamine |
| GPCR | G-protein-coupled receptors |
| GTPase | guanosine-5'-triphosphatase |
| h | hour |
| HCl | hydrochloric acid |
| HEPES | 4-(2-hydroxyethyl)-1-piperazineethanesulfonic acid |
| HMH | Hkr1 Msb2 homology |
| IPTG | isopropyl β-D-1-thiogalactopyranoside |
| Kbp | kilo base pair |
| KCl | potassium chloride |
| LiAc | lithium acetate |
| LiCl | lithium chloride |
| log | logarithmic |
| *M. grisea* | *Magnaporthe grisea* |
| mA | milliampere |
| MAPK | mitogen-activated protein kinase |
| $MgCl_2$ | magnesium chloride |
| µm | micrometer |
| min | minute |
| ml | milliliter |
| mM | milimolaire |
| mRNA | messanger RNA |
| M | molaire |

| | |
|---|---|
| MM | minimal medium |
| MTL | mating type locus |
| NaAc | sodium acetate |
| NaCl | sodium chloride |
| NaOH | sodium hydroxide |
| ng | nanogram |
| nm | nanometer |
| $O.D._{600nm}$ | optical density at 600nm |
| ORF | open reading frame |
| PCR | polymerase chain reaction |
| PEG | polyethylenglycol |
| PKA | protein kinase A |
| RNA | ribonucleic acid |
| RT | room temperature |
| RT-PCR | Real time polymerase chain reaction |
| S. cerevisiae | *Saccharomyces cerevisiae* |
| SDS | sodium dodecyl sulfate |
| SSC | standard saline citrate |
| SS-DNA | single-strand DNA |
| STR | serine Threonine rich |
| Tab. | table |
| TAE | tris-Acetat-EDTA |
| TM | transmembran |
| Tris | trishydroxymethylaminomethane |
| WT | wild-type |
| X-gal | 5-bromo-4-chloro-3-indolyl- beta-D-galactopyranoside |
| YNB | yeast nitrogen base |
| YPD | yeast extract-Pepton-Dextrose |

# 9. Supplementary data

Table 1: Expression ratios in mutants relative to the wild-type strain from microarray experiment. Data were statistically analyzed with SAM software, which calculated q-values reflecting variation among the six ratios for each gene (a low q-value indicates a low level of variation).

Genes commonly regulated in *msb2*, *sho1* and *msb2 sho1* mutants : 1

| | | | ***msb2* / *sho1* / *sho1 msb2*** |
|---|---|---|---|
| **orf19 number** | **Gene name** | **Function** | **Fold regulation (q-value)** |
| *orf19.6442* | *PRP8* | U5 snRNP protein. pre-mRNA splicing factor | 0.52 (0.00) / 0.61 (0.00) / 0.64 (0.00) |

Genes commonly regulated in *msb2* and *sho1* mutants: 3

| **orf19 number** | **Gene name** | **Function** | **Fold regulation (q-value)** |
|---|---|---|---|
| *orf19.3374* | *ECE1* | cell elongation protein | 0.58 (0.00) / 3.88 (0.00) |
| *orf19.11943* | *IFL1* | cell wall organisation and biogenesis | 0.56 (0.00) / 0.46 (0.00) |
| *orf19.8613* | *IPF6787* | similar to *Saccharomyces cerevisiae* Bsp1p | 0.56 (0.00) / 0.55 (0.00) |

Genes commonly regulated in *sho1* and *sho1 msb2* mutants: 12

| | | | ***sho1 / sho1 msb2*** |
|---|---|---|---|
| **orf19 number** | **Gene name** | **Function** | **Fold regulation (q-value)** |
| *orf19.2355* | *ALS10* | agglutinin like protein | 4.15 (0.00) / 1.69 (0.00) |
| *orf19.1321* | *HWP1* | hyphal wall protein | 2.99 (0.00) / 1.80 (0.49) |
| *orf19.11525* | *IPF7217* | response to stress | 2.12 (0.00) / 0.63 (0.00) |
| *orf19.4051* | *HTS1* | histidine tRNA synthetase | 1.93 (0.00) / 0.66 (0.00) |
| *orf19.7676* | *IPF4959* | D-xylulose reductase | 1.78 (0.00) / 0.57 (0.00) |
| *orf19.6586* | *IPF1617* | unknown function | 1.61 (4.08) / 1.61 (0.00) |
| | *FUN34.5EOC* | unknown function | 1.58 (0.00) / 0.66 (0.65) |
| *orf19.6608* | *IPF7940* | unknown function | 1.58 (0.92) / 0.65 (0.00) |
| *orf19.3822* | *SCS7* | required for hydroxylation of ceramide | 1.51 (4.08) / 0.63 (0.00) |
| *orf19.1172* | *PHO84* | inorganic phosphate transport protein | 0.66 (2.53) / 0.54 (0.00) |
| | *IPF2268.3* | unknown function | 0.64 (2.53) / 1.90 (0.00) |
| *orf19.4772* | *SHO1* | protein involved in the Hog1p signal | 0.26 (0.00) / 0.46 (0.00) |

| | | | |
|---|---|---|---|
| | | transduction | |

Genes commonly regulated in *msb2* and *sho1 msb2* mutants: 2

| | | | ***msb2 - sho1 msb2*** |
|---|---|---|---|
| **orf19 number** | **Gene name** | **Function** | **Fold regulation (q-value)** |
| *orf19.9332* | *IFR1* | unknown function | 1.56 (3.33) / 0.63 (0.00) |
| *orf19.10861* | *IPF4820* | putative complex I intermediate associated protein Cia30p | 0.64 (4.64) / 0.66 (0.66) |

Genes only regulated in *msb2* mutant: 8

| **orf19 number** | **gene name** | **function** | **Fold regulation** | **q-value** |
|---|---|---|---|---|
| *orf19.3376* | *IPF13247* | unknown function | 0.66 | 4.64 |
| *orf19.5430* | *IPF1128* | similar to *Saccharomyces cerevisiae* Bud21p | 0.65 | 4.64 |
| *orf19.1490* | *IPF6003* | similar to *Saccharomyces cerevisiae* Msb2p | 0.64 | 0.00 |
| *orf19.5270* | *IPF2059* | unknown function | 0.63 | 4.64 |
| *orf19.3926* | *IPF10934* | similar to *Saccharomyces cerevisiae* Rny1p | 0.63 | 4.64 |
| *orf19.3542* | *LEM3* | lipid translocator | 0.61 | 3.33 |
| *orf19.5291* | *IPF17024* | phospholipid metabolic process | 0.59 | 0.00 |
| *orf19.641* | *IPF14630* | similar to *Saccharomyces cerevisiae* Erj5p | 0.56 | 0.00 |

Genes only regulated in *sho1* mutant: 65

| **orf19 number** | **Gene name** | **Function** | **Fold regulation** | **q-value** |
|---|---|---|---|---|
| *orf19.5636* | *RBT5* | repressed by Tup1p protein 5 | 3.01 | 0.00 |
| *orf19.5674* | *PGA10* | putative GPI-anchor protein | 2.71 | 0.00 |
| *orf19.1691* | *IPF6518* | unknown function | 2.69 | 0.00 |
| *orf19.4035* | *PGA4* | putative GPI-anchhored protein | 2.51 | 0.00 |
| *orf19.5635* | *PGA7* | putative GPI-anchhored protein | 2.29 | 0.00 |
| *orf19.3128* | *SLY1* | hydrophilic suppressor of Ypt1p | 2.28 | 0.00 |
| *orf19.4048* | *DES1* | putative delta-4 sphingolipid desaturase | 2.27 | 0.00 |
| *orf19.4716* | *GDH3* | NADP-glutamate dehydrogenase | 2.22 | 0.00 |
| *orf19.4040* | *ILV3* | dihydroxyacid dehydratase | 2.10 | 0.00 |
| *orf19.9896* | *URA2* | multifunctional pyrimidine biosynthesis protein | 2.08 | 2.93 |
| *orf19.3117* | *IPF12297* | mycelial surface antigen | 2.04 | 0.00 |

| | | | | |
|---|---|---|---|---|
| *orf19.789* | *PYC2* | pyruvate carboxylase 2 | 1.96 | 0.00 |
| *orf19.5372* | *IPF6235* | *Candida albicans* Tca2p retrotransposon | 1.94 | 0.00 |
| *orf19.4045* | *EST1* | telomere capping | 1.77 | 0.00 |
| *orf19.4459* | *IPF11849* | unknown function | 1.77 | 0.00 |
| *orf19.1408* | *GLK1* | aldohexose specific glucokinase | 1.76 | 0.00 |
| *orf19.7077* | *FRE7* | ferric reductase transmembrane component | 1.75 | 0.00 |
| *orf19.3198* | *OBPA* | similar to *S. cerevisiae* Osh7p | 1.74 | 0.00 |
| *orf19.3829* | *PHR1* | GPI-anchored pH responsive glycosyl transferase | 1.73 | 2.93 |
| *orf19.3575* | *CDC19* | pyruvate kinase | 1.72 | 0.00 |
| *orf19.5634* | *FRE5* | ferric reductase transmembrane component | 1.71 | 0.00 |
| *orf19.4752* | *MSN4* | similar to *S. cerevisiae* Msn4p transcriptional activator | 1.67 | 4.08 |
| *orf19.3651* | *PGK1* | phosphoglycerate kinase | 1.67 | 0.00 |
| *orf19.4044* | *MUM2* | ubiquitin C-terminal hydrolase | 1.66 | 0.00 |
| *orf19.2396* | *IFR2* | unknown function | 1.65 | 0.00 |
| *orf19.5645* | *MET15* | O-acetylhomoserine O-acetylserine sulphydrylase | 1.64 | 0.00 |
| *orf19.4033* | *PRP22* | RNA-dependent ATPase | 1.63 | 0.00 |
| *orf19.5437* | *RHR2* | DL-glycerol phosphatase | 1.63 | 0.00 |
| *orf19.675* | *IPF3964* | similar to *S. cerevisiae* Yel077cp | 1.63 | 0.00 |
| *orf19.6920* | *IPF2195* | unknown function | 1.63 | 0.00 |
| *orf19.4013* | *IPF3352* | unknown function | 1.62 | 0.00 |
| *orf19.4618* | *FBA1* | fructose-bisphosphate aldolase | 1.61 | 0.00 |
| *orf19.2337* | *ALP1* | amino-acid permease | 1.61 | 0.00 |
| *orf19.5779* | *RNR1* | ribonucleoside-diphosphate reductase | 1.59 | 0.00 |
| *orf19.4076* | *MET10* | sulfite reductase flavin-binding subunit | 1.59 | 0.92 |
| *orf19.7504* | *IPF407* | unknown function | 1.58 | 0.00 |
| *orf19.9345* | *SCW1* | glucanase | 1.58 | 0.00 |
| *orf19.767* | *ERG3* | C5.6 desaturase | 1.57 | 0.92 |
| *orf19.3239* | *CTF18* | chromosome transmission in mitosis | 1.57 | 0.00 |
| *orf19.5673* | *OPT7* | oligopeptide transporter | 1.56 | 0.00 |
| *orf19.6139* | *FRE30.3* | strong similarity to ferric reductase Fre2p | 1.56 | 0.00 |

| | | | | |
|---|---|---|---|---|
| *orf19.8243* | *EFG1* | enhanced filamentous growth factor | 1.55 | 0.92 |
| *orf19.395* | *ENO1* | enolase I (2-phosphoglycerate dehydratase) | 1.55 | 0.00 |
| *orf19.3710* | *YHB5* | flavohemoglobin (by homology) | 1.54 | 2.53 |
| *orf19.903* | *GPM1* | phosphoglycerate mutase | 1.52 | 0.00 |
| *orf19.4036* | *APM1* | AP-1 complex subunit. mu1 subunit | 1.51 | 0.00 |
| *orf19.2496* | *FRP1* | member of the FRP family | 1.51 | 0.92 |
| *orf19.5348* | *TPS3* | alpha.alpha-trehalose-phosphate synthase | 1.51 | 0.92 |
| *orf19.9993* | *IPF15822* | unknown function | 1.51 | 0.00 |
| *orf19.6745* | *TPI1* | triose phosphate isomerase | 1.50 | 0.92 |
| *orf19.13651* | *IPF4866* | similar to *Saccharomyces cerevisiae* Yuh1p | 0.66 | 2.93 |
| *orf19.3618* | *YWP1* | adhesion protein | 0.65 | 4.08 |
| *orf19.6816* | *IPF2400* | putative aldehyde reductase | 0.65 | 2.53 |
| *orf19.8730* | *CDC8* | dTMP kinase | 0.65 | 5.99 |
| *orf19.4222* | *SST2* | GTPase activator | 0.63 | 3.07 |
| *orf19.2531* | *CSP37* | hyphal cell wall protein | 0.63 | 1.13 |
| *orf19.655* | *PHO84* | high-affinity inorganic phosphate/H+ symporter | 0.63 | 1.13 |
| *orf19.1367* | *IPF8989* | similar to *Saccharomyces cerevisiae* Ntw1p | 0.62 | 5.99 |
| *orf19.7319* | *SUC1* | putative zinc finger protein Suc1p | 0.58 | 5.99 |
| *orf19.6178* | *FBP1* | fructose-1.6-bisphosphatase | 0.58 | 4.08 |
| *orf19.10708* | *MTALPHA2* | transcription factor | 0.57 | 0.00 |
| *orf19.997* | *IPF6785* | unknown function | 0.56 | 4.08 |
| | *PRE6* | 20S proteasome subunit | 0.45 | 0.00 |
| *orf19.10713* | *PAP12* | poly(A) polymerase | 0.40 | 0.00 |
| *orf19.1716* | *URA3* | orotidine-5 -monophosphate decarboxylase | 0.31 | 0.00 |

Genes only regulated in *sho1 msb2* mutant : 192

| **orf19 number** | **Gene name** | **Function** | **Fold regulation** | **q-value** |
|---|---|---|---|---|
| *orf19.1364* | *IPF16939* | unknown function | 15.23 | 4.98 |
| | *IPF14348.3* | unknown function | 4.95 | 0.00 |
| *orf19.4980* | *SSA4* | cahsp70 mRNA for heat shock | 3.91 | 0.00 |
| *orf19.7654* | *CPR6* | cyclophylin | 3.37 | 0.00 |
| *orf19.5749* | *SBA1* | Hsp90p (Ninety) Associated Co-chaperone | 2.87 | 0.00 |

| | | | | |
|---|---|---|---|---|
| | *IPF11391* | unknown function | 2.87 | 0.49 |
| *orf19.7085* | *IPF525* | unknown function | 2.78 | 0.00 |
| *orf19.3396* | *HCH1* | Protein folding | 2.76 | 0.00 |
| *orf19.4998* | *IPF1798* | putative transcription factor | 2.54 | 0.65 |
| *orf19.5277* | *IPF4706* | Similar to *Saccharomyces cerevisiae* Upf3p | 2.49 | 0.49 |
| *orf19.7291* | *GCD14* | translational repressor of Gcn4p | 2.43 | 1.26 |
| *orf19.9564* | *KAR2* | dnaK-type molecular chaperone | 2.41 | 0.00 |
| *orf19.6515* | *HSP90* | heat shock protein | 2.39 | 0.00 |
| *orf19.13747* | *HSP104* | heat shock protein | 2.33 | 0.00 |
| *orf19.10702* | *STI1* | stress-induced protein | 2.32 | 0.00 |
| *orf19.2260* | *IPF16141* | Similar to *Saccharomyces cerevisiae* Bcd1p | 2.31 | 1.26 |
| *orf19.1816* | *ALS3* | agglutinin-like protein | 2.16 | 1.60 |
| *orf19.2770* | *IPF7081* | unknown function | 2.16 | 1.26 |
| *orf19.6301* | *RPS620B* | unknown function | 2.12 | 0.00 |
| *orf19.6300* | *RPS620A* | unknown function | 2.08 | 0.00 |
| *orf19.882* | *HSP78* | heat shock protein | 2.06 | 0.00 |
| *orf19.6408* | *YDJ1* | mitochondrial and ER import protein | 1.99 | 0.00 |
| *orf19.5409* | *IPF1098* | Similar to *Saccharomyces cerevisiae* Ist1p | 1.98 | 1.26 |
| *orf19.7602* | *IPF661* | Similar to *Saccharomyces cerevisiae* Aha1p | 1.97 | 0.00 |
| *orf19.4715* | *NUM11* | nuclear migration protein | 1.97 | 0.20 |
| *orf19.1065* | *SSA1* | heat shock protein of Hsp70p family | 1.95 | 0.00 |
| *orf19.9405* | *ARO10* | putative pyruvate decarboxylase | 1.94 | 0.22 |
| *orf19.10345* | *IPF10963* | similar to *Saccharomyces cerevisiae* Tid3p | 1.90 | 0.85 |
| *orf19.5474* | *IPF2690.3F* | unknown function | 1.89 | 0.00 |
| *orf19.8136* | *IPF10391* | similar to DnaJ proteins | 1.89 | 0.00 |
| *orf19.1445* | *ESC4* | Negative regulation of DNA transposition | 1.89 | 0.85 |
| *orf19.5531* | *CDC37* | cell division control protein | 1.88 | 0.00 |
| *orf19.7156* | *FAA24* | long-chain-fatty-acid--CoA ligase | 1.85 | 0.85 |
| *orf19.3861* | *SIS1* | heat shock protein | 1.85 | 0.00 |
| *orf19.190* | *YAL011* | mitochondrial transit peptide | 1.84 | 0.20 |
| *orf19.2253* | *IFT1* | unknown function | 1.83 | 0.65 |
| *orf19.11788* | *IPF16988* | unknown function | 1.82 | 0.20 |
| *orf19.4424* | *IPF5556* | acid phosphatase | 1.81 | 0.00 |

| | | | | |
|---|---|---|---|---|
| *orf19.7539* | *IPF333* | unknown function | 1.81 | 0.85 |
| *orf19.11257* | *SSK2* | MAP kinase kinase kinase | 1.80 | 1.26 |
| *orf19.8332* | *IPF20079* | similar to *S.cerevisiae* Ymr074cp | 1.79 | 2.68 |
| *orf19.304* | *IPF1471* | aminotriazole resistance protein | 1.79 | 0.22 |
| *orf19.320* | *IPF6755* | unknown function | 1.79 | 0.20 |
| *orf19.7818* | *IPF13416* | unknown function | 1.78 | 0.00 |
| | *IPF4137.3F* | unknown function | 1.78 | 0.22 |
| *orf19.3524* | *CRK1.5F* | protein kinase | 1.76 | 1.26 |
| *orf19.1296* | *PRP31* | pre-mRNA splicing protein | 1.75 | 0.00 |
| *orf19.5469* | *IPF2690.5F* | unknown function | 1.74 | 0.00 |
| *orf19.11088* | *PEX17* | peroxisomal peripheral membrane protein | 1.73 | 2.68 |
| *orf19.7492* | *IPF424* | similar to *S.cerevisiae* Swc4cp | 1.71 | 0.49 |
| *orf19.5126* | *IPF14559.3F* | RNA binding | 1.70 | 0.22 |
| *orf19.5268* | *NUT2* | negative transcription regulator from artifical reporters | 1.69 | 0.00 |
| *orf19.5506* | *PLC1* | 1-phosphatidylinositol-4.5-bisphosphate phosphodiesterase | 1.69 | 2.68 |
| *orf19.2432* | *HAC1* | transcription factor | 1.68 | 0.20 |
| *orf19.866* | *RAD32* | DNA repair protein | 1.67 | 0.49 |
| *orf19.4987* | *NUP49* | nuclear pore protein | 1.67 | 1.26 |
| *orf19.5742* | *ALS9.5EOC* | agglutinin-like protein | 1.67 | 0.49 |
| *orf19.9371* | *PEX14* | peroxisomal protein | 1.66 | 0.00 |
| *orf19.6973* | *IPF7556* | proteolysis | 1.66 | 1.60 |
| *orf19.4054* | *CTA24* | transcriptional regulation | 1.65 | 0.00 |
| *orf19.1168* | *ZCF3* | unknown function | 1.64 | 0.65 |
| *orf19.7053* | *GAC1* | ser/thr phosphoprotein phosphatase 1. regulatory chain | 1.63 | 1.26 |
| *orf19.5823* | *SGT2* | glutamine-rich tetratricopeptide repeat containing protein | 1.62 | 0.00 |
| *orf19.1341* | *IPF7926* | putative protein kinase | 1.62 | 0.65 |
| *orf19.7739* | *IPF14895* | similar to *S. cerevisiae* Mic17p | 1.61 | 0.65 |
| *orf19.5641* | *CAR2* | ornithine aminotransferase | 1.61 | 1.60 |
| *orf19.11* | *IPF11566* | unknown function | 1.61 | 0.49 |

| | | | | |
|---|---|---|---|---|
| *orf19.4622* | *IPF11090.EXON1* | weak similarity to glutenin | 1.61 | 1.03 |
| *orf19.2238* | *LTE1* | Guanyl-nucleotide exchange factor | 1.60 | 0.49 |
| | *CTA24.3* | transcriptional activator | 1.59 | 0.22 |
| *orf19.1757* | *IPF6857* | putative transcriptional regulator | 1.59 | 0.85 |
| *orf19.4492* | *IPF4776* | similar to *S. cerevisiae* Ebp2p | 1.58 | 1.26 |
| *orf19.3281* | *IPF298* | similar to *S. cerevisiae* Yer051wp | 1.58 | 1.26 |
| | *CTA241.EXON2* | transcriptional activator | 1.58 | 0.00 |
| *orf19.6688* | *IPF2615* | unknown function | 1.58 | 0.00 |
| | *HSP10.3* | 10 kDa mitochondrial heat shock chaperonin | 1.58 | 0.00 |
| *orf19.4909* | *CBK1* | serine/threonine protein kinase | 1.57 | 0.00 |
| *orf19.2849* | *AQY1* | similarity to plasma membrane and water channel proteins | 1.57 | 0.85 |
| *orf19.13252* | *IPF11217* | similar to *S. cerevisiae* Lhs1p chaperone of the ER lumen | 1.56 | 0.00 |
| | *IPF15772* | unknown function | 1.56 | 1.60 |
| *orf19.6193* | *TAF145* | transcription factor | 1.55 | 4.98 |
| *orf19.34* | *GIT1* | glycerophosphoinositol transporter | 1.55 | 0.65 |
| *orf19.2722* | *CGR1* | cell growth protein | 1.55 | 2.68 |
| *orf19.2925* | *CIN4* | GTP-binding protein | 1.54 | 1.26 |
| *orf19.884* | *HSP78* | heat shock protein of clpb family | 1.53 | 0.00 |
| *orf19.7167* | *IPF20175* | unknown function | 1.53 | 0.00 |
| *orf19.11979* | *IPF4792* | unknown Function | 1.53 | 0.00 |
| *orf19.2989* | *IPF16795* | glycerate/formate-dehydrogenase | 1.53 | 0.65 |
| *orf19.9369* | *CDC43* | geranylgeranyltransferase I | 1.53 | 0.00 |
| *orf19.831* | *IPF16057* | unknown function | 1.52 | 0.85 |
| *orf19.3949* | *YTA7* | 26S proteasome subunit | 1.52 | 0.00 |
| | *IPF6712.3F* | unknown function | 1.52 | 0.00 |
| *orf19.1087* | *IPF19578* | unknown function | 1.52 | 0.00 |
| *orf19.1091* | *IPF16935* | putative ortholog of *S. cerevisiae* Nop8p | 1.52 | 0.22 |
| *orf19.6377* | *IPF5425* | similar to *S. cerevisiae* Ppm1p carboxy methyltransferase | 1.51 | 0.00 |

| | | | | |
|---|---|---|---|---|
| *orf19.6326* | *IPF5729* | similar to *S. cerevisiae* Sfg1p | 1.51 | 0.20 |
| *orf19.10868* | *IPF19902* | unknown function | 1.51 | 1.26 |
| *orf19.3210* | *IPF12399* | unknown function | 1.51 | 0.65 |
| *orf19.5281* | *IPF4697* | similar to *Saccharomyces cerevisiae* Scp160p | 1.51 | 0.00 |
| *orf19.11626* | *IPF11262* | similar to *Saccharomyces cerevisiae* Ybr014cp | 1.51 | 0.22 |
| *orf19.3831* | *IPF15927.3F* | similar to *Saccharomyces cerevisiae* Pxr1p | 1.51 | 0.00 |
| *orf19.1235* | *HOM3* | aspartokinase | 1.50 | 0.00 |
| *orf19.6757* | *IPF3485* | aldo/keto reductase | 0.67 | 2.68 |
| *orf19.5114* | *GRD19* | probable golgi membrane protein-sorting protein | 0.66 | 0.00 |
| *orf19.922* | *ERG16* | cytochrome P450 lanosterol 14a-demethylase | 0.66 | 0.00 |
| *orf19.3888* | *PGI1* | glucose-6-phosphate isomerase | 0.66 | 0.00 |
| *orf19.5663* | *IPF5282* | similar to *Saccharomyces cerevisiae* Ymr034cp | 0.66 | 0.00 |
| *orf19.7219* | *FTR1* | high affinity iron permease | 0.66 | 0.00 |
| *orf19.7611* | *TRX1* | thioredoxin | 0.66 | 0.00 |
| *orf19.3656* | *COX15* | cytochrome oxidase assembly factor | 0.66 | 0.00 |
| *orf19.8176* | *HXK2* | hexokinase II | 0.66 | 0.00 |
| *orf19.2336* | *IPF8682* | unknown function (cell wall component) | 0.66 | 0.00 |
| *orf19.4268* | *IPF9525* | similar to *Saccharomyces cerevisiae* Utp13p | 0.66 | 0.00 |
| *orf19.4381* | *VTC2* | putative polyphosphate synthetase | 0.66 | 0.00 |
| *orf19.3696* | *TOM22* | mitochondrial outer membrane receptor complex subunit | 0.66 | 1.03 |
| *orf19.4826* | *IDH1* | isocitrate dehydrogenase (NAD+) subunit1 | 0.65 | 0.00 |
| *orf19.3358* | *LSC1* | succinate-CoA ligase / synthetase | 0.65 | 0.00 |
| *orf19.6787* | *ERV14* | membrane protein | 0.65 | 0.00 |
| *orf19.7459* | *IPF2908* | similar to *Saccharomyces cerevisiae* Ybr238cp | 0.65 | 0.00 |
| *orf19.5517* | *IPF20104* | alcohol dehydrogenase | 0.65 | 0.00 |
| *orf19.7115* | *SAC7* | GAP for Rho1p | 0.65 | 0.00 |
| *orf19.4611* | *PRS4* | ribose-phosphate pyrophosphokinase 3 | 0.65 | 0.65 |
| *orf19.6068* | *SVF1* | similar to *Saccharomyces cerevisiae* Svf1p | 0.65 | 0.00 |
| *orf19.1585* | *ZRT2* | zinc transport protein | 0.64 | 0.00 |
| *orf19.3442* | *EBP2* | NADPH dehydrogenase | 0.64 | 0.00 |
| *orf19.6385* | *ACO1* | aconitate hydratase | 0.64 | 0.00 |
| *orf19.1743* | *ACS1* | acetyl-coenzyme-A synthetase | 0.64 | 0.00 |

| | | | | |
|---|---|---|---|---|
| *orf19.2774* | *LAB5* | lipoic acid synthase | 0.64 | 0.00 |
| *orf19.6632* | *ACO2* | aconitate hydratase | 0.64 | 0.00 |
| *orf19.11011* | *CYT12* | cytochrome-c1 | 0.64 | 0.00 |
| | *LSC2.3EOC2* | succinate-CoA ligase beta subunit | 0.64 | 0.49 |
| *orf19.2023* | *HGT7* | sugar transporter | 0.64 | 0.00 |
| *orf19.5113* | *ADH2* | alcohol dehydrogenase I | 0.63 | 0.00 |
| *orf19.6881* | *YTH1* | mRNA cleavage and polyadenylation specificity factor | 0.63 | 0.00 |
| *orf19.3130* | *IPF7819* | similar to *Saccharomyces cerevisiae* Ylr243wp | 0.63 | 0.65 |
| *orf19.5680* | *IPF5471* | unknown function | 0.63 | 0.00 |
| *orf19.7538* | *PIF2* | DNA helicase | 0.63 | 0.00 |
| *orf19.2942* | *DIP5* | dicarboxylic amino acid permease | 0.63 | 0.00 |
| *orf19.5193* | *FMA1* | unknown function | 0.63 | 0.22 |
| *orf19.7312* | *ERG13* | 3-hydroxy-3-methylglutaryl coenzyme A synthase | 0.63 | 0.20 |
| *orf19.12101* | *ERG251* | C-4 sterol methyl oxidase | 0.63 | 0.20 |
| *orf19.1187* | *CPH2* | transcriptional activator of hyphal growth | 0.63 | 0.00 |
| *orf19.3917* | *IPF10032.3F* | unknown function | 0.62 | 0.00 |
| *orf19.10660* | *GRP4* | putative reductase | 0.62 | 0.00 |
| *orf19.2270* | *SMF12* | manganese transporter | 0.62 | 0.00 |
| *orf19.220* | *PIR1* | putative cell wall protein of the PIR family | 0.62 | 0.00 |
| *orf19.2608* | *ADH5* | probable alcohol dehydrogenase | 0.62 | 0.00 |
| *orf19.3608* | *MSH3* | DNA mismatch repair | 0.62 | 0.20 |
| *orf19.5576* | *IPF16189.3F* | protein similar to S. cerevisiae Ydr531wp | 0.61 | 0.00 |
| *orf19.5459* | *IPF4160* | protein similar to S. cerevisiae Pbp1p | 0.61 | 0.49 |
| *orf19.9988* | *IPF14850* | unknown function | 0.61 | 0.20 |
| *orf19.2451* | *PGA45* | putative GPI-anchored protein of unknown function | 0.60 | 0.00 |
| *orf19.5343* | *ASH1* | GATA-like transcription factor | 0.60 | 0.22 |
| *orf19.951* | *IPF1548* | unknown function | 0.60 | 0.00 |
| *orf19.7655* | *RPO21* | DNA-directed RNA polymerase II. 215 KD subunit | 0.60 | 0.00 |
| *orf19.1387* | *IPF12383* | similar to *Saccharomyces cerevisiae* Cfd1p | 0.60 | 0.00 |

| | | | | |
|---|---|---|---|---|
| *orf19.8467* | *IPF3415* | similar to *Saccharomyces cerevisiae* Yim1p | 0.60 | 0.00 |
| *orf19.5698* | *IPF5446* | similar to *Saccharomyces cerevisiae* Mrpl1p | 0.60 | 0.00 |
| *orf19.1868* | *RNR22* | ribonucleoside-diphosphate reductase | 0.59 | 0.00 |
| | *FUM12.53F* | fumarate hydratase. internal fragment | 0.59 | 0.00 |
| *orf19.5801* | *RNR21* | ribonucleoside-diphosphate reductase | 0.59 | 0.00 |
| *orf19.5611* | *GRP3* | similar to *Saccharomyces cerevisiae* Gre2p | 0.57 | 1.03 |
| *orf19.2670* | *IPF12162* | similar to *Saccharomyces cerevisiae* Htd2p | 0.57 | 0.22 |
| *orf19.689* | *PLB1* | phospholipase B | 0.57 | 0.00 |
| *orf19.7231* | *FTR2* | high affinity iron permease | 0.57 | 0.00 |
| | *ATP1.EXON2* | F1F0-ATPase complex. F1 alpha subunit | 0.57 | 0.00 |
| *orf19.6561* | *LAT1* | Dihydrolipoamide S-acetyltransferase | 0.56 | 0.00 |
| *orf19.6741* | *IPF3506* | unknown function | 0.56 | 0.85 |
| *orf19.3675* | *GAL7* | UDP-glucose-hexose-1-phosphate uridylyltransferase | 0.56 | 0.00 |
| *orf19.7405* | *IPF2645* | unknown function | 0.55 | 0.00 |
| *orf19.2021* | *HGT8* | sugar transporter | 0.55 | 0.00 |
| *orf19.4082* | *DDR48* | stress protein | 0.55 | 0.00 |
| *orf19.5949* | *FAS2* | fatty-acyl-CoA synthase. alpha chain | 0.55 | 0.00 |
| *orf19.1448* | *APT1* | adenine phosphoribosyltransferase | 0.55 | 0.65 |
| *orf19.11687* | *FET33* | cell surface ferroxidase | 0.54 | 0.00 |
| *orf19.9578* | *IPF4119* | unknown function | 0.54 | 0.49 |
| *orf19.2020* | *HGT6* | sugar transporter | 0.53 | 0.00 |
| *orf19.3908* | *IPF15492* | unknown function | 0.53 | 1.03 |
| *orf19.7514* | *PCK1* | phosphoenolpyruvate carboxykinase | 0.52 | 0.00 |
| *orf19.1306* | *IPF6679* | unknown function | 0.51 | 0.00 |
| *orf19.3433* | *OYE23* | NADPH dehydrogenase | 0.49 | 0.00 |
| *orf19.6105* | *MVD1.3* | mevalonate pyrophosphate decarboxylase | 0.48 | 0.00 |
| *orf19.8138* | *QDR1* | putative antibiotic resistance proteins | 0.48 | 0.00 |
| *orf19.4624* | *HRT2* | similar to ScHrt2p | 0.48 | 0.00 |
| *orf19.7765* | *FAD2* | delta-12 fatty acid desaturase | 0.46 | 0.00 |
| *orf19.7772* | *EBP1* | NADPH dehydrogenase | 0.43 | 0.00 |
| *orf19.5288* | *IFE2* | putative alcohol dehydrogenase | 0.38 | 0.00 |
| *orf19.3707* | *YHB1* | nitric oxide dioxygenase | 0.38 | 0.00 |

| | | | | |
|---|---|---|---|---|
| | *STF2* | ATP synthase regulatory factor | 0.36 | 0.00 |
| *orf19.2659* | *IPF20056* | similar to *Saccharomyces cerevisiae* Yer067wp | 0.27 | 0.00 |
| *orf19.934* | *IPF18109* | unknown function | 0.04 | 4.98 |
| *orf19.2233* | *PRE2* | 20S proteasome subunit (beta5) | 0.02 | 4.98 |

Table 2: List of genes predicted to encode protein with a minimum of 3 TM domains and a C-terminal tail cytoplasmic constituted by at least 30 a.a. Only genes without strong homolog and with a protein of unknown function were selected.

| **Ca number** | **common name** | **orf19 name** | **Number of TM domains** | **a.a. in N-terminal tail** | **a.a. in C-terminal tail** |
|---|---|---|---|---|---|
| *CA2599* | *IPF11176* | *orf19.52* | 3 | 150 | |
| | *IPF11434* | *orf19.6462* | 3 | | 60 |
| *CA3023* | *IPF11508* | *orf19.3904* | 3 | | 90 |
| *CA0589* | *IPF13080* | *orf19.1162.1* | 3 | | 60 |
| *CA0109* | *IPF13723* | *orf19.7892* | 3 | 260 | |
| *CA2588* | *IPF15098* | *orf19.4376* | 3 | 120 | |
| *CA2906* | *IPF15523* | *orf19.4521* | 3 | | 60 |
| *CA6142* | *IPF1879* | *orf19.5903* | 3 | 430 | |
| *CA0071* | *IPF19290* | *orf19.621* | 3 | 50 | |
| *CA5825* | *IPF2489* | *orf19.7480* | 3 | | 80 |
| *CA6192* | *IPF29314* | *orf19.1764* | 3 | 70 | |
| *CA0903* | *IPF4401* | *orf19.1480* | 3 | 70 | |
| *CA4091* | *IPF5005* | *orf19.6650* | 3 | 70 | |
| *CA5522* | *IPF708* | *orf19.5370* | 3 | 80 | |
| *CA4187* | *IPF7524* | *orf19.12003* | 3 | | 50 |
| *CA5394* | *IPF9400* | *orf19.937* | 3 | | 70 |
| | *IPF9464* | *orf19.11550* | 3 | 50 | |
| *CA2621* | *IPF9499* | *orf19.2808* | 3 | 330 | |
| *CA3362* | *IPF9789* | *orf19.9489* | 3 | 190 | |
| *CA5157* | *IPF993* | *orf19.4595* | 3 | 200 | |
| *CA2732* | *IPF10327* | *orf19.2113* | 4 | 90 | 240 |
| *CA3025* | *IPF11503* | *orf19.3902* | 4 | | 110 |
| *CA0055* | *IPF12442* | *orf19.10917* | 4 | | 60 |
| *CA3604* | *IPF12942* | *orf19.4933* | 4 | 75 | 120 |
| *CA1019* | *IPF13485* | *orf19.3769* | 4 | 320 | 210 |
| *CA3302* | *IPF13784* | *orf19.2313* | 4 | 60 | 200 |
| *CA0859* | *IPF14495* | *orf19.4466* | 4 | 180 | 80 |
| *CA3937* | *IPF14686* | *orf19.9557* | 4 | | 90 |
| *CA3020* | *IPF15492* | *orf19.3908* | 4 | | 70 |
| *CA6077* | *IPF16* | *orf19.5984* | 4 | | 160 |
| *CA4889* | *IPF1629* | *orf19.6581* | 4 | | 220 |
| *CA0282* | *IPF17417* | *orf19.12160* | 4 | | 60 |
| *CA3021* | *IPF17640* | *orf19.3906* | 4 | | 60 |
| *CA3022* | *IPF17642* | *orf19.3905* | 4 | | 70 |
| *CA0843* | *IPF18853* | *orf19.8656* | 4 | | 80 |
| *CA2537* | *IPF20108* | *orf19.3184* | 4 | 80 | |
| *CA1619* | *IPF2067* | *orf19.11558* | 4 | | 220 |
| *CA5454* | *IPF257.3f* | *orf19.3261* | 4 | 70 | |

| | | | | | |
|---|---|---|---|---|---|
| *CA5799* | *IPF4176* | *orf19.5449* | 4 | 60 | |
| *CA6054* | *IPF4952* | *orf19.7672* | 4 | | 100 |
| *CA5624* | *IPF501* | *orf19.7073* | 4 | | 80 |
| *CA3073* | *IPF6108* | *orf19.4811* | 4 | 100 | |
| *CA4603* | *IPF6230* | *orf19.10803* | 4 | 160 | |
| *CA0293* | *IPF6624* | *orf19.6489* | 4 | | 80 |
| *CA2185* | *IPF6880* | *orf19.4247* | 4 | 140 | |
| *CA3748* | *IPF7385* | *orf19.3430* | 4 | 160 | |
| *CA3548* | *IPF12179* | *orf19.3872* | 5 | | 50 |
| *CA3550* | *IPF13228* | *orf19.3874* | 5 | 320 | |
| *CA0832* | *IPF14225* | *orf19.9244* | 5 | 230 | |
| *CA2510* | *IPF1472* | *orf19.305* | 5 | | 60 |
| *CA0482* | *IPF14763* | *orf19.7765* | 5 | | 110 |
| *CA1220* | *IPF14985* | *orf19.4134* | 5 | | 70 |
| *CA0325* | *IPF15222* | *orf19.3781* | 5 | | 220 |
| *CA5459* | *IPF276* | *orf19.3267* | 5 | | 100 |
| *CA2327* | *IPF4782* | *orf19.11972* | 5 | 130 | |
| *CA4086* | *IPF5014* | *orf19.6642* | 5 | 143 | |
| *CA5609* | *IPF538* | *orf19.7091* | 5 | 80 | |
| *CA4709* | *IPF5895* | *orf19.6941* | 5 | 70 | |
| *CA5543* | *IPF5988* | *orf19.7305* | 5 | 150 | |
| *CA3594* | *IPF6076* | *orf19.4922* | 5 | 84 | |
| *CA2493* | *IPF7227* | *orf19.4048* | 5 | 65 | |
| *CA3845* | *IPF7944* | *orf19.6605* | 5 | 50 | |
| *CA2427* | *IPF9898* | *orf19.3406* | 5 | | 200 |
| *CA5142* | *IPF1022* | *orf19.4579* | 6 | 100 | |
| *CA2806* | *IPF11702* | *orf19.5780* | 6 | 75 | 150 |
| *CA0427* | *IPF11995* | *orf19.2761* | 6 | 50 | |
| *CA2530* | *IPF12782* | *orf19.3176* | 6 | 90 | 200 |
| *CA1791* | *IPF13967* | *orf19.5205* | 6 | 110 | |
| *CA1204* | *IPF14524* | *orf19.8486* | 6 | | 300 |
| *CA0553* | *IPF16653* | *orf19.5534* | 6 | 50 | 80 |
| *CA3133* | *IPF16939* | *orf19.1364* | 6 | 60 | |
| *CA5652* | *IPF19815* | *orf19.7354* | 6 | 140 | 80 |
| *CA4249* | *IPF4293* | *orf19.538* | 6 | 70 | |
| *CA1508* | *IPF9977* | *orf19.4525* | 6 | 80 | 60 |
| *CA2934* | *IPF11515* | *orf19.3329* | 7 | 80 | |
| *CA1687* | *IPF12275* | *orf19.3658* | 7 | | 150 |
| *CA0676* | *IPF13097* | *orf19.8772* | 7 | | 70 |
| *CA2853* | *IPF17057* | *orf19.1070* | 7 | | 60 |
| *CA2208* | *IPF17255* | *orf19.696* | 7 | | 90 |
| *CA0117* | *IPF19231* | *orf19.916* | 7 | 50 | |
| *CA1039* | *IPF4012* | *orf19.2501* | 7 | | 220 |
| *CA2947* | *IPF6298* | *orf19.1964* | 7 | | 130 |
| *CA5509* | *IPF743* | *orf19.5353* | 7 | | 70 |
| *CA4685* | *IPF9013* | *orf19.881* | 7 | 70 | |
| *CA3810* | *IPF9230* | *orf19.2492* | 7 | | 130 |
| *CA5013* | *IPF13941* | *orf19.5234* | 8 | 190 | |
| *CA1488* | *IPF17402.5eoc* | *orf19.4064* | 8 | | |
| *CA1713* | *IPF19743* | *orf19.3332* | 8 | 150 | 220 |
| *CA5481* | *IPF19810* | *orf19.12773* | 8 | 70 | |
| *CA4955* | *IPF4580* | *orf19.6522* | 8 | 120 | |

| | | | | | |
|---|---|---|---|---|---|
| *CA4372* | *IPF5282* | *orf19.5663* | 8 | | 120 |
| *CA1883* | *IPF5479* | *orf19.2209* | 8 | 240 | 130 |
| *CA5168* | *IPF6032* | *orf19.4607* | 8 | 90 | 50 |
| *CA5508* | *IPF745* | *orf19.5352* | 8 | | 170 |
| *CA5018* | *IPF7558* | *orf19.6971* | 8 | 120 | |
| *CA4483* | *IPF9156* | *orf19.1881* | 8 | | 130 |
| *CA3527* | *IPF9934* | *orf19.8603* | 8 | 60 | 70 |
| *CA1474* | *IPF10208* | *orf19.1096* | 9 | 90 | |
| *CA4834* | *IPF1217* | *orf19.2063* | 9 | | 280 |
| *CA1721* | *IPF14652* | *orf19.2653* | 9 | 260 | |
| *CA1448* | *IPF14728* | *orf19.192* | 9 | | 170 |
| *CA0794* | *IPF15639* | *orf19.552* | 9 | 100 | |
| *CA2001* | *IPF17074* | *orf19.2792* | 9 | 160 | |
| *CA0349* | *IPF19026* | *orf19.1813* | 9 | | 190 |
| *CA1957* | *IPF3887* | *orf19.768* | 9 | 430 | |
| *CA3595* | *IPF6079* | *orf19.4923* | 9 | | 130 |
| *CA2211* | *IPF13921* | *orf19.4749* | 10 | 170 | |
| *CA5274* | *IPF1764* | *orf19.4985* | 10 | 100 | |
| *CA5430* | *IPF191* | *orf19.3232* | 10 | 70 | 40 |
| *CA5798* | *IPF4181* | *orf19.5447* | 10 | 140 | 70 |
| *CA2438* | *IPF5505* | *orf19.2198* | 10 | | 90 |
| *CA1325* | *IPF6678* | *orf19.1307* | 10 | 50 | 120 |
| *CA3241* | *IPF7493* | *orf19.4682* | 10 | 100 | 90 |
| *CA6062* | *IPF8307* | *orf19.6005* | 10 | 190 | 110 |
| *CA4936* | *IPF8369* | *orf19.13498* | 10 | 60 | |
| *CA0480* | *IPF8610* | *orf19.2633* | 10 | 50 | 70 |
| *CA3747* | *IPF10153* | *orf19.2170* | 11 | | 230 |
| *CA5756* | *IPF1065* | *orf19.5392* | 11 | 60 | |
| *CA1016* | *IPF11142* | *orf19.473* | 11 | | 60 |
| *CA3189* | *IPF11607* | *orf19.2149* | 11 | 80 | |
| *CA4833* | *IPF1216* | *orf19.2064* | 11 | 100 | |
| *CA0189* | *IPF12201* | *orf19.11600* | 11 | 70 | |
| *CA6118* | *IPF126* | *orf19.5932* | 11 | | 90 |
| *CA0954* | *IPF13162* | *orf19.1142* | 11 | 240 | |
| *CA3769* | *IPF13465* | *orf19.2898* | 11 | | 60 |
| *CA4659* | *IPF17754* | *orf19.4446* | 11 | | 130 |
| *CA5030* | *IPF2988* | *orf19.6984* | 11 | 320 | |
| *CA6050* | *IPF4939* | *orf19.7666* | 11 | 120 | |
| *CA5626* | *IPF498* | *orf19.7071* | 11 | 90 | |
| *CA5600* | *IPF559* | *orf19.7100* | 11 | 200 | |
| *CA3069* | *IPF6117* | *orf19.4805* | 11 | | 90 |
| *CA1546* | *IPF6671* | *orf19.8891* | 11 | | 100 |
| *CA3414* | *IPF9240* | *orf19.6141* | 11 | 50 | |
| *CA4573* | *IPF9431* | *orf19.6884* | 11 | 50 | |
| *CA1281* | *IPF10171* | *orf19.644* | 12 | | 70 |
| *CA2053* | *IPF11029* | *orf19.5720* | 12 | 60 | |
| *CA0164* | *IPF11694* | *orf19.4335* | 12 | 60 | |
| *CA4380* | *IPF12736* | *orf19.5673* | 12 | 60 | |
| *CA2339* | *IPF13377* | *orf19.2350* | 12 | 50 | |
| *CA2571* | *IPF13769* | *orf19.13590* | 12 | 50 | |
| *CA1963* | *IPF14040* | *orf19.2397* | 12 | 50 | |
| *CA6173* | *IPF1479* | *orf19.309* | 12 | 80 | 40 |

| | | | | | |
|---|---|---|---|---|---|
| *CA4635* | *IPF1524* | *orf19.341* | 12 | 170 | 40 |
| *CA0793* | *IPF16273* | *orf19.553* | 12 | 70 | |
| *CA4885* | *IPF1636* | *orf19.6577* | 12 | 160 | |
| *CA5287* | *IPF1922* | *orf19.7148* | 12 | 120 | |
| *CA4330* | *IPF2087* | *orf19.4090* | 12 | 70 | |
| *CA5240* | *IPF3032* | *orf19.5023* | 12 | 60 | 40 |
| *CA3915* | *IPF3277* | *orf19.4384* | 12 | 70 | |
| *CA5836* | *IPF428* | *orf19.7490* | 12 | 70 | |
| *CA3686* | *IPF4890* | *orf19.13642* | 12 | 60 | |
| *CA6053* | *IPF4949* | *orf19.7670* | 12 | 240 | |
| *CA1816* | *IPF7020* | *orf19.136* | 12 | 140 | |
| *CA5023* | *IPF7547* | *orf19.6976* | 12 | 60 | |
| *CA3833* | *IPF8192* | *orf19.6592* | 12 | 80 | |
| *CA0966* | *IPF9136* | *orf19.6249* | 12 | 70 | 240 |
| *CA3966* | *IPF9376* | *orf19.1427* | 12 | 50 | |
| *CA2435* | *IPF9483* | *orf19.10898* | 12 | 60 | |
| *CA2619* | *IPF9490* | *orf19.2810* | 12 | 120 | 50 |
| *CA2703* | *IPF12193* | *orf19.4655* | 13 | 200 | |
| *CA5570* | *IPF1992* | *orf19.7336* | 13 | 70 | |
| *CA4263* | *IPF2277* | *orf19.6656* | 13 | | 50 |
| *CA4020* | *IPF5324* | *orf19.3444* | 13 | 160 | |
| *CA1324* | *IPF6676* | *orf19.1308* | 13 | 80 | |
| *CA3356* | *IPF9560* | *orf19.9497* | 13 | 100 | |
| *CA0778* | *IPF12884* | *orf19.4779* | 14 | 70 | |
| *CA2221* | *IPF9670* | *orf19.5100* | 17 | | 300 |